

# GEOLOGICA ULTRAIECTINA

Mededelingen van het  
Instituut voor Aardwetenschappen der  
Rijksuniversiteit te Utrecht

No. 55

## HIGH-RESOLUTION SEISMIC PROFILING

DEVELOPMENT OF ACQUISITION, PROCESSING, AND INTERPRETATION  
FOR THE PRACTICAL IMPLEMENTATION OF THE METHOD IN SHALLOW  
SUB-SURFACE EXPLORATION AND ENGINEERING

JAN BROUWER

# GEOLOGICA ULTRAIECTINA

Mededelingen van het  
Instituut voor Aardwetenschappen der  
Rijksuniversiteit te Utrecht

No. 55

## HIGH-RESOLUTION SEISMIC PROFILING

DEVELOPMENT OF ACQUISITION, PROCESSING, AND INTERPRETATION  
FOR THE PRACTICAL IMPLEMENTATION OF THE METHOD IN SHALLOW  
SUB-SURFACE EXPLORATION AND ENGINEERING

JAN BROUWER

**X. X. - 3**

CIP-GEGEVENS KONINKLIJKE BIBLIOTHEEK, DEN HAAG

Brouwer, Jan

High-resolution seismic profiling : development of acquisition, processing, and interpretation for the practical implementation of the method in shallow sub-surface exploration and engineering / Jan Brouwer. - [Utrecht : Instituut voor Aardwetenschappen der Rijksuniversiteit Utrecht]. - Ill., fig., tab. - (Geologica Ultraiectina ; no. 55)  
Proefschrift Utrecht. - Met lit. opg.  
ISBN 90-71577-08-2  
SISO 562 UDC 550.3 (043.3)  
Trefw.: geofysica.

# **HIGH-RESOLUTION SEISMIC PROFILING**

**DEVELOPMENT OF ACQUISITION, PROCESSING, AND INTERPRETATION  
FOR THE PRACTICAL IMPLEMENTATION OF THE METHOD IN SHALLOW  
SUB-SURFACE EXPLORATION AND ENGINEERING**

## **HOGE RESOLUTIE SEISMIEK**

**DE ONTWIKKELING VAN ACQUISITIE, PROCESSING EN INTERPRETATIE  
VOOR DE PRAKTISCHE TOEPASSING VAN DE METHODE  
BIJ DE VERKENNING VAN DE ONDIEPE ONDERGROND**

(met een samenvatting in het Nederlands)

### **PROEFSCHRIFT**

**TER VERKRIJGING VAN DE GRAAD VAN DOCTOR AAN  
DE RIJKSUNIVERSITEIT TE UTRECHT OP GEZAG VAN  
DE RECTOR MAGNIFICUS PROF. DR. J.A. VAN GINKEL  
VOLGENS BESLUIT VAN HET COLLEGE VAN DEKANEN  
IN HET OPENBAAR TE VERDEDIGEN OP DONDERDAG  
1 DECEMBER 1988 DES NAMIDDAGS TE 12.45 UUR**

**DOOR**

**JAN BROUWER**

**GEBOREN OP 13 OKTOBER 1958 TE LEEUWARDEN**

PROMOTOR: PROF. DR. K. HELBIG

*Aan Liesbeth, Robert Jan, Marloes en  
Femke*

*'There is a theory which states that if ever anyone discovers exactly what the Universe is for and why it is here, it will instantly disappear and be replaced by something even more bizarre and inexplicable.*

*There is another which states that this has already happened.*

*From: The restaurant at the end of the Universe by Douglas Adams.*

*The research described in this thesis was carried out at the:*

*Department of Exploration Geophysics,  
Institute for Earth Sciences,  
University of Utrecht,  
Budapestlaan 4, P.O. Box 80.021,  
3508 TA Utrecht,  
The Netherlands.*

## Contents

### Chapter 1

Introduction and summary .....	11
References .....	12

### Chapter 2

High-resolution 3D reflection seismics on a tidal flat: acquisition, processing, and interpretation .....	15
2.1 Introduction .....	15
2.2 Location and target .....	16
2.3 Equipment .....	16
2.4 Field layout .....	19
2.4.1 General considerations .....	19
2.4.2 Considerations for 3D surveys on tidal shoals .....	19
2.5 Implementation .....	19
2.6 Field parameters and data acquisition .....	21
2.7 Processing .....	23
2.8 Display .....	26
2.9 Results .....	26
2.10 Geological interpretation .....	32
2.11 Conclusions .....	32
2.12 References .....	34

### Chapter 3

Onshore high-resolution seismic profiling .....	37
3.1 Introduction .....	37
3.2 Acquisition .....	38
3.2.1 Introduction .....	38
3.2.2 Field equipment .....	40
3.2.2.1 Seismic sources .....	40
3.2.2.2 Seismic receivers .....	41
3.2.2.3 Cables and interfacing .....	43
3.2.2.4 Seismograph, storage and display .....	43
3.2.3 Field setup .....	45
3.2.3.1 Introduction .....	45
3.2.3.2 Offset .....	45
3.2.3.3 Geophone distance .....	47
3.3 Processing .....	48



## Contents

3.3.1	Introduction .....	48
3.3.2	Basic processing scheme .....	48
3.3.3	High-resolution processing .....	51
3.4	Field examples .....	56
3.4.1	Introduction .....	56
3.4.2	Example 1: Winterswijk .....	57
3.4.2.1	Setting and targets .....	57
3.4.2.2	Acquisition parameters .....	57
3.4.2.3	Results .....	58
3.4.3	Example 2: Portugal .....	60
3.4.3.1	Setting and targets .....	60
3.4.3.2	Acquisition parameters .....	61
3.4.3.3	Results .....	61
3.4.4	Example 3: Zwolle .....	63
3.4.4.1	Setting and targets .....	63
3.4.4.2	Acquisition parameters .....	64
3.4.4.3	Results .....	64
3.4.5	Example 4: Denekamp .....	66
3.4.5.1	Setting and targets .....	66
3.4.5.2	Acquisition parameters .....	66
3.4.5.3	Results .....	67
3.4.6	Example 5: Spain .....	68
3.4.6.1	Setting and targets .....	68
3.4.6.2	Acquisition parameters .....	68
3.4.6.3	Results .....	69
3.4.7	Example 6: Texel .....	71
3.4.7.1	Setting and targets .....	71
3.4.7.2	Acquisition parameters .....	71
3.4.7.3	Results .....	72
3.5	References .....	75
 <i>Chapter 4</i>		
High-resolution seismic profiling: a case history .....		77
4.1	Introduction .....	77
4.2	Geological setting .....	78
4.3	Geophysical setting .....	79
4.4	Definition of acquisition conditions .....	81
4.5	Refraction interpretation .....	82
4.6	Description of the raw data .....	83
4.7	First arrival interpretation .....	87

## Contents

4.8	Guided waves .....	89
4.9	Processing strategy .....	91
4.10	Actual processing parameters .....	94
4.11	Discussion .....	98
4.12	References .....	100
<i>Chapter 5</i>		
	Ray-tracing statics .....	103
5.1	Introduction .....	103
5.2	Are static corrections really static? .....	104
5.3	Standard methods in theory .....	106
5.4	Standard methods in practice .....	107
5.5	Ray-tracing statics .....	112
5.6	Topographic corrections and lateral inhomogeneities .....	113
5.7	Conclusions .....	119
5.8	References .....	119
<i>Chapter 6</i>		
	Calibration of the seismic stratigraphic response of tidal deposits .....	121
6.1	Introduction .....	122
6.2	Sedimentologic framework .....	123
6.3	Seismic characteristics .....	125
6.4	Test section .....	126
6.5	Heuristic relations .....	129
6.5.1	One-dimensional features .....	130
6.5.2	Multi-dimensional features .....	130
6.6	Conclusions .....	131
6.7	References .....	131
	Samenvatting (Summary in Dutch) .....	133
	Acknowledgements .....	135
	Curriculum Vitae .....	136

## *Chapter 1*

# INTRODUCTION AND SUMMARY

In the last few years there has been a general increase in the activities in the field of high-resolution seismic profiling. A growing interest in shallow sub-surface exploration probably underlies this development. Major attention is paid to the adaptation of high-resolution seismic profiling for engineering purposes. Commercial applicability is one of the main points of interest and improvements are principally found in the field of data acquisition.

At the University of Utrecht the interest in the development of high-resolution seismic profiling dates from 1976. The wish to obtain information on recent sedimentary structures in tidal areas resulted in a feasibility study by Herber, Runia and Helbig (1981). No direct commercial application was thought of during this study. Data proved to be of very good quality, mainly due to the absence of a weathering layer and the relatively low noise level. Further developments were focussed on the improvement of processing and interpretation methods, and on the adaptation of acquisition techniques in order to increase vertical- and lateral resolution. A processing and interpretation package was written and expanded by staff and students and field equipment was updated. Doornenbal and Helbig (1983) gave a detailed description of the activities in the period 1981 to 1983. It was stressed by the authors that the results pertained to tidal areas only.

The research presented in this thesis addresses the further development of high-resolution seismic profiling towards a method for shallow sub-surface exploration. Within this context three major aspects are presented. In the first place the extension of the method towards the acquisition, processing, and interpretation of 3-D high-resolution seismic data is described in chapter 2. The second aspect this thesis addresses is the development of onshore high-resolution seismic profiling. A general description of onshore profiling is given in chapter 3 and some field examples are presented. In chapter 4 a case history of an onshore seismic survey is presented emphasizing the possibility to combine refraction- and reflection information in processing and interpretation. The problems relating to the static correction of high-resolution seismic data are discussed in chapter 5. A method for static corrections that can generally be used in seismic profiling, including standard surveys, is

presented. Finally, the relationship between high-resolution seismic data and geology is dealt with. Chapter 6 discusses the correlation between clastic tidal deposits and their seismic facies.

The development of high-resolution seismic profiling has by no means reached an end. Hence, the overview presented in this thesis is not complete. Further research has to be carried out addressing, e.g., the problems that arise from weathering layer effects and the time-to-depth conversion (Brouwer, Douma, and Helbig, 1985).

#### REFERENCES

- Brouwer, J.H., Douma, J., and Helbig, K. 1985. A new look at migration. *First Break* 3 (12) 9-15.
- Doornenbal, J.C. and Helbig, K. 1983. High resolution reflection seismics on a tidal flat in the Dutch delta: acquisition, processing and interpretation. *First Break* 1 (5) 9-20.
- Herber, M.A., Runia, D.J., and Helbig, K. 1981. The shallow structure of the Roggenplaat (The Netherlands) as deduced from high-resolution multi-channel profiling. *Geologie en Mijnbouw* 60, 225-236.

## *Chapter 2*

# **HIGH-RESOLUTION 3-D REFLECTION SEISMICS ON A TIDAL FLAT: ACQUISITION, PROCESSING, AND INTERPRETATION**

Shallow sub-surface structures may show strong lateral variations. These variations can usually not be described by a two-dimensional symmetry. Hence standard 2-D acquisition methods give a corrupted image of the sub-surface and correct processing of the data is impossible. In this chapter a method to acquire, process, and interpret high-resolution 3-D data is presented. The author of this thesis was mainly involved in the processing and interpretation of the data and the development of 3-D display- and picking algorithms.

## **2.1 INTRODUCTION**

It is generally accepted that complex geological structures require full 3-D data acquisition, processing, and display. 3-D seismics has the reputation to be expensive and to require large computers and thus be beyond the means of small university units. This is certainly correct for large-scale surveys as in prospecting for oil, but we show here that

---

This chapter has been published as:

Corsmit, J., Versteeg, W.H., Brouwer, J.H. and Helbig, K. 1987. High-resolution 3D reflection seismics on a tidal flat: acquisition, processing and interpretation. *First Break* 6 (1) 9-23.

shallow high-resolution surveys can be carried out in full 3-D technology at no more than nominal expenditure.

The survey described here was designed to test the possibility of expanding the mandatory field work to cover 3D seismics. It provided a starting point for the development of the necessary software and display technology. J. Corsmit and W.H. Versteeg (then students at Utrecht) were asked to develop the field technique, acquire a data set for test purposes, write the necessary expansions to the existing 2D processing package (Doornenbal and Helbig 1983) and carry out the preliminary interpretation. J. Brouwer and K. Helbig were involved in planning and supervision and are responsible for some of the display technology.

The acquisition phase lasted two weeks. Three people were continuously involved, but a routine survey of this magnitude could, in principle, be carried out by two people (a total of about 120 man-hours). The data were originally processed on a HP-1000 minicomputer. Processing was time consuming since it was combined with programme development. To reprocess the data on our current Gould PN 6000 super-minicomputer takes about 8 hours connect time (with known parameters). Interactive processing of a comparable new data set would require about 32 hours. Several of the illustrations were prepared on the Gould PN 6000.

## 2.2 LOCATION AND TARGET

The survey was carried out on the *Plaat van Oude Tonge* (Fig. 2.1), an intertidal shoal in the Eastern Scheldt inlet, where 2D surveys have been carried out since 1981 by students of the University of Utrecht as part of their field work (see Doornenbal and Helbig 1983). While most of the shallow features in the early lines are subhorizontal, lines 8102 and 8103 show an interesting dune-like structure at traveltimes between 15 ms and 40 ms (Fig. 2.2). This structure was the target of our survey. Since the two lines recorded in 1981 did not intersect - accessibility is restricted by the Grevelingen dam and a hardened causeway on the shoal itself - the detailed geometry of the structure and consequently its classification and probable origin were still uncertain. In particular, it was not clear whether the two anti-forms represented a single dune-like structure striking NW-SE or two separate features striking NE-SW. The latter strike appears to be more common in the area for the aeolian deposits of the Twente Formation (van Staalduinen et al., 1979).

## 2.3 EQUIPMENT

The equipment used in this survey was described by Doornenbal and Helbig (1983). The source was a 30 kg steel ball, dropped from a height of 3 m onto a steel plate of about

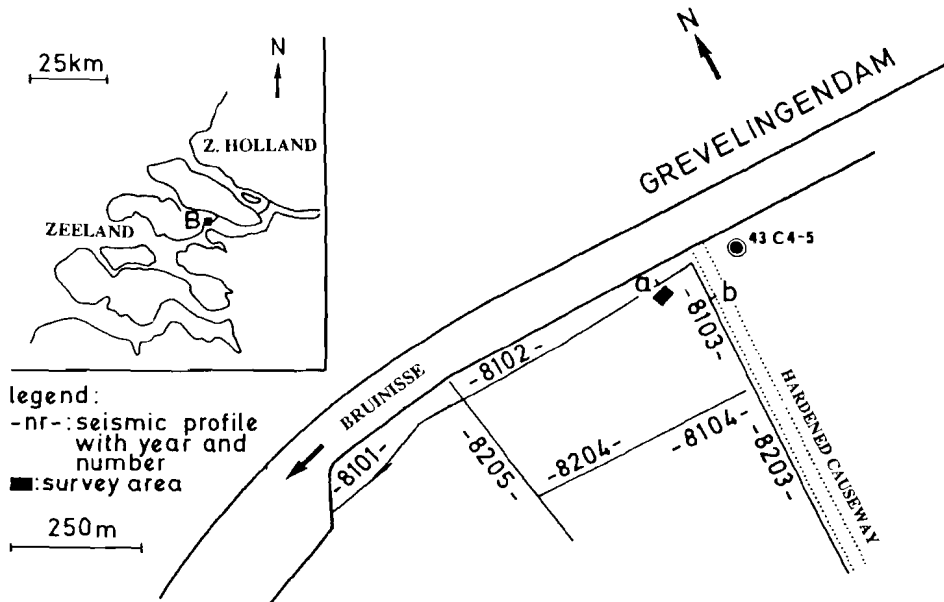


**Fig. 2.1.** Location of some 2-D lines shot in recent years on the Plaat van Oude Tonge and borehole location 43 C4-5. The markers a and b, indicated on line 8102 and 8103, correspond to the markers on the profiles in Fig. 2.2. Inset: Topographical map showing the location of the survey area in the south-western part of the Netherlands.

30 kg mass. Under the survey conditions the signal observed during the first 50 ms after the impact has a peak frequency of about 250 Hz. Twenty-four 100 Hz electrodynamic geophones (GS 100/QSC 27) were laid out simultaneously. A simple roll-along switch allowed the selection of twelve consecutive channels. The recording unit was a twelve-channel enhancement seismograph (Nimbus ES 1200) with 1024 words of 10 bits each per channel, a cathode ray tube display, analog output for hard copy, and data storage on magnetic cartridge tapes. The storage unit did not have read-after-write or field-playback facilities, so that data quality and the field performance had to be judged on the CRT or paper display. The recording unit was triggered by a pulse from a piezoelectric switch built into the impact plate of the source.

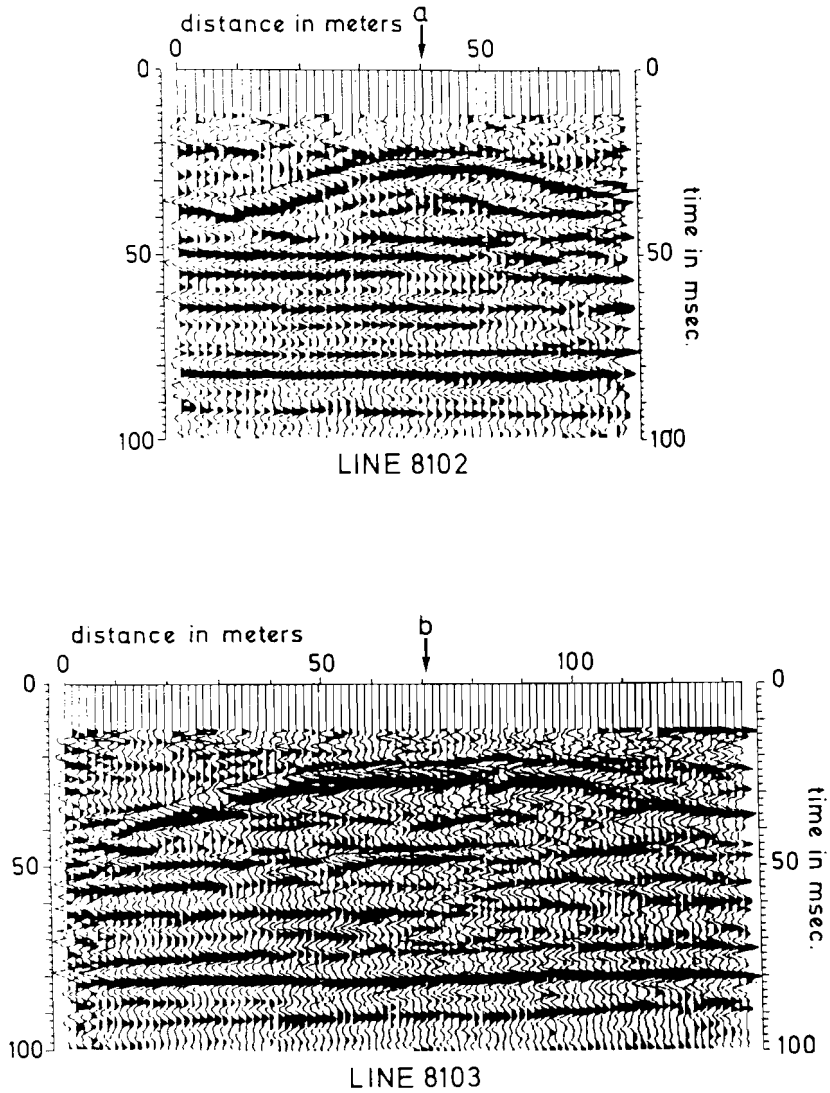


**Fig. 2.2.** High-resolution stacked timesection, shot in 1981. Survey parameters for these sections were: record length 200 ms, sampling rate 0.2 ms, six-fold CDP-coverage, 12 recording channels, off-end spread, geophone spacing 3 m, one geophone per station, near-trace offset 15 m. The location of markers a and b, is given in Fig. 2.1.



## 2.4 FIELD LAYOUT

### 2.4.1 General Considerations

The ideal 3D survey should be designed so that:

- the data points (i.e. the "nominal" reflection points in a vertically inhomogeneous medium) of different source-receiver pairs exactly coincide so that binning is unnecessary;
- the common data points (CDP's) lie on a regular - preferably square - grid;
- each CDP gather consists of the same number of traces;
- each CDP gather has a range of source-geophone distances that are distributed fairly regularly in the  $x^2-t^2$  domain to allow reliable determination of the stacking velocity by least-squares regression;
- the source-geophone azimuths are evenly distributed to allow the determination of azimuth-corrected stacking velocities;
- any chosen field technique can easily be adapted to different targets.

### 2.4.2 Considerations For 3D Surveys On Intertidal Shoals

On intertidal shoals the low-water period lasts about six hours. Therefore

- the survey grid must be relocatable after high-water;
- no equipment can be left in the survey area during high-water;
- since it takes one to two hours to move a complete 24-channel layout with two persons, moving the geophone spread within a low-water period is inefficient and should be avoided.

## 2.5 IMPLEMENTATION

A square grid of data points was generated from building blocks based on a regularly spaced strip, twelve geophones long and two geophones wide (Fig. 2.3). The geophone spacing is used as the unit of distance in the following discussion. The spacing of data points is, of course, half a distance unit.

Twenty-four source locations with an interval spacing of two distance units were combined with these 24 geophone positions. The resulting 576 source-receiver points are located in two strips of 13 by 3 distance units. 48 data points at the narrow ends of the

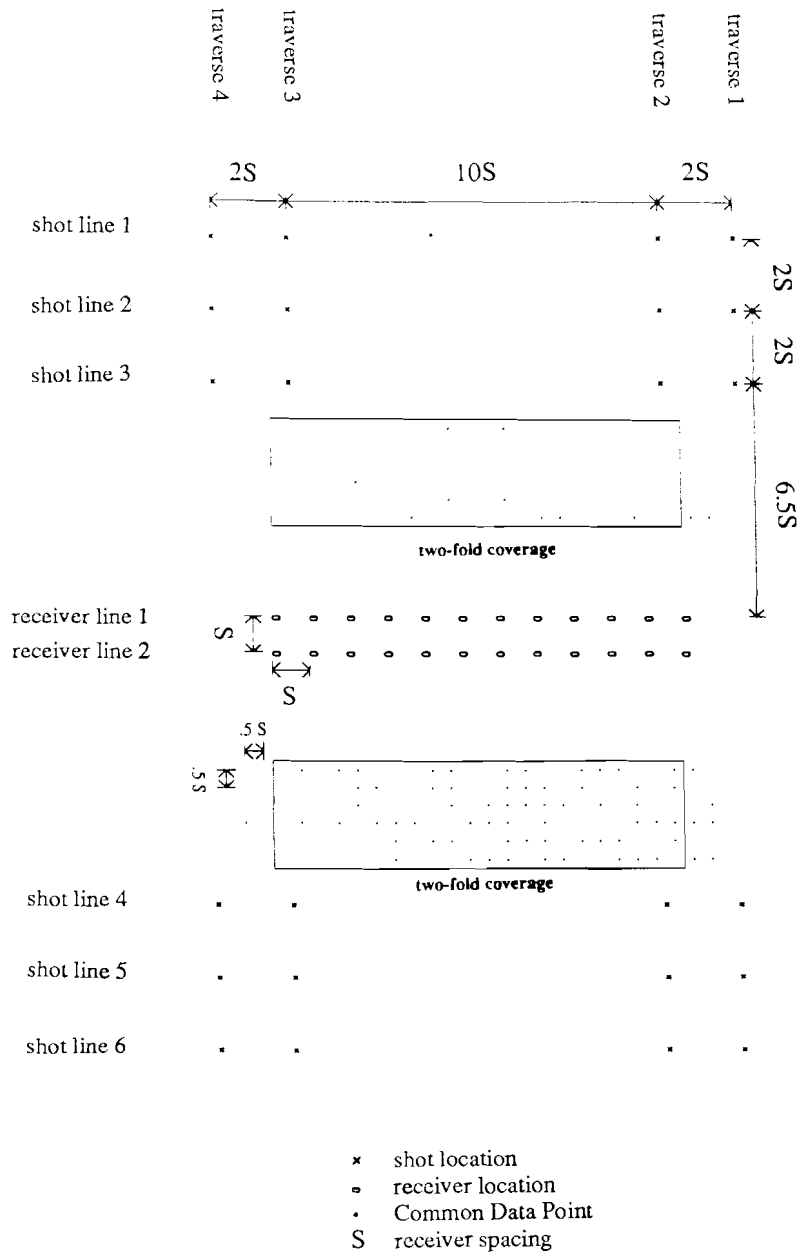


**Fig. 2.3.** Basic field geometry. The geophone stations are located on two parallel lines (the receiver lines). The shot locations are placed on four traverses perpendicular to the receiver lines. Each shot location is used twice, once for each geophone spread.

strips are singly covered; the 264 data points in the central parts of the strips have two-fold coverage. Each source location was used twice with each geophone spread, once with geophones 1 to 12 and once with geophones 13 to 24. With a 24-channel acquisition unit these observations could have been obtained as a single record (Fig. 2.4).

Once the 576 traces were recorded, the entire layout was shifted by 3 distance units in the direction at right angles to the orientation of the geophone spreads to expand the area covered by the square grid of data points. After the recording of three layouts, a contiguous doubly covered area measures 22 data points in the direction of the geophone spread and 36 data points in the direction of the shot traverse, and is lined on either side by two lines of 36 singly covered data points.

A further shift of the entire layout in the shot traverse direction results in a central four-fold grid. This four-fold grid consists of unit areas of 22 by 6 data points. The corresponding unit data volumes are the basic units for data processing. The azimuths within the four-fold area are reasonably distributed.

The grid of data points belonging to one strip consists at both ends of three unit areas of double coverage. If full coverage of the entire grid is wanted, the survey should start and end with shooting the first and last three geophone spreads from one side.

Shifts in the geophone spread direction by 12 distance units result in a homogeneous four-fold coverage since the two-fold lines at both sides of the strip overlap precisely.

## 2.6 FIELD PARAMETERS AND DATA ACQUISITION

In the summer of 1983 a unit data volume was acquired for test purposes. This preliminary survey was set out to test field performance and timing, to establish standard parameters (vertical stack, sampling rate and recording time, and amplification factor), to verify that for the chosen distance unit the reflections from the target depth occurred in the "window" between first arrivals and the surface waves, and to obtain test data for the software that had been developed.

The following parameters were chosen: distance unit 2 m (i.e. geophone spacing 2 m, data point spacing 1 m, source point spacing 4 m, offsets between 13 m and 34 m), three-fold vertical stack, sampling rate 0.2 ms, recording time 204.8 ms, a fixed amplifier gain setting of 40 dB (factor 100) throughout. No acquisition filter (other than that provided by the 100 Hz geophones) was used.

The survey took place in the late autumn of 1983 during nine low-tide periods spread over two weeks. With a total of 288 source points, 792 traces were recorded corresponding to 22 by 36 uniformly four-fold data points, arranged in a strip oriented at right angles to the supposed strike of the target structure. Positioning accuracy was maintained by using a theodolite and a measuring chain, and the field operations were documented carefully.

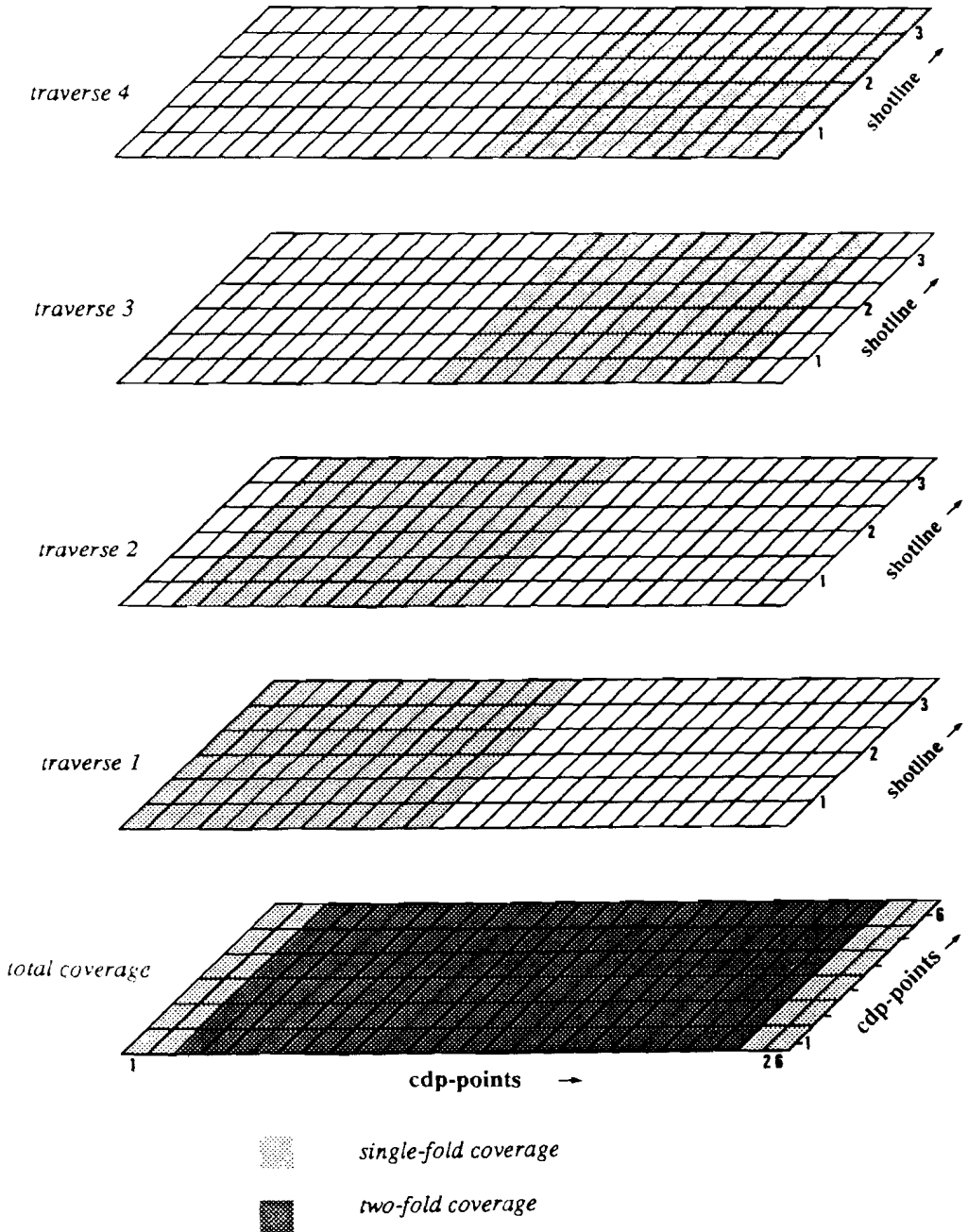


**Fig. 2.4.** The source-receiver configuration generates two areas of 26 x 6 grid points. In each area we find a square grid of 22 x 6 two-fold covered CDP's. The grid points at the boundaries of each area have single fold coverage.

## 2.7 PROCESSING

The processing sequence consisted of:

- reading field cartridges into a data base on standard tape;
- sorting into CSP gathers (Fig. 2.5) and generating headers containing information on field parameters and geometry (optional: display of CSP gathers);
- muting and trace editing;
- suppression of surface waves and high-frequency noise by frequency filtering;
- deconvolution;
- construction of CDP gathers (Fig. 2.6);
- determination of the stacking velocity function by optimisation of "constant velocity stacks". Early in the processing the dependence of the stacking velocity on the apparent dip (i.e. on azimuth) was investigated by using "common azimuth gathers" (Fig. 2.7). No significant azimuth effect was detected, most likely because the accuracy of velocity determination at four-fold coverage was only 10%. Therefore the azimuth dependence was not taken further into account.

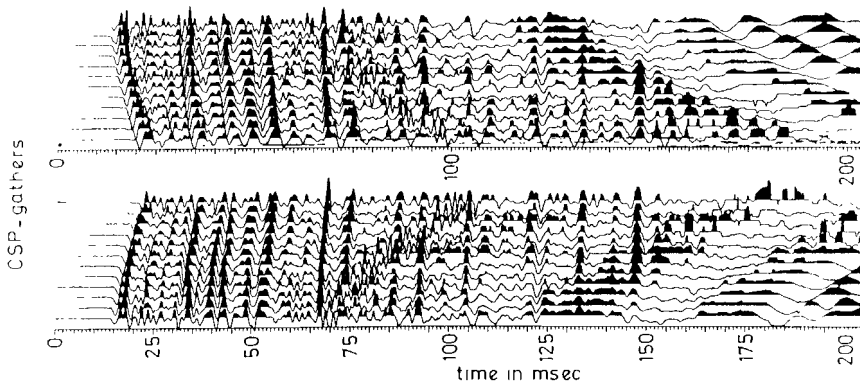


**Fig. 2.5.** A Common Shotpoint Gather for both 12-channel geophone spreads in the same strip. The trace sequence versus distance is opposite in the two spreads. Between 65 and 105 ms a relatively slow event of high frequency can be distinguished. This is the soundwave through the air. The low-frequency noise is the groundroll.

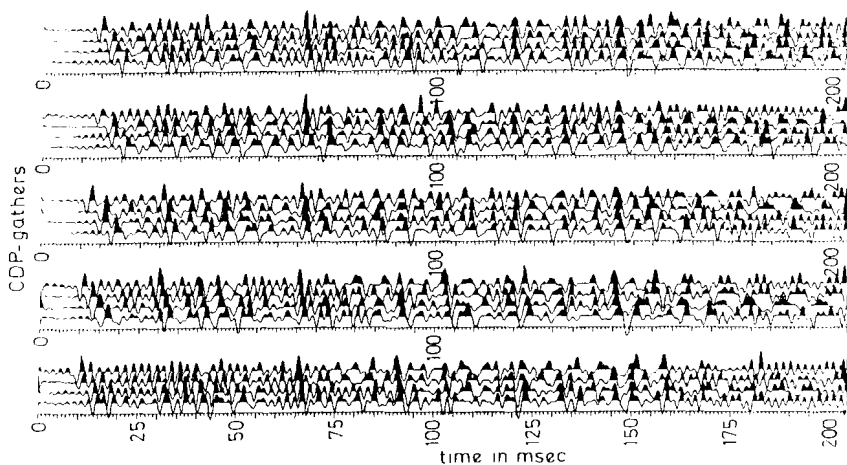


**Fig. 2.6.** A few CDP-gathers after muting, bandpass filtering (120-550 Hz) and deconvolution (spiking).

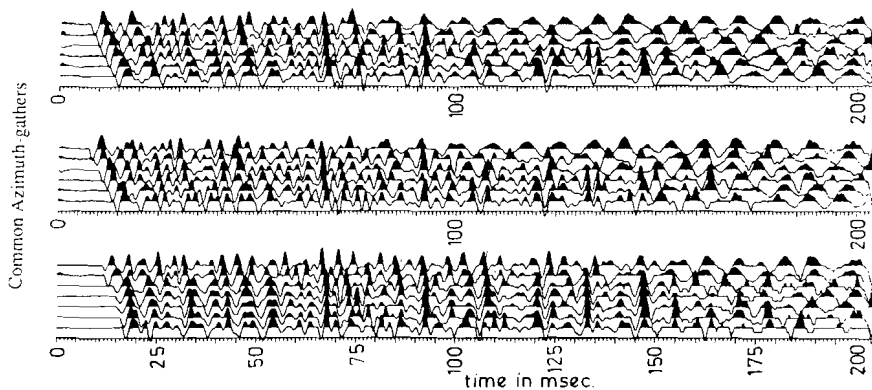


**Fig. 2.7.** Set of common azimuth gathers. Design criteria within such gathers are: preferably a regularly spaced and large range of offsets, variation in azimuth less than  $5^\circ$  and the selected traces as close to the central CDP as possible. Each displayed gather in this figure has the same central CDP. The azimuths of the displayed gathers vary over nearly  $40^\circ$ .

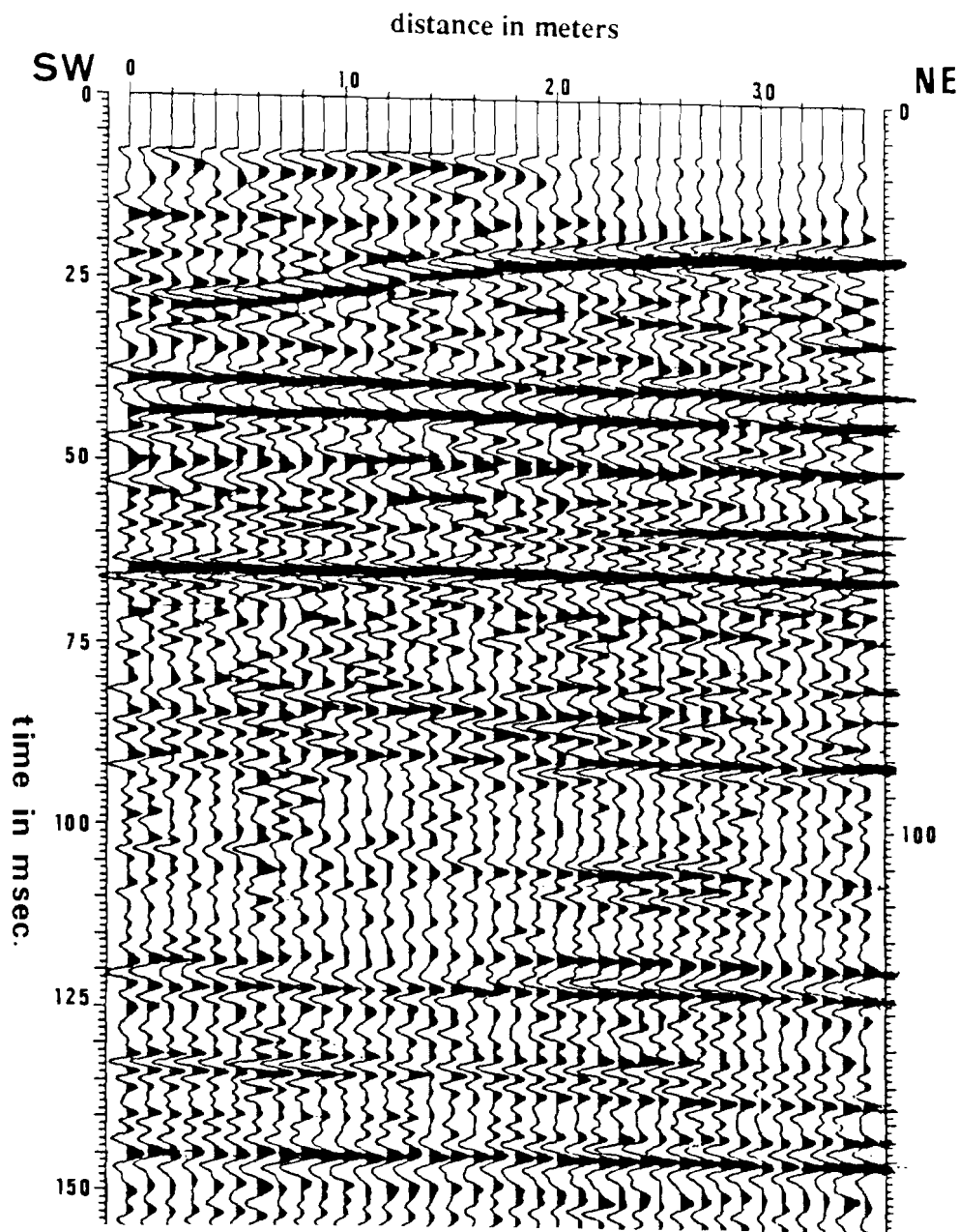


Fig. 2.8. A vertical timesection through the data volume, perpendicular to the expected strike of the dune.

## 2.8 DISPLAY

3D surveys are a particular challenge to the display technology: the interpreter has to see the data from different aspects to understand the geometrical relations between different events. The original software package contained three plotting modes for the display of the  $x,y,t$ -data volume:

- vertical time sections through the data volume with arbitrary location and azimuth (Fig. 2.8);
- horizontal sections through the data volume at arbitrary times (time slices) as contours of equal amplitude (Fig. 2.9);
- time maps of arbitrary reflection events as iso-time contours ("horizon slices") based on automatic picking routines (Fig. 2.10).

After the completion of the investigation, an additional set of 3D display utilities was written for use on a colour terminal. These utilities permitted a fast and flexible interpretation of the data set as described above. The following display modes became available:

- the stereometric combination of two arbitrary perpendicular vertical time sections and a time slice or horizon slice (Figs. 2.11 and 2.12). In these figures amplitudes are coded according to the displayed grey scale.
- the stereometric combination of the four limiting time sections and arbitrary time slices or "horizon slices" (Figs. 2.13 and 2.14).
- the stereometric display of a stack of time slices or a stack of "horizon slices" (Figs. 2.15 and 2.16).

There are many display methods. The strength of 3D seismic display methods is not found in any single method but in the possibility of looking at the data set in a number of ways.

## 2.9 RESULTS

In Fig. 2.8 the top of the dune is represented as a strong reflector with negative reflection amplitude. This apparent negative amplitude is caused by the negative polarity of the source wavelet. Figure 2.14 shows the shape of the dune in three dimensions. A shift in arrival time is introduced by picking the negative peaks as representing the top of the dune instead of the onset of the reflected wavelet.

It can also be seen that the amplitude decreases at the flanks of the dune. This is illustrated by the change in grey level along the flanks of the dune (Fig. 2.14). The change



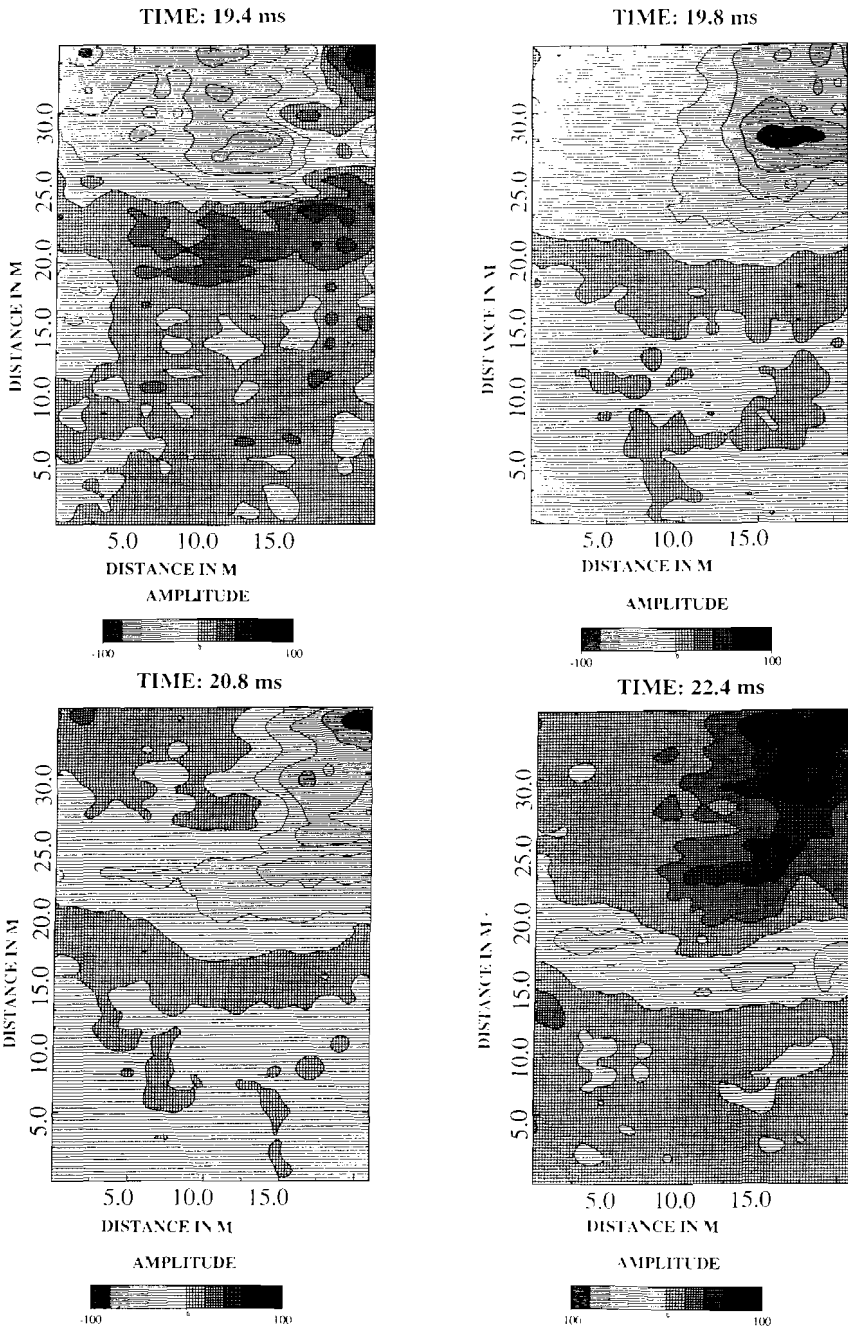


**Fig. 2.9.** Timeslices ("horizontal" cut through the 3-D data volume). For each slice the amplitudes are scaled between -100 and 100. The following relative amplitudes are plotted according to the shading on the linear scale bar.

in amplitude is partly caused by geometrical spreading and a change in dip. Nevertheless, the remaining amplitude decrease must be due to changes in the contrast in seismic impedance, probably caused by changes in grain size, sorting and degree of water saturation.

The time slices in Fig. 2.9 clearly show the orientation of the dune. Its main axis strikes N35°W. This is perpendicular to the strip direction of the acquisition geometry.

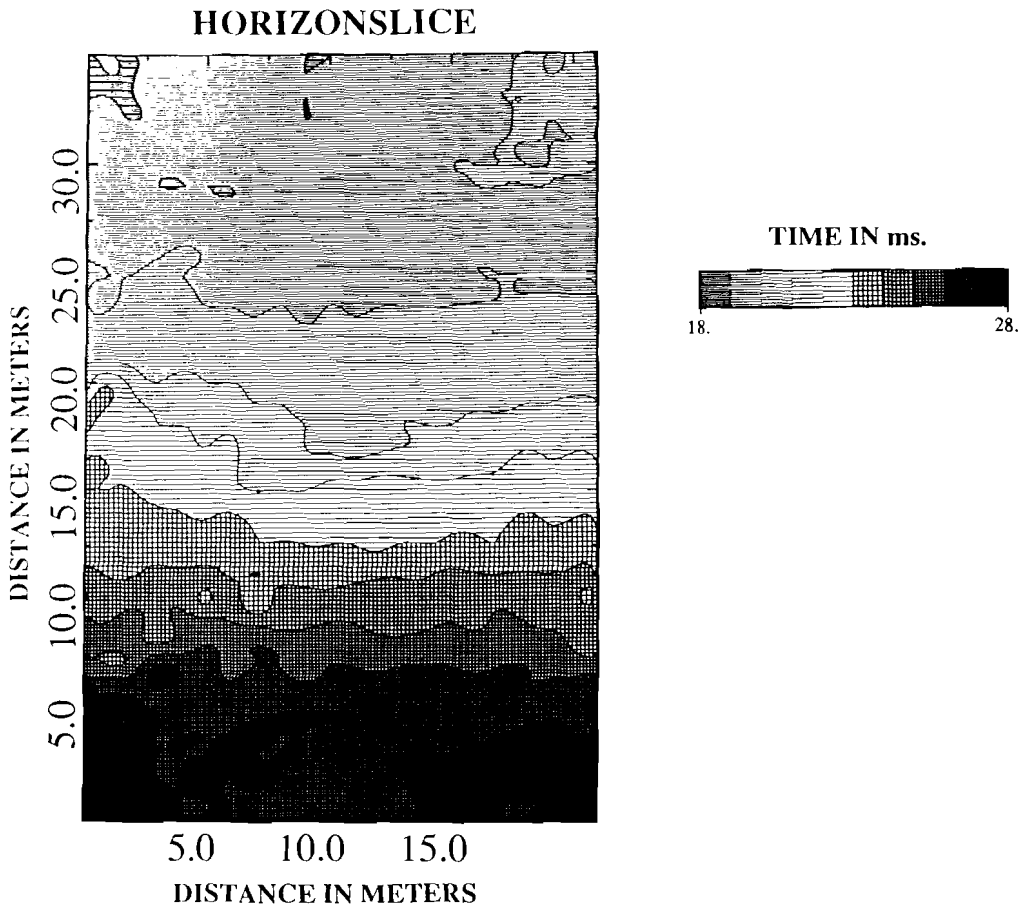


**Fig. 2.10.** A time map of the dune. In this figure the time of the negative reflector is plotted in milliseconds from 18-28 ms according to the shading on the linear bar.

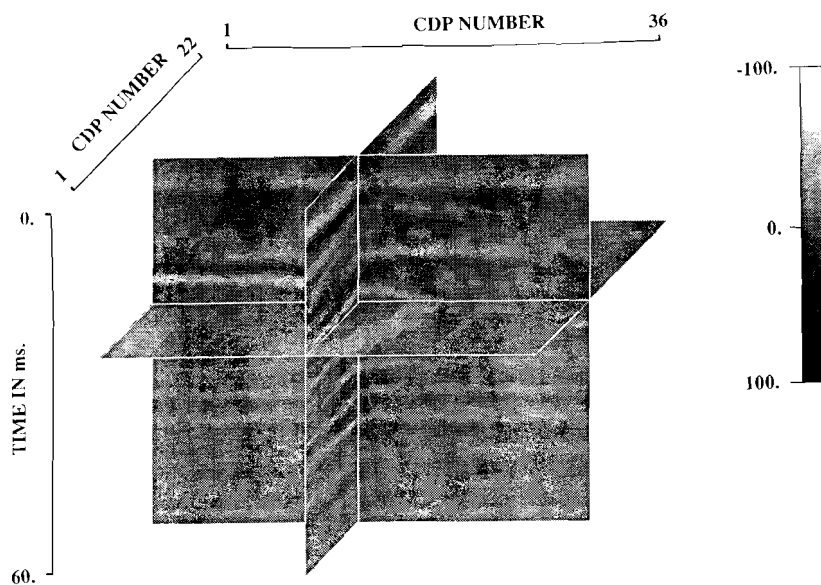


**Fig. 2.11.** Stereometric combination of two arbitrary perpendicular vertical time sections and a time slice. Amplitudes are scaled between -100 and 100 according to the displayed grey scale.

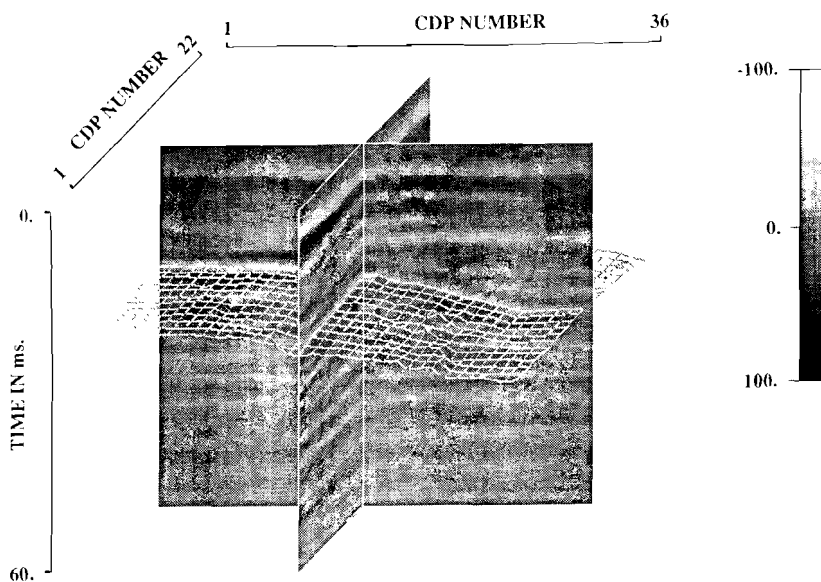


**Fig. 2.12.** Stereometric combination of two arbitrary perpendicular vertical time sections and a horizon slice.

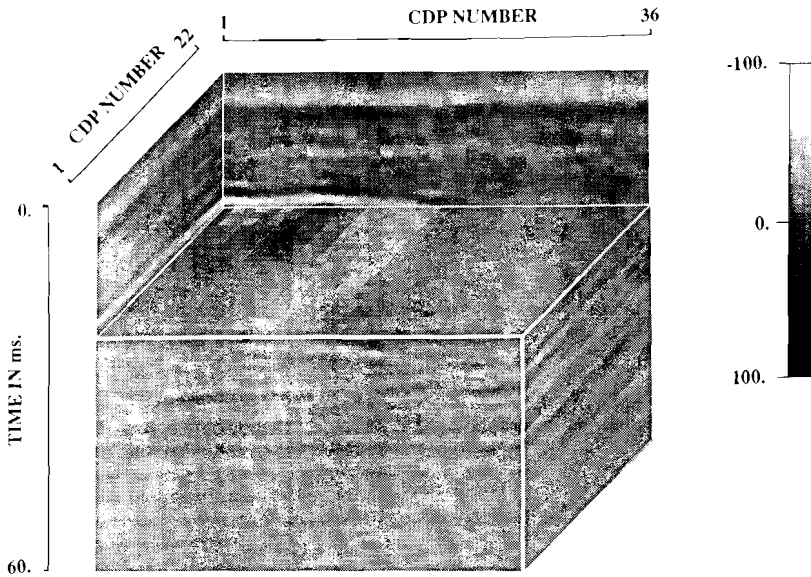


Fig. 2.13. Stereometric combination of the four limiting time sections and an arbitrary time slice.

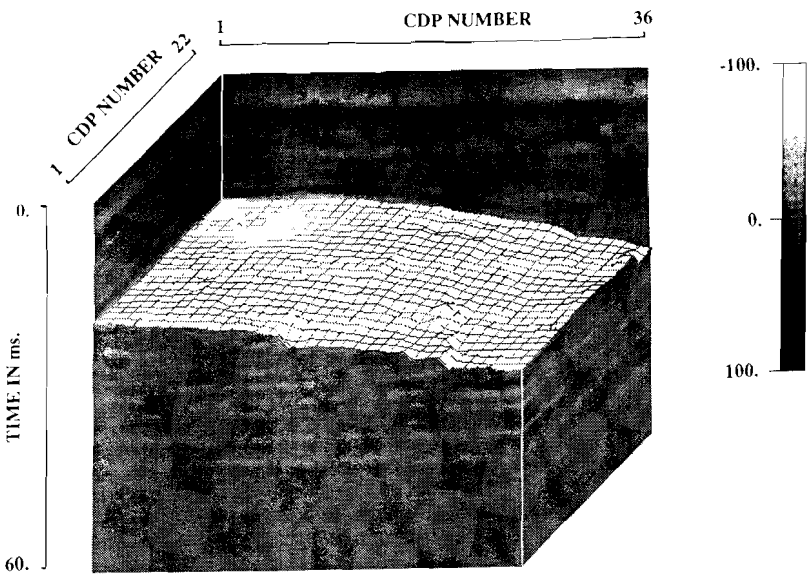


Fig. 2.14. Stereometric combination of the four limiting time sections and an arbitrary horizon slice.

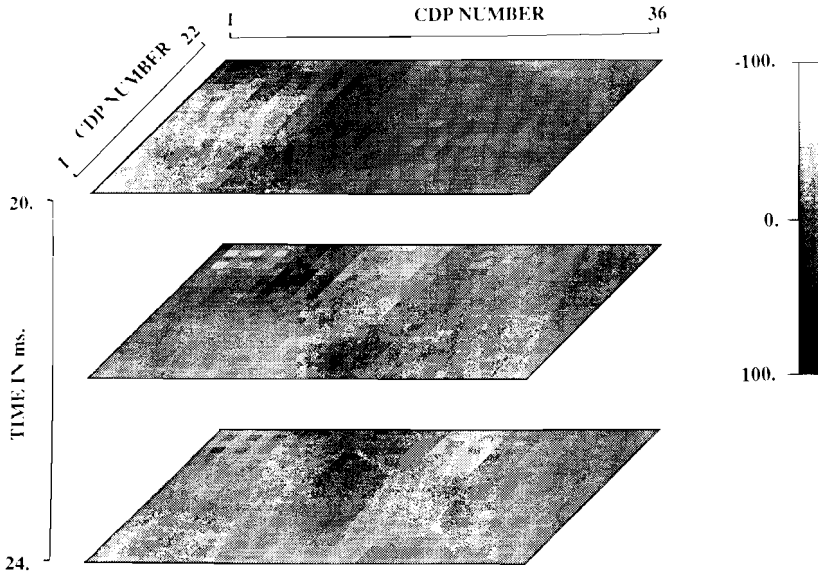


Fig. 2.15. Stereometric display of a stack of time slices.

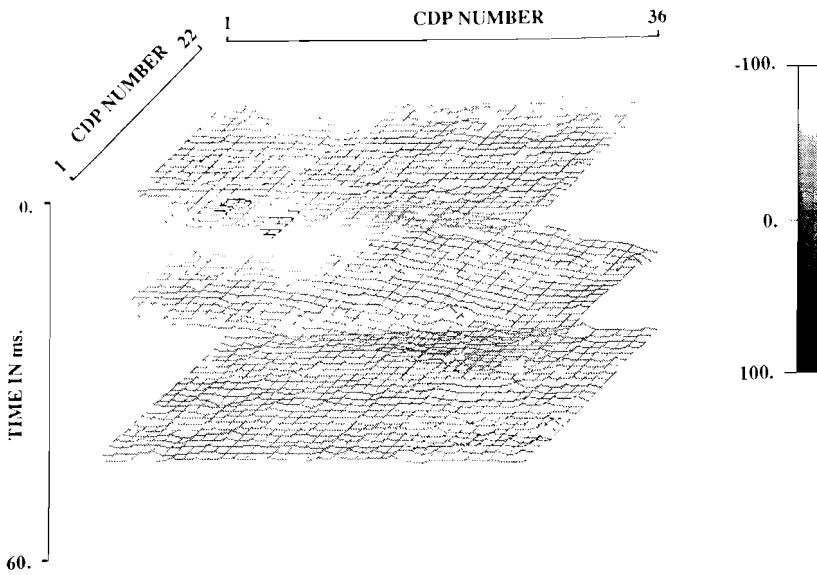


Fig. 2.16. Stereometric display of a stack of horizon slices.

## 2.10 GEOLOGICAL INTERPRETATION

Geological information about the survey area came from a schematic stratigraphic column that was compiled during an extensive study of the regional geology of the Province of Zeeland (van Staalduinen et al. 1979). Detailed information was obtained from a shallow borehole near seismic line 8103 (for location, see Fig. 2.1). The geological formations that can be expected in the seismic data are described in Fig. 2.17.

The time section of Fig. 2.8 served to fit the seismic data to the geology. Clear events can be recognized in the first 150 ms. At 65 ms an abrupt change in reflection strength and reflector configuration can be seen. Just before 65 ms we see parallel, discontinuous reflections with moderate amplitudes. In addition, some bifurcating and undulating reflections are found. After 65 ms the reflections become weaker. The 65 ms boundary can be interpreted as the top of the Maassluis Formation. The strength of the reflection can be explained by a depositional hiatus after the deposition of the Maassluis Formation.

Between 38 ms and 65 ms many parallel reflections of variable continuity and amplitude are found. These reflections have been identified with the Tegelen and Eem Formations (Fig. 2.17). A distinction between these two Formations was not possible from the seismic record.

The base of the Twente Formation is found at 38 ms. The top of this Formation is a buried-dome unconformity capped by the Westland Formation. We interpret this unconformity as representing the top of a dune. The reflections in the Twente Formation are curved and of high amplitude, while those of the Westland Formation are mainly horizontal and weak. The deepest reflectors of the Westland Formation show clear onlap features.

## 2.11 CONCLUSIONS

These acquisition and processing techniques resulted in data that allowed detailed interpretation. The high resolution reveals some internal structures in the dune. The 3D figures show some relief in the flanks of the dune. These structures may have been caused by erosion from surface water run-off.

The flank of the dune strikes N35°W. This is in contradiction with the general NE-SW trend of the ridges of the Westland Formation. Subsequent surveys have shown that the N35°W trend of the dune is consistent over a larger area and is not due to the small scale of this survey.

Though the data set is small by any standard, the project has demonstrated that 3D acquisition and processing lies within the reach of a department with limited resources. However, even at this small scale the acquisition is too time consuming to make it part of the curriculum, since mandatory assignments must correspond to a reasonably steep part of the "learning curve". On the other hand, the tedium of a full week of routine data

CHRONO-STRATIGRAPHY		BOREHOLE 43 C4-5	LITHOSTRATIGRAPHY	
QUATERNARY	HOLOCENE			Westland Formation Sequence of fine to coarse sands with intercalations of clay and peat layers. These sediments were deposited in tidal channels and on tidal flats during various transgressive phases.
	PLEISTOCENE	Lower	18 m	Twente Formation Aeolian deposits, known as coversands. Through horizontal lamination, these medium-fine sands are assumed to have been transported by storms forming a system of SW-NE trending ridges. Thin loam layers may be intercalated in well-sorted material.
			24 m	Eem Formation Shallow marine, beach, estuarine and fluvial deposits related to the rivers Rhine, Meuse and Scheldt. Composition: medium-coarse to very coarse sands with intercalations of clay or gravel. These sediments may be over- or underlain by peat.
			26.5 m	Non-deposition
	Middle			
	Upper	26.5 m	Tegelen Formation Fluvial equivalence of Maassluis Formation. Medium-fine to coarse sands with gravel and clay intercalations as lenses or layers. They were deposited as channel fill in a broad fluvial channel with E-W trend. Dehydration resulted in strong compaction.	
			Maassluis Formation Marine nearshore deposits, coarse and fine sands containing shell fragments with some intercalated sandy clay beds or clay lenses. During the regression following their deposition dehydration resulted in enhanced compaction.	

Fig. 2.17. Stratigraphic column of Quaternary formations and facies, including information from borehole 43 C4-5 (van Staaldunen et al. 1979).

acquisition is likely to be accepted by students who have a stake in the results. Without a breakthrough in automation the acquisition of 3D data will remain a thesis assignment.

Even then the question remains whether other university departments could follow our lead. The paramount requirement is a suitable survey area comparable to the tidal flats. There should be no weathered layer, the ground should provide sufficient resistance to surface impacts or small explosions so that high-frequency signals can be generated by simple means, and the area should be easily accessible in the technical and the legal sense. Under favorable conditions of sedimentation beaches (below the high-water line) should

have such properties. However, the area should also be interesting scientifically so that the seismic survey does not degenerate into a laboratory experiment that, by accident, is carried out in the field.

If a suitable survey area exists, only minor difficulties remain. Any enhancement seismograph with at least twelve channels and permanent digital storage will do. Together with cables, geophones, a self-built source and some means of transportation the equipment currently comes to not more than 60000 US\$. The software we have used has evolved slowly, so that the effort is not easily estimated. If it had to be done again we would budget eighteen man-months, twelve for the basic (2D) package, two to three months for the 3D extensions, and a similar time to develop the display package. Most of our programmes are written in FORTRAN (a few exceptions are subroutines written in C) and the whole package runs under UNIX on a 32-bit computer. Graphical output is possible on a large Versatec plotter, a pen plotter, a laser printer, and for interactive work on colour terminals or on the semi-graphical Qume QVT-211GX.

#### ACKNOWLEDGMENTS

The authors have to thank many people who made this survey possible. Especially J.W.H. Dankbaar for his critical remarks on the geophysical aspects of this survey and J. Tempels who kept the equipment going in all circumstances and who arranged transportation and accommodation.

#### 2.12 REFERENCES

- Doornenbal, J.C. and Helbig, K. 1982. High-resolution reflection seismics on a tidal flat in the Dutch delta: acquisition, processing and interpretation. *First Break* 1 (5) 9-20.
- van Staaldin, C.J., van Adrichem Boogaert, H.A., Bless, M.J.M., Doppert, J.W. Chr., Harsveld, H.M., van Montfrans, H.M., Oele, E., Wermuth, R.A. and Zagwijn, W.H. 1979. The geology of The Netherlands. *Mededelingen Rijks Geologische Dienst* 31-2, 9-49.



## *Chapter 3*

# **ONSHORE HIGH-RESOLUTION SEISMIC PROFILING**

The method of high-resolution seismic profiling showed excellent results on tidal flats. However, adaptation of the method for onshore exploration involves more than the choice of a different location. This chapter gives a general overview of the acquisition and processing of onshore shallow seismic data. In addition some field examples are presented. This chapter was written in cooperation with Drs. P. Jongerius.

### **3.1 INTRODUCTION**

In the last few years seismic profiling has been introduced in the exploration of the shallow subsurface (Doornenbal and Helbig 1983, Hunter et al 1984, Jongerius et al 1987, Steeples and Knapp 1985). Several applications have been proposed, e.g. in groundwater exploration, civil engineering and mining. Shallow seismic profiling is extensively described, but actual field data are poorly documented. This inaccessibility of field examples may be the main problem the average geoscientist encounters in rating shallow seismic profiling at its true value. It also may be the major reason why shallow seismic profiling has not yet been commercially accepted on a large scale and remains as research subject.

At the University of Utrecht shallow reflection seismic exploration, originally set up as a field course on the tidal flats of Zeeland (Doornenbal and Helbig 1983), has become a valuable tool in the study of recent tidal deposits (Jongerius and Helbig 1988). A high frequency source, suitable geophones, and consistent quality control in the field are the basic ingredients for the acquisition of high-resolution seismic reflection data. A method that works well on tidal flats was expected to work equally well on land. Thus, starting 1984, onshore-shallow seismic surveys were carried out by students and members of the

exploration geophysics department. However, differing surface and subsurface conditions influenced the data quality and adaptation of acquisition and processing techniques was necessary.

In this paper an overview is given of the onshore seismic activities at the University of Utrecht in the last 4 years. A brief discussion of basic seismic acquisition and processing techniques is given as a frame in which the specific problems we encountered in the acquisition and processing of onshore data will be emphasized. In addition a series of examples of onshore shallow seismic surveys of different quality are presented.

A part of the seismic surveys presented are data collected by students during their course in exploration geophysics at the University of Utrecht. The other examples are studies carried out by the authors as part of a research on the applications of high-resolution seismic profiling. All examples contain a short description of the subsurface build-up with emphasis on possible seismic reflectors. The results are presented as time sections with a short description of acquisition and processing (processing is in most examples a major key to interpretable results). A short conclusion is drawn in each example.

The aim of this research was not to solve geological problems, but to test the seismic response in different surface and subsurface conditions without a specific target. We realize that the examples presented are incomplete because of the lack of well-data or VSP needed for a reliable geologic interpretation. However, for a rough interpretation of the seismic sections lithologic core data and knowledge of the regional geology were available in all surveys described and used to predict the seismic response qualitatively as well as quantitatively. Attention was paid to the seismic quality of the studies in relation to the field conditions and acquisition parameters.

## 3.2 ACQUISITION

### 3.2.1 Introduction

Seismic data acquisition can be described by three basic constituents.

- field equipment; the hardware needed to perform data acquisition.
- field setup; spread geometry, timing parameters, amplifier settings, etc.
- field conditions; surface conditions, noise elements, environmental influences, etc.

As we have little influence on the field conditions, improvement of data quality should be found in the adaptation of field equipment and setup. Although the equipment and setup are described separately it should be emphasized that it is the interaction of the three constituents of seismic data acquisition that determines the quality of the field data.

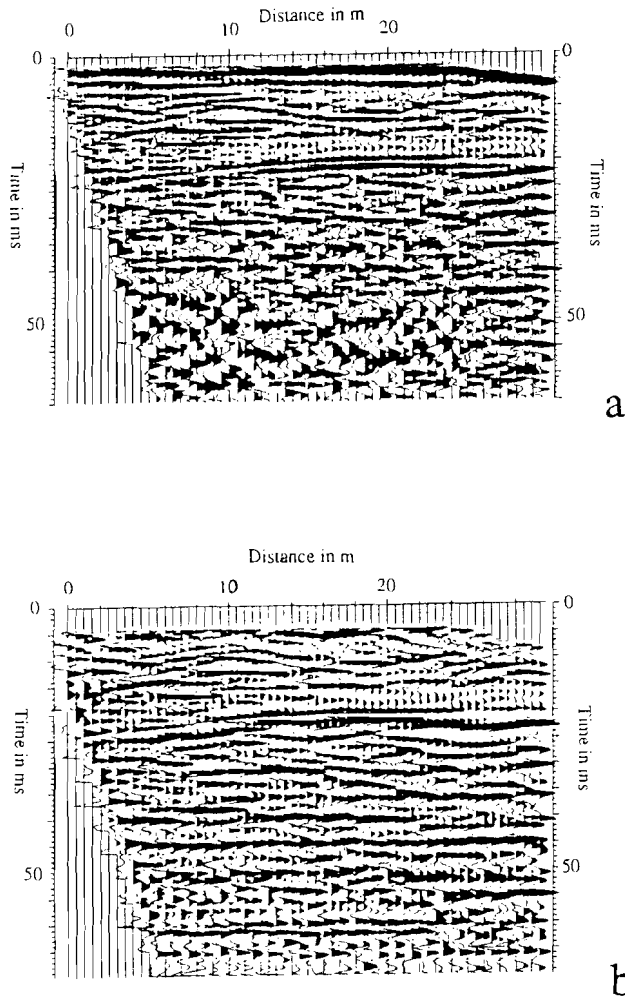


**Fig. 3.1ab.** Two stacked sections (data acquired at the "plaat van Oude Tonge") showing changes in characteristic frequency in the same seismic profile as a function of source energy. In Fig. 3.1a (top) a high-frequency source was used.

To illustrate this figure 3.1 shows the stacked sections for different sources under almost ideal field conditions. It can be seen that an increase of the frequency of the source signal immediately affects the data quality. Resolution increases for shallow structures.

Deeper reflections become less clear due to a decrease in source energy. On the other hand less favorable field conditions might completely obscure improvements in data quality as expected from changes in equipment and setup.

### 3.2.2 Field Equipment

In figure 3.2 the field equipment is shown as part of the "Seismic Chain". Based on this concept a description is given of the specific equipment used. In addition we discuss what improvements in data quality can be expected from changes in field equipment.

#### 3.2.2.1 Seismic Sources

The University of Utrecht started seismic data acquisition on tidal flats using a weight drop system as the source of seismic energy (Doornenbal and Helbig 1983). The spectrum of the source was satisfactory and the energy was sufficient to achieve the desired depth penetration. Either higher frequencies or better penetration could be obtained by using different combinations of weights, baseplates, and dropping heights. Increasing the number of drops at one position was alternatively used to increase penetration depth. However, one has to be sure the source signal can be reproduced to preserve high frequency information. The last few years some field tests using a so called "shotpipe" were performed. This shotpipe was developed as an attempt to achieve better penetration by generating seismic energy beneath the weathered layer. On land seismic energy is sometimes captured in this layer due to a large contrast in seismic impedance at its top and base. Deeper reflections are relatively weak and are obscured by internal multiples in the weathering layer. Although some of these deeper reflections can be unveiled during the processing sequence, a significant improvement can be expected from new acquisition techniques. Figure 3.3 shows a comparison between field records acquired with the shotpipe and weight drop method.

At present only preliminary conclusions can be drawn with respect to the different sources used. In general, the weight drop method is still, as we see it, the best source to be used in high-resolution seismic data acquisition. Only on a few occasions on land the shotpipe has given slightly better results. This only happened under very difficult surface and subsurface conditions. In places where reasonable data quality is obtained with the weight drop source the shotpipe is not doing any better.

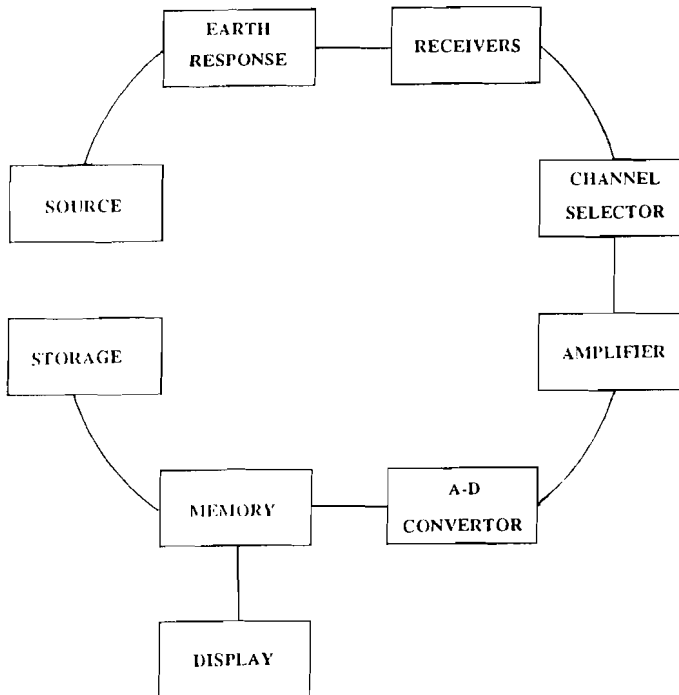


Fig. 3.2. Seismic chain.

### 3.2.2.2 Seismic Receivers

Signal frequencies generated and measured in high-resolution seismic data acquisition are, in general, an order of magnitude higher than those in seismic exploration for oil and gas (figure 3.4 shows the characteristic spectra of tidal flat data and land exploration data). As frequency decreases with increasing source energy, a high frequency source works at a much lower energy level than the sources in standard seismic exploration. Therefore, it is not at all obvious that standard seismic receivers should be used in shallow seismic exploration. The frequency response of those receivers can be disturbed within the frequency band of the data (spurious frequencies). Nevertheless, the receivers used in high-resolution seismic acquisition are standard geophones. Not because they are so good, but just because of the poor availability of alternative receivers (e.g. accelerometers etc.).

The frequency response of a geophone can be described by its natural frequency and

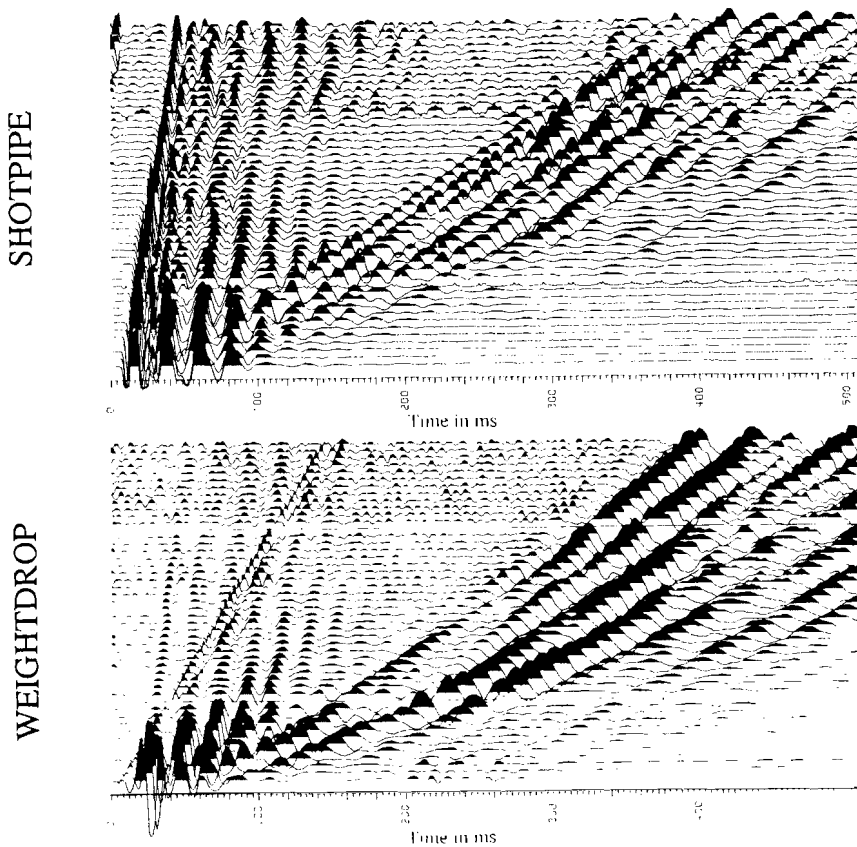
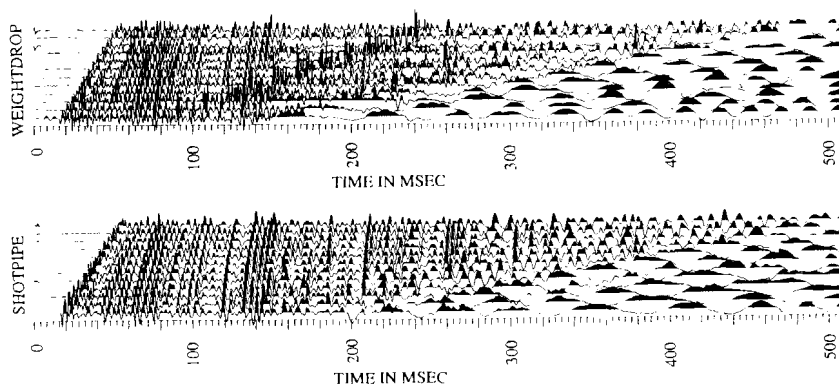


Fig. 3.3a. Comparison of weightdrop and shotpipe records on land.

its damping. The geophones we use vary in natural frequency from 10 Hz to 100 Hz. Geophones can be seen as high pass filters showing a low cut at their natural frequency. It is reasonable to use broadband seismic receivers in order to achieve full spectral coverage of the seismic signal. Afterwards, noise elements that differ in spectral bandwidth from the seismic signal can eventually be removed by using digital frequency filters. Thus the use of geophones with low natural frequencies might be suggested.

When signal-to-noise ratios are extremely low problems might occur in the simultaneous recording of noise and signal due to a limited range of the A-D converters. Either the noise level is too high to be digitized (clipping) or the signal level is too low. Of course this problem is most prominent when fixed point A-D converters are used. Under these conditions, and when frequency bands of signal and noise are sufficiently separated, it can be useful to perform some sort of analog filtering before data are being digitalized. Sometimes even the geophones itself can be used to perform such a frequency filtering. For instance, low frequency surface waves can be suppressed using geophones with



**Fig. 3.3b.** Comparison of weightdrop and shotpipe records on tidal flats.

relatively high natural frequency.

### 3.2.2.3 Cables and Interfacing

The total number of geophones used in the field was 24. The geophones are permanently connected to the cable using a waterproof sealing in order to avoid bad contacts. Especially in moist areas one could best use fixed connections although the geophones can not easily be exchanged in case of damage. In order to be most flexible in the choice of the field configuration we use cables with a small number of geophones per cable segment. Thus the 24 channels are distributed over 4 cable segments (6 geophones per segment).

The 24 field geophones are interfaced with the 12 channel amplifier unit by a home-made roll-along switch. Any series of 12 consecutive geophones can be selected and connected to the amplifier unit.

### 3.2.2.4 Seismograph, Storage and Display

All the surveys presented were carried out with an OYO McSeis 1500 enhancement seismograph except for the Portugal fieldwork (example 2) which was done using a

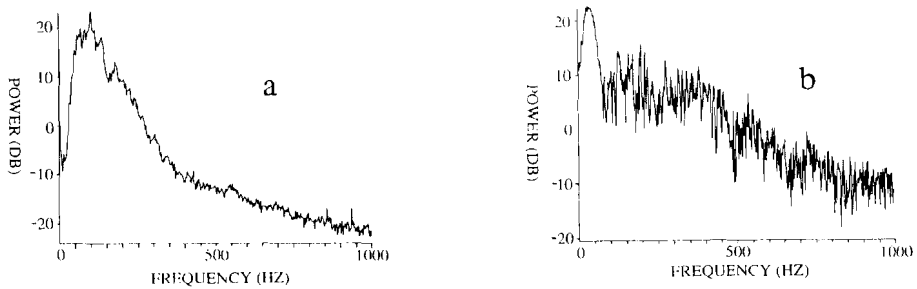


**Fig. 3.4.** Differences in spectral shape for seismic land data (left) and tidal data (right).

NIMBUS. The OYO McSeis uses a 12 bit fixed point A-D converter which causes some problems in amplitude resolution. The NIMBUS has only 10 bits resolution. Sampling rates for the OYO McSeis can be selected in a range from 50 microseconds to 5 milliseconds. The NIMBUS has somewhat different sampling rates. As the number of channels is usually small in high-resolution seismic acquisition, multiplexing is rarely necessary.

Storage of the data on the OYO McSeis is done on floppy disc (5 1/4", 360 kbyte, random access). The NIMBUS uses cartridge tapes (150 kbyte, sequential access). Especially when large data volumes are to be stored there might be need for a winchester disc, or a streamer tape unit (eg., one month of field work at 100 shots a day will add up to 250 floppy discs). The use of cartridge tapes is even more expensive (750 tapes are needed for the same fieldwork). A serious disadvantage of the NIMBUS is that data on tape can not easily be restored in the memory of the enhancement seismograph.

Since intensive processing of the data is foreseen, for which purpose the field processor is insufficient, we should have a fast way of interchanging data between field equipment and a more powerful computer. Transmission of data by means of a connection between the field processor and this computer using standard serial interfaces is time consuming. It takes eg. about 2.5 minutes to transmit 1 record from the OYO McSeis to another computer using the built in serial transmission facility (RS232). To transmit the whole survey mentioned above would take about 125 hours. Therefore, a better solution is to choose a storage medium that can be accessed both by the field unit and a more powerful computer.

The field display is one of the most important parts of the seismic equipment. Without a good display facility in the field it is impossible to perform the necessary quality control, select or adjust field parameters, or keep record of the changes in data quality due to e.g. weather conditions.



### 3.2.3 Field Setup

#### 3.2.3.1 Introduction

Field parameters like geophone spacing, initial offset, recording time, and delay time depend on a number of factors. Depth of the zone of interest, desired time- and lateral resolution, in combination with some pre-knowledge of the geology and the characteristic velocities and wavelengths of noise and signal influence the choice of the field configuration. The optimal field setup should give an unaliased sampled image of the total wavefield, both in time and space. Depth of interest and subsurface velocity distribution essentially determine the total sampling length (total record time and maximum spatial distance between shot and receiver). Apparent wavelength and frequency of signal and noise affect the sampling (sample time and receiver spacing). Rigdon and Hoover (1987), and Ongkiehong and Askin (1988), gave a consistent description of a general method to determine field parameters. The method they apply essentially supports the use of geophone groups in order to discriminate between noise and signal. Differences in apparent wavelength and velocity between signal and noise determine the actual group configuration. Inter-group spacing and initial offset can be chosen relatively independent of the need to suppress unwanted noise since this is done within the separate (source-receiver) groups. Depth of the zone of interest and velocity distribution within this zone determine the maximum useful offset.

Penetration depth and wavelength are essentially scaled by the same factor in high-resolution-seismic profiling thus resulting in a field configuration that is scaled likewise. Therefore, the total number of channels needed will not differ for standard and high-resolution seismic surveys. However, the actual number of channels available in high-resolution seismic profiling is relatively small (12,24,...). Usually only one geophone per group is used, since, for a fixed number of receivers, an increase in the number of receivers per group would mean a decrease of the number of groups. The use of single-geophone groups implicitly means that no wavenumber filtering is performed in the field. Applicability of the method described is questionable as far as shallow reflection surveys are concerned unless the number of recording channels is drastically increased.

One has to take into account that shallow reflections can exhibit apparent velocities that do not differ that much from the velocities of e.g. surface waves and ground-coupled sound wave. Differences in apparent wavelength between noise and signal will only occur for very small offsets.

#### 3.2.3.2 Offset

The seismic dataset consists of a number of characteristic wavetypes. In general we

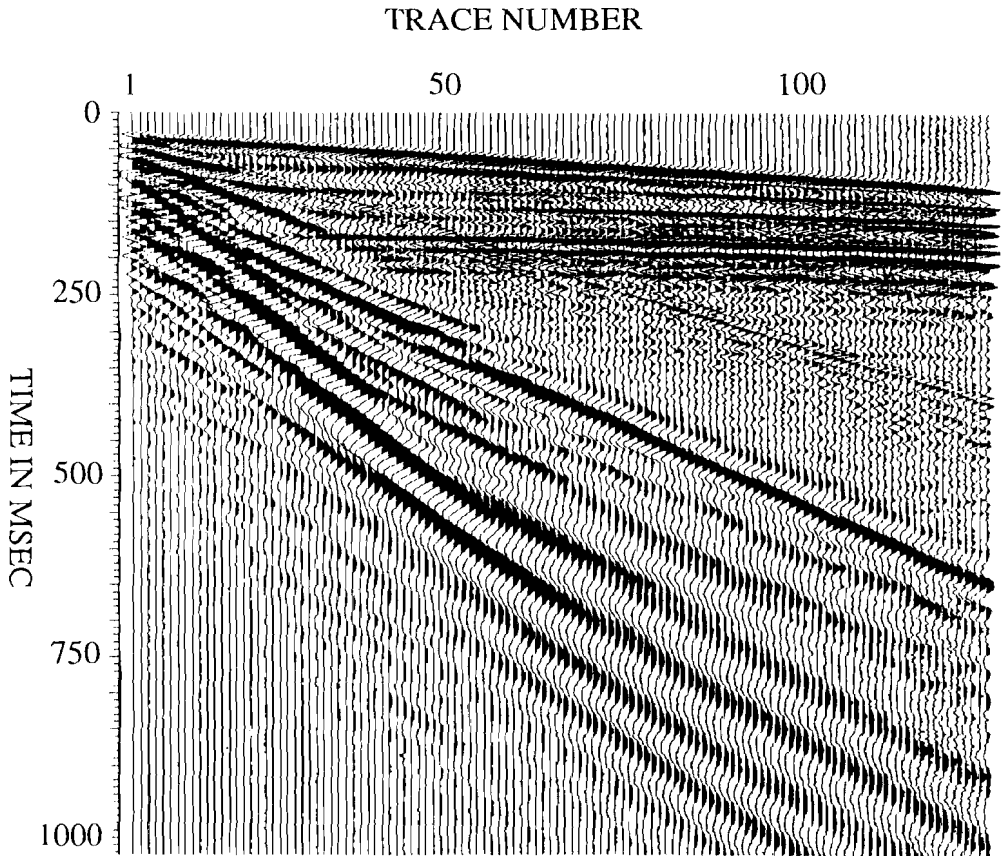


Fig. 3.5. Characteristic seismic shot record.

find P- and S-waves, surface waves, and the ground-coupled sound wave. By using vertical geophones we limit ourselves mainly to the recording of P-waves, surface waves, and the ground-coupled sound wave. For the moment we will forget about the S-waves. In practice field records resemble figure 3.5. The P-waves we are interested in are found in the wedge formed by the refracted waves and the surface waves. This zone can be seriously disturbed by the ground-coupled sound wave. The choice of the optimal initial offset depends on the severeness of the disturbance due to surface- and sound wave at small offsets and the loss

of shallow information due to large offsets. Any seismic survey should start with the determination of the velocities, amplitudes and frequencies of all the present wavetypes. Knowledge of these parameters in combination with the definition of the desired depth penetration will simplify a proper choice of the offset. The possibility to remove, e.g., surface waves afterwards by means of digital frequency or velocity filters may facilitate the choice of the optimal initial offset. However, the use of digital filters in the processing sequence also introduces limitations for the field configuration.

### 3.2.3.3 Geophone Distance

We limit ourselves to a brief discussion of some of the elements that influence the choice of receiver spacing. We implicitly assume the number of recording channels to be constant.

In order to obtain reliable stacking velocities, it is necessary to cover a large part of the reflection hyperbola. The use of short receiver distances possibly yields badly defined velocities. On the other hand, for large offsets the assumed hyperbolic shape of the reflection curve is violated.

The subsurface sampling has to be close enough to permit correct imaging of the dipping geological features. One has to take into account that the slope of a reflector is the derivative of time with respect to offset.

Large receiver spacing causes wave number aliasing. In general the distance between the receivers should not exceed half of the apparent wavelength of the signal. One has to take into account the problems that might occur in the processing sequence later on due to aliasing problems in the acquisition stage.

The number of shots needed to cover the area of interest largely determines the costs of a seismic survey. There might be reasons for reducing the number of shots and thus increasing shot separation. However, lateral resolution decreases and even aliasing might occur when shot- and receiver separation is increased, and CDP-coverage decreases if only the distance between shots is increased. It is a deplorable practice to determine field parameters based on a commercial point of view; one has to realize that high-resolution surveys are expensive and resolution has to be paid for.

The amplitude of the seismic signal decreases with travelled distance. In the presence of noise there is a maximum pathlength between shot and receiver where the signal can still be recorded. For given depth of interest this results in a maximum distance between shot and last receiver. Increasing the source energy will increase this distance but will also decrease the characteristic frequency and thus the resolution of our seismic signal. Repeating the shot at one place will also increase the source energy but slows down the daily progress and one has to be sure the source signal can be reproduced. A qualitative evaluation should take place in the field.

One of the most important factors in the determination of a suitable field configuration is the seismic response of the weathering layer. Changes in the thickness of this layer, its

velocity and the topography may cause drastic changes in the signature of the seismic data.

### 3.3 PROCESSING

#### 3.3.1 Introduction

Processing of seismic data consists of manipulating the original field data and presenting them in a way suitable for interpretation. Due to the increase in data volume and the development of new time-consuming processing methods the processing of seismic data has become a major part of seismic data handling. The need for preservation of high frequencies and shallow reflections in high-resolution seismic surveys has a serious drawback on data processing. Geological features of interest are at the limit of the seismic detectability. Small changes in acquisition conditions can completely obscure the geological structures in the dataset. Processing generally should compensate for all those changes in seismic data quality that have no cause in geological structures in the area of interest, but that are due to changes in, e.g., the weathering layer response.

#### 3.3.2 Basic Processing Scheme

The processing of high-resolution seismic data can best be described in relation to the processing of standard seismic data. Therefore we first give a basic scheme for seismic data processing in general and then highlight the specific problems that occur in the processing of high-resolution seismic data and specifically onshore high-resolution seismic data. A comparison between processing of tidal flat data and onshore data is made in figures 3.6 and 3.7.

Onshore field data can be described as the recording of a voltage  $A$  that is the band limited equivalent of particle velocity at given receiver location  $(x_r, y_r, z_r)$ . The signal at position  $x_r, y_r, z_r$  is induced by an initial signal generated by the seismic source. The actual size and shape of the seismic source is not taken into account. Defining a point source at position  $(x_s, y_s, z_s)$  thus implies that the distance between source and receiver should be large with respect to the characteristic wavelength of the source signal. All processing steps somehow deal with the problem of finding the geological model that caused this time response (1).

$$A(t; x_s, x_r, y_s, y_r, z_s, z_r) \quad (1)$$

1- A spread geometry with shots and receivers in line, choosing the shotline as the  $x$ -axis will yield  $y_s=y_r=y_m=0$ . We then get:

$$A(t; x_s, x_r, y_m=0, z_s, z_r) \quad (2)$$

2- Further processing steps are based on the assumption that source and receiver coordinates are in a horizontal plane at datum level  $z_d$  on top of a homogeneous layer.  $z_s$  and  $z_r$  will usually not be at datum level (topography), nor will the top layer be homogeneous (weathering layer). Therefore, a correction has to take place that compensates for topographic and weathering layer effects. This correction is a constant time shift as long as reflection depth is large with respect to the thickness of the weathered layer and the offset.

$$A(t; x_s, x_r, y_m=0, z_d) \quad (3)$$

3- When we define the  $x$ -coordinate of the midpoint as:

$$x_m = (x_r + x_s) / 2 \quad (4)$$

and the offset from this midpoint as:

$$\delta = (x_r - x_m) = (x_r - x_s) / 2 \quad (5)$$

we get:

$$A(t; x_m, \delta, y_m=0, z_d) \quad (6)$$

4- When we compensate for the offset  $\delta$  (NMO-correction) we get:

$$A(t; x_m, y_m=0, z_d) \quad (7)$$

This is the time response we would expect for a shot-receiver coincident experiment with both shot and receiver at  $x_m, y_m=0, z_d=0$  for a horizontally layered subsurface.

The steps 1 to 4 all deal with the reduction of the number of independent variables of the seismic dataset. Steps 5 and 6 theoretically deal with the conversion of seismic amplitude into reflectivity and the time-to-depth conversion.

5- Deconvolution theoretically removes the influence of the shape of the source signal from the recorded seismic signal. It is based on the assumption that the recorded seismic signal can be seen as the convolution of the source signal with the earth's unit pulse response. This only holds for plane waves. When the exact shape of the source signal is known to be  $G$  a suitable inverse operator  $G^{-1}$  can be deduced. Convolution of this operator with  $A$  yields a reflectivity series  $I$ :

$$I(t; x_m, y_m=0, z_d) = G^{-1} * A(t; x_m, y_m=0, z_d) \quad (8)$$

When we have no exact knowledge of the waveshape  $G$  we can still determine a  $G^*$  based on eg. statistical assumptions on this waveshape. Using this  $G^*$  however, deconvolution will merely be a signal enhancement operation.

6- Time-to-depth migration transforms the time response at  $z_d$  into a model of the subsurface at  $t=0$ . This model still contains multiple reflections.

$$I(z; x_m, y_m=0, t=0) \quad (9)$$

It should be stated that there is a great variety of migration algorithms, some yielding a real depth model others resulting in a time domain representation of the data set.

In addition to these operations a number of data enhancement algorithms can be chosen. Among these are:

- data muting; remove part of the data from the recorded seismic signals.
- digital filtering; improvement of the signal-to-noise ratio of the seismic data due to the suppression of a part of the data, characterized by differing frequency, wavelength, or both, by applying digital filtering techniques.
- data stacking; the stacking of seismic data sharing the same midpoint but having not necessarily the same offsets (after NMO-correction). Due to the stacking of the data the signal-to-noise ratio generally will increase.

### *3.3.3 High-resolution processing*

The problems encountered in the processing of high-resolution seismic data are related to:

- static corrections.

High-resolution seismic surveys are usually small scale projects. Not much attention is paid to the determination of topography, weathering layer thickness and weathering layer velocity. In order to determine these parameters a geodetic survey as well as a refraction survey should be carried out. To perform refraction seismics as a subsidiary project would probably take as much time as the reflection measurements itself. Therefore a solution is sought in the combination of reflection and refraction measurements in one operation. It still has to be shown that the usual way of applying static corrections is employable also in shallow seismic surveys. For shallow seismic reflections at depths comparable to the thickness of the weathered layer the time correction that has to be performed in order to have both shot and receiver positions at datum level on top of a homogeneous layer depends on this depth. Until a good method has been developed one should always compare the unstacked common-offset-sections with the stacked sections to determine if the stacking procedure really worked well.

- number of channels.

The number of channels in high-resolution seismic profiling is usually small. This may give problems in the determination of stacking velocities and the use of wavenumber and/or velocity filters. Due to the small CDP-coverage each bad trace will cause a severe loss of data quality.

- time-to-depth conversion.

Time-to-depth transformation can be seen as an operation inherent to migration. Without migration one can only perform a time-to-distance conversion. As we usually do not have velocity information from well logs and the accuracy of the stacking velocities is moderate, the time-to-depth (distance) conversion of the data is problematic. Therefore fitting the data to lithological information is a bit tricky.

- resolution losses.

It should be stated that most of the processing steps mentioned, such as eg. frequency filtering and data stacking, are basically intended to increase the signal-to-noise ratio. They are not guaranteed to preserve seismic resolution, although some of the events might become sharper.

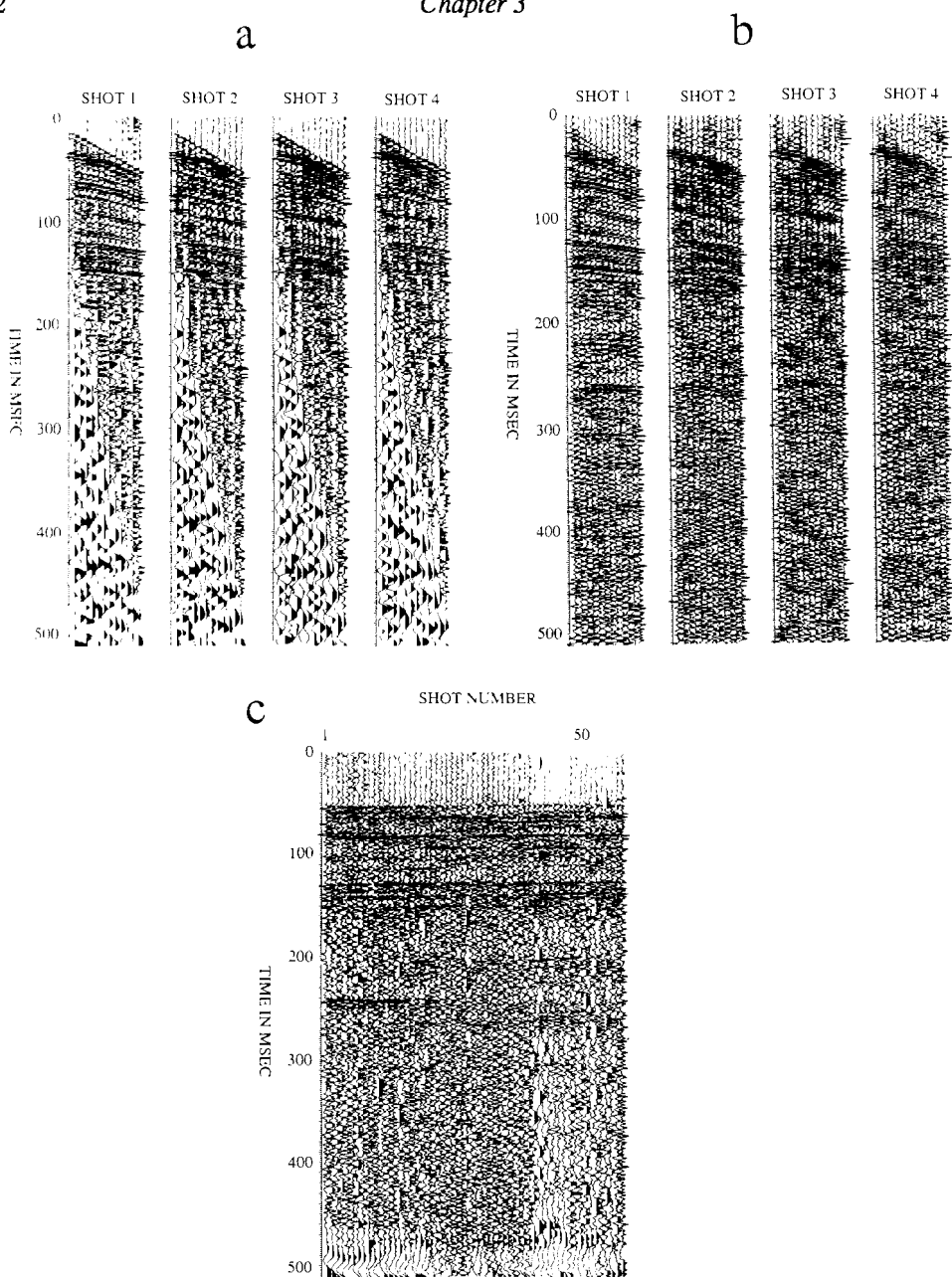


**Fig. 3.6.** Compilation of intermediate results of tidal data processing.  
a- raw Common-Shot-Point  
b- filtered CSP  
c- Common-Offset-Section



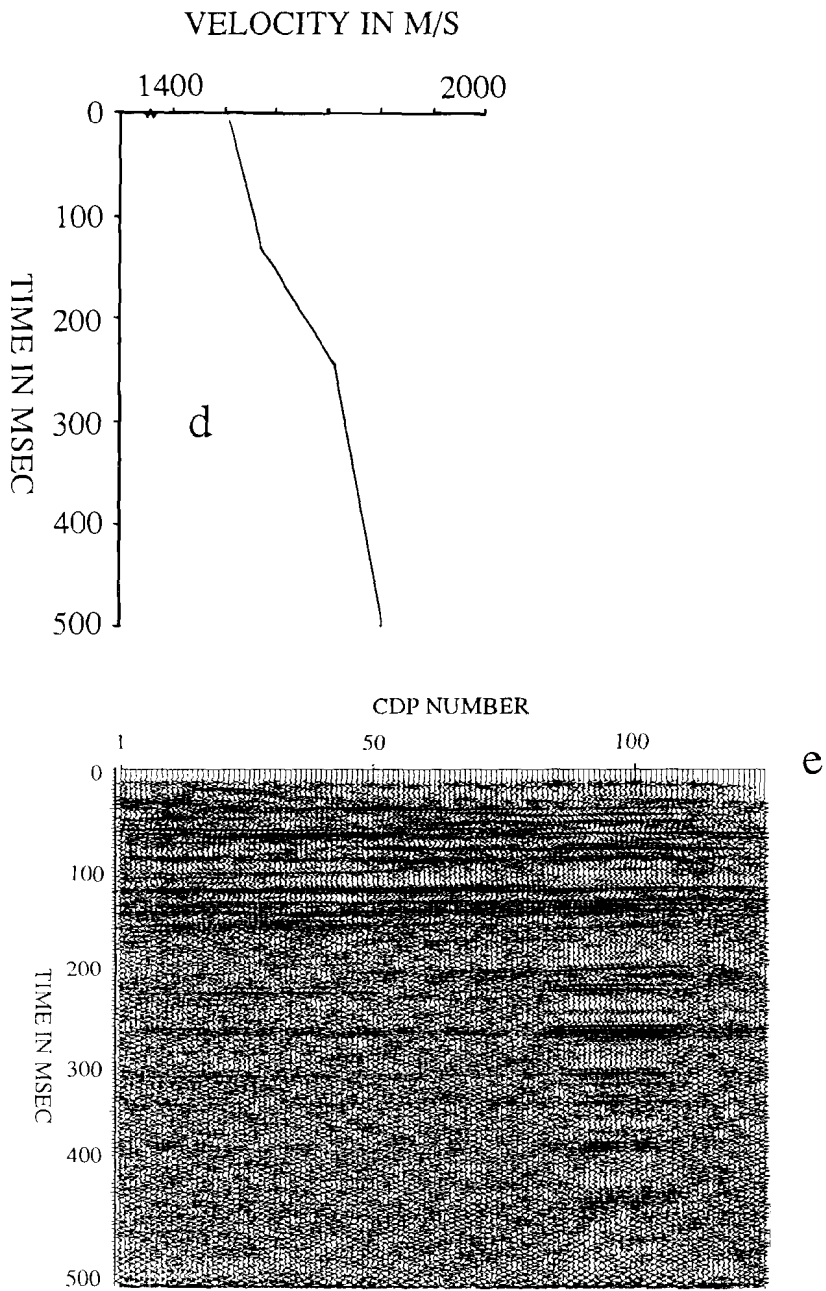
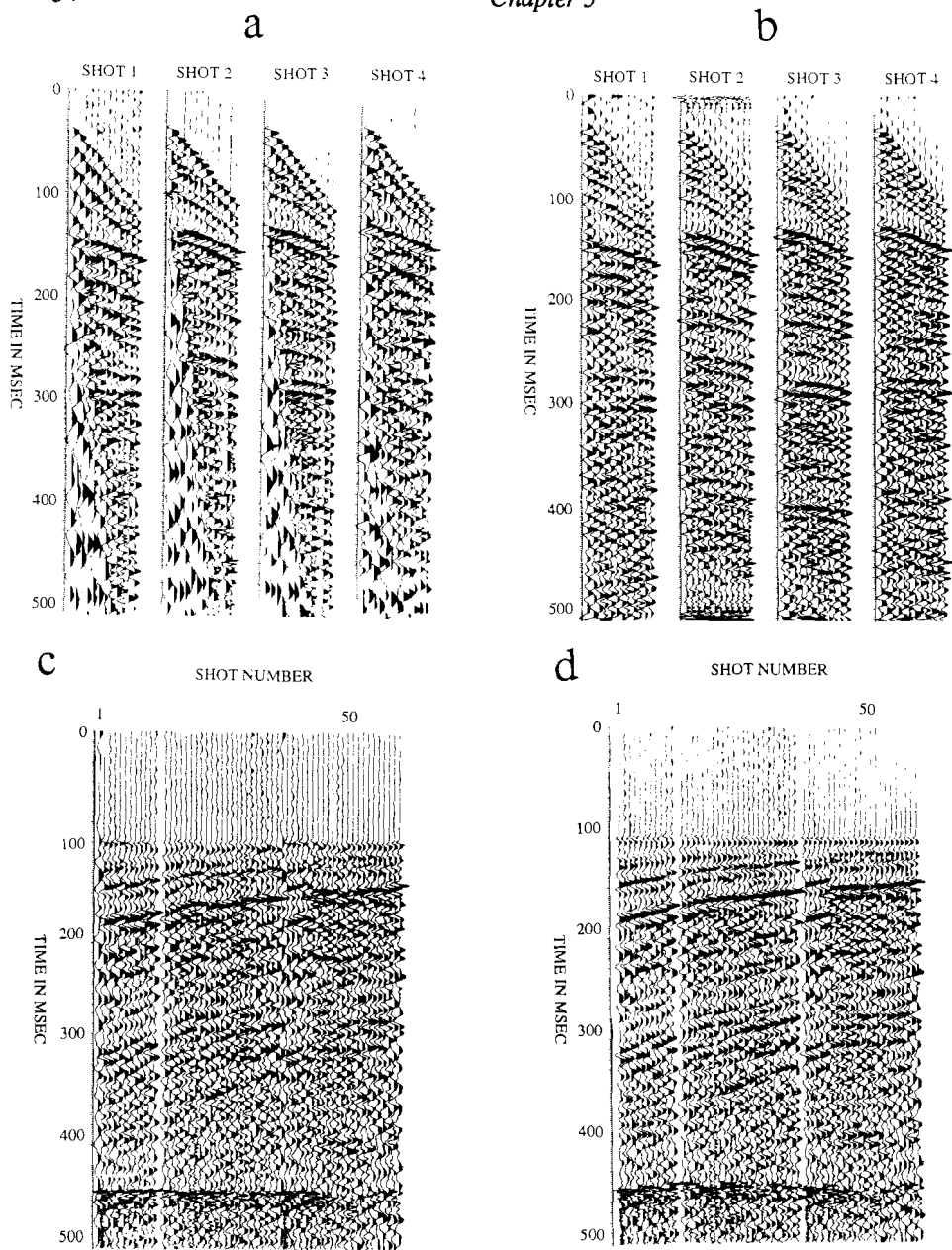
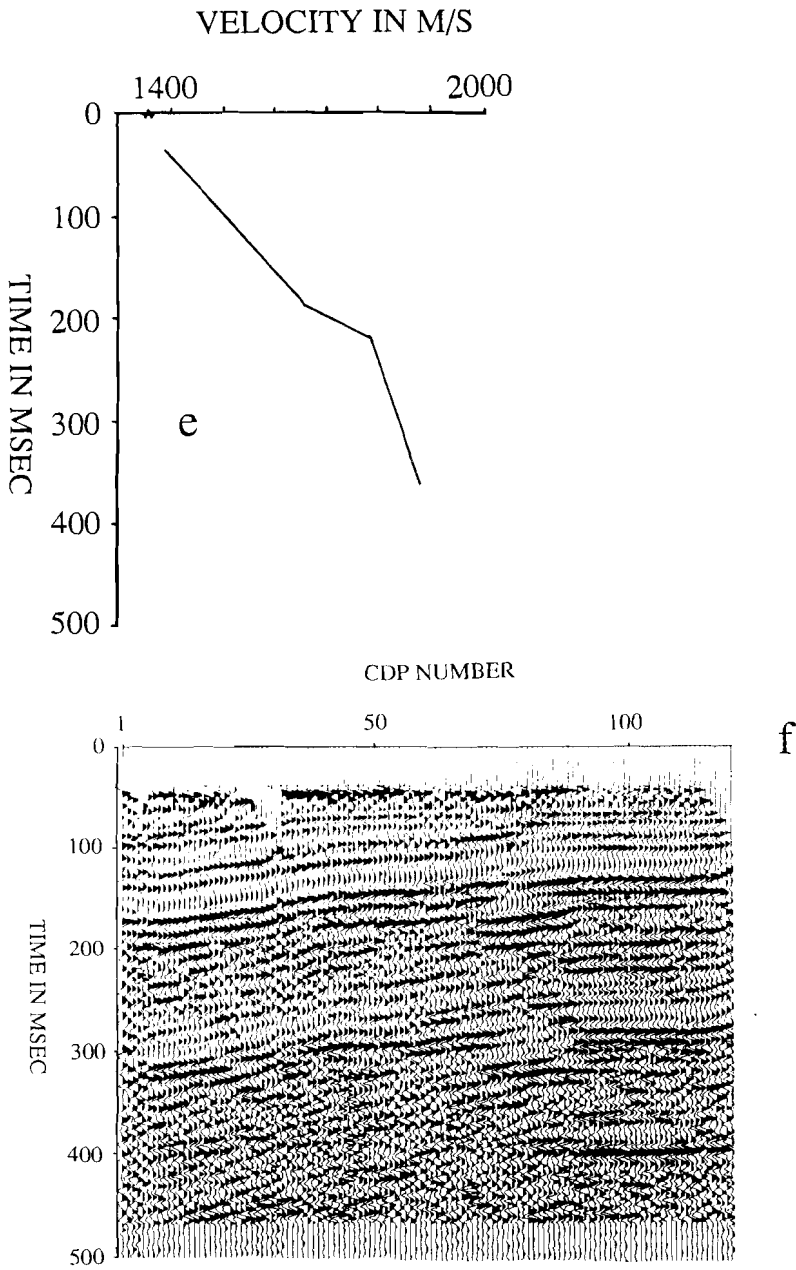


Fig. 3.6. (continued) Compilation of intermediate results of tidal data processing.  
d- Stack velocity profile  
e- Stacked section



**Fig. 3.7.** Compilation of intermediate results of onshore data processing.

- a- raw Common-Shot-Point
- b- filtered CSP
- c- Common-Offset-Section
- d- COF section after static corrections



**Fig. 3.7. (continued)** Compilation of intermediate results of onshore data processing.  
e- Stack velocity profile  
f- Stacked section

### 3.4 FIELD EXAMPLES

#### 3.4.1 Introduction

In the next paragraph some field examples of on-shore high-resolution seismic surveys are presented. For each example the geological setting and the geophysical targets are described in a brief introduction. The location of the survey areas in the Netherlands are given in figure 3.8. Acquisition parameters- and conditions, estimated costs per shot, and the ratio of acquisition time versus processing time are given for each field example. Finally the results are discussed.

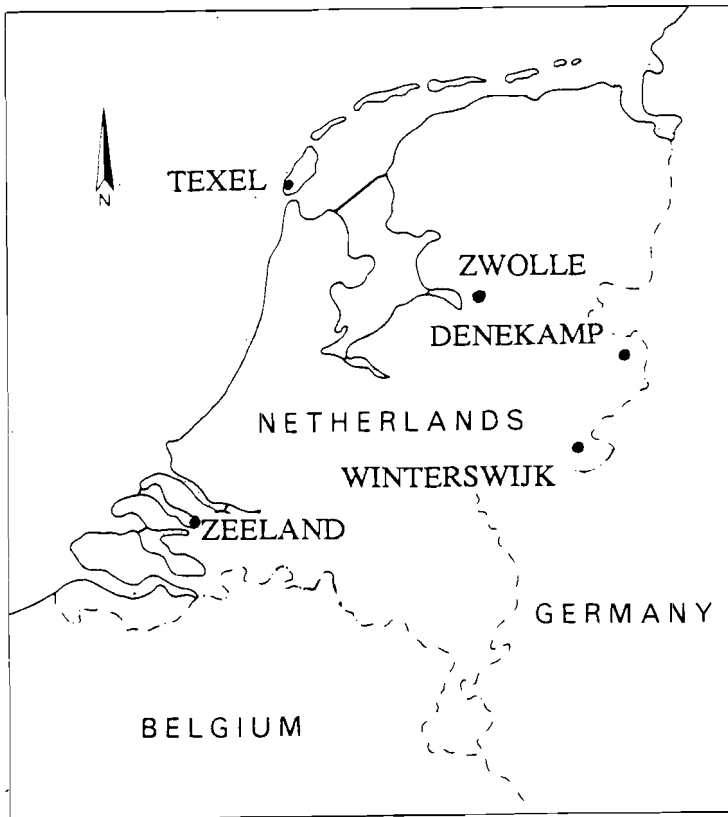


Fig. 3.8. Map of survey areas in the Netherlands.

### 3.4.2 Example 1: Winterswijk

#### 3.4.2.1 Setting and Targets

The main target of the seismic study was the mapping of Mesozoic sediments which come close to the surface in the study area. They are covered by Tertiary and Quaternary sands and shales. The Paleozoic formations are covered by Triassic continental sands, shales and silts (Lower and Main Buntsantstein). After a period a erosion, which resulted in the Hardegsen unconformity, the Triassic continental sequence was covered by Triassic marine shales, limestones and marls (Röt and Muschelkalk). The Triassic sedimentation was interrupted by the Early Kimmerian activity (unconformity), which was followed by a transgression during the Lower Jurassic (Lias shales). During the Upper Cretaceous (Santonian) orogeny, the sediments were faulted and uplifted. The orogeny was followed by a period in which most of the Cretaceous and Jura were eroded. After erosion, Tertiary and Quaternary sands and shales were deposited. The distribution of these sediments was largely controlled by Late Oligocene faulting, which resulted in NW-SE orientated basins and grabens. Expected seismic reflectors in the area are the Hardegsen unconformity, the Kimmerian unconformity and the base of the Tertiary.

#### 3.4.2.2 Acquisition Parameters

AREA	WINTERSWIJK
SOURCE	WEIGHTDROP 40 kg
RECEIVERS TYPE	50 Hz GEOPHONE
UNIT DISTANCE	11 m
IN-LINE OFFSET	33 m
ACQ/PROC RATIO	.5
SURFACE CONDITIONS	ROADSIDE
COSTS PER SHOT	\$ 25,-
NOISE SOURCES	WIND

**Table 3.1.** Acquisition overview Winterswijk.

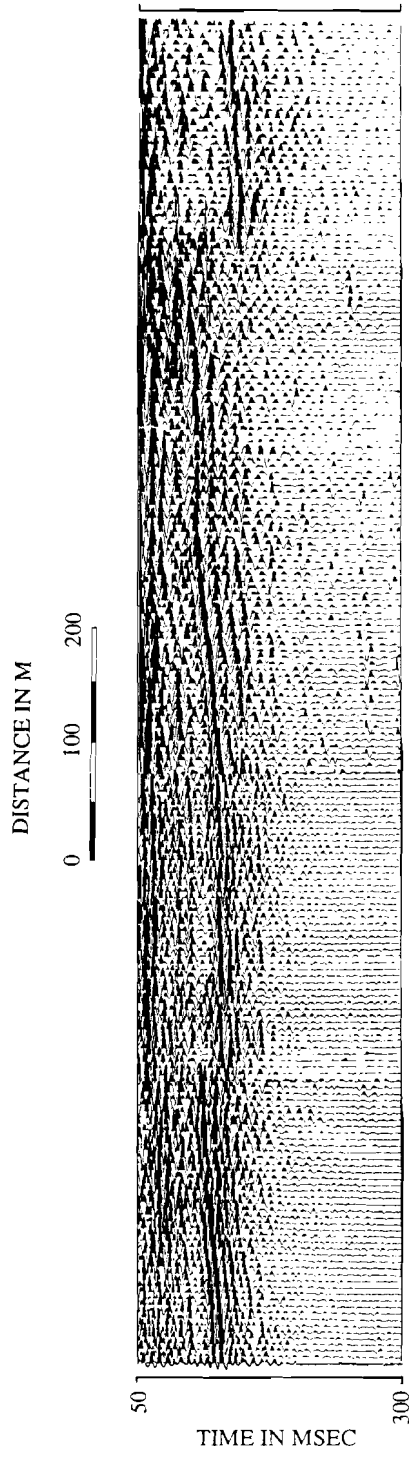
## 3.4.2.3 Results

Figure 3.9 shows a compilation of six successive sections. The sections are originally shot as one survey, but changes in surface conditions caused a strong variation in seismic quality along the profile. All sections are displayed without automatic gain control, and no correction for spherical spreading was applied.

One clear reflector is recognizable and is easy to delineate along the profile. Small scale faulting is obvious, but some confusion may be caused by small vertical offsets between successive sections (different processing). Based on well information and standard seismic sections (Bredewout and Gouly, 1987) the strong reflector is interpreted as the Early Kimmerian Unconformity. Stack velocities are used to calculate the approximate depth of the reflector.

The seismic quality of the sections is reasonable and allows to study the zone between standard seismic targets and near surface targets.

**Fig. 3.9.** Seismic section recorded at the Winterswijk location (next page).



## 3.4.3 Example 2: Portugal

## 3.4.3.1 Setting and Targets

This survey was carried out in Algarve in the Southern part of Portugal. The demand on groundwater is great in this area, because most of the land is used for horticulture of citrus, which requires an intensive irrigation. Most of the groundwater is extracted from a Miocene aquifer. The hydro-geology department of the Free University of Amsterdam studies this area extensively using resistivity, gravimetric, and electro-magnetic surveys to get an insight in the hydro-geological characteristics and extension of the Miocene coastal aquifer, but geological information is scarce. The non-seismic methods give an understanding of the structures of the subsurface and the aquifers. However, interpretations based on these methods are not unique.

In the area studied less-pervious Cretaceous marly limestones are present, with local beds of karstified limestones or dolomite, which form highly productive groundwater zones (figure 3.10 a). The Cretaceous is discordantly overlain by the Miocene. The lithology of the Miocene varies considerably and may consist of unconsolidated sands, sandstones, marls and fossiliferous limestones. In the studied area, the Miocene sands, sandstones, and limestones represent the most important coastal aquifer. Most of the aquifer is covered by less-pervious Plio-Quaternary conglomerate or by Holocene clays.

An expected seismic reflector is the unconformity between south-dipping Cretaceous and the overlying Miocene sediments. The strong variation of lithologies within Miocene might also result in seismic reflections.

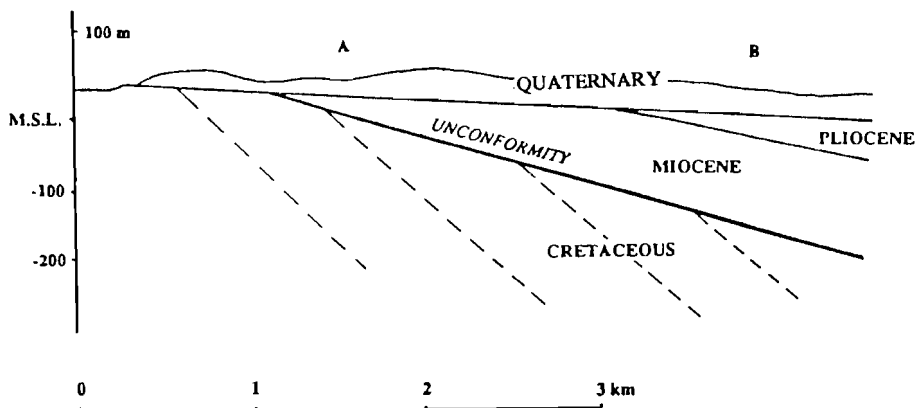


Fig. 3.10a. Model belonging to the Portugal survey.



## 3.4.3.2 Acquisition Parameters

AREA	PORTUGAL
SOURCE	WEIGHTDROP 25 kg
RECEIVERS TYPE	10 Hz GEOPHONE
UNIT DISTANCE	11 m
IN-LINE OFFSET	33 m
ACQ/PROC RATIO	1
SURFACE CONDITIONS	SANDY ROADS
COSTS PER SHOT	\$ 30,-
NOISE SOURCES	IRREGATION SYSTEMS

**Table 3.2.** Acquisition overview Portugal.

## 3.4.3.3 Results

Two seismic profiles (perpendicular and parallel to the strike direction of the Cretaceous) are presented in figures 3.10b and 3.10c. The seismic quality of the lines differs significantly. The profile located near the coast (figure 3.10b) shows good data quality and several sharp reflectors can be recognized. The section may be divided into three seismic facies zones: A lower part below the strong reflector at 190 ms consisting of flat parallel reflections (possibly products of the processing or multiple remains), a middle part from 60 ms to 190 ms of slightly west dipping reflectors, covered by a third zone of flat reflections. Using the stacking velocities the bases of zones two and three can be calculated at 171 m and 51 m depths respectively. The quality of the dip section (figure 3.10c) is moderate, most probably caused by the surface conditions. The seismogram shows at 110 ms (depth 94 m) an unconformity of south dipping reflections covered by flat laying reflections.

The observed seismic patterns agree reasonably well to the described regional geology. The strong reflector at the base of zone 2 in profile 1 and the unconformity in profile 2 are easy to correlate with the expected unconformity between the dipping Cretaceous and the Miocene. The seismic method seems useful in this study and shows to be a fast and easy method to delineate the base of the Miocene aquifer. The two seismic lines are part of a larger survey with profiles of a comparable quality.

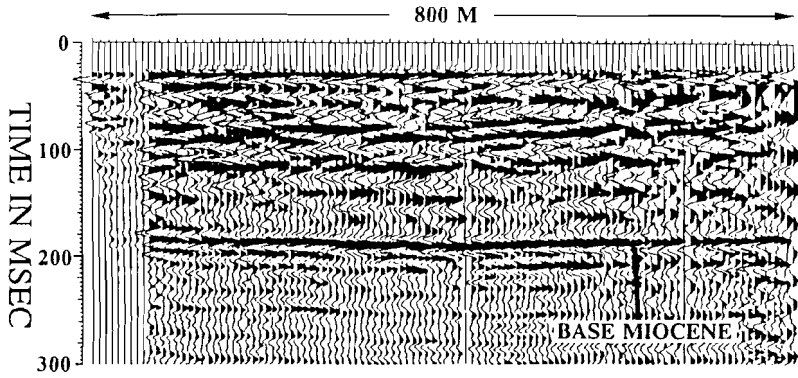


Fig. 3.10b. Strike section belonging to the Portugal survey.

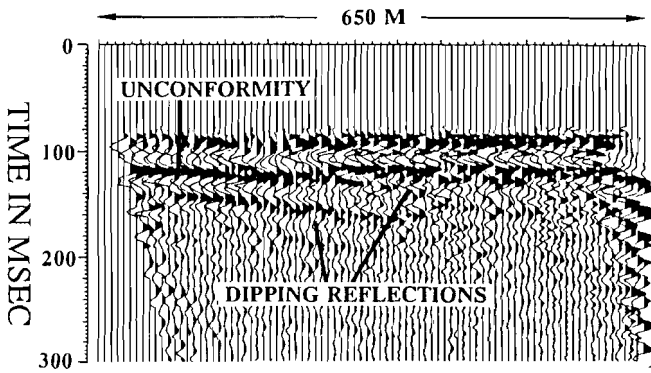


Fig. 3.10c. Dip section belonging to the Portugal survey.

## 3.4.4 Example 3: Zwolle (Engelse werk)

## 3.4.4.1 Setting and Targets

The aim of this survey was to test the use of high-resolution seismic profiling in a geologically complicated situation on land. This survey was carried out south of Zwolle to study the internal structure of ice-pushed ridges. These ridges are formed during the Saalien. Lower and Middle Pleistocene peri-glacial and fluvial deposits are stacked together with Saalien fluvial, massflow and alluvial fan deposits in thrust-sheets of about 25 m - 50 m thick (figure 3.11a). From a seismic point of view it may be important that the base of the thrusts consists of thin clay and loam layers of the Kedichem formation with a thickness of 3 to 4 meter. Their lithology differs from the other sheet sediments, which contain predominantly medium-fine to coarse sands. The specific lithologic character of the base may provide a seismic impedance contrast, detectable with high-resolution seismic profiling. To study these small scale tectonic phenomena, the seismic parameters were designed for a resolution on meter scale and a target depth between 0 and 100 m.

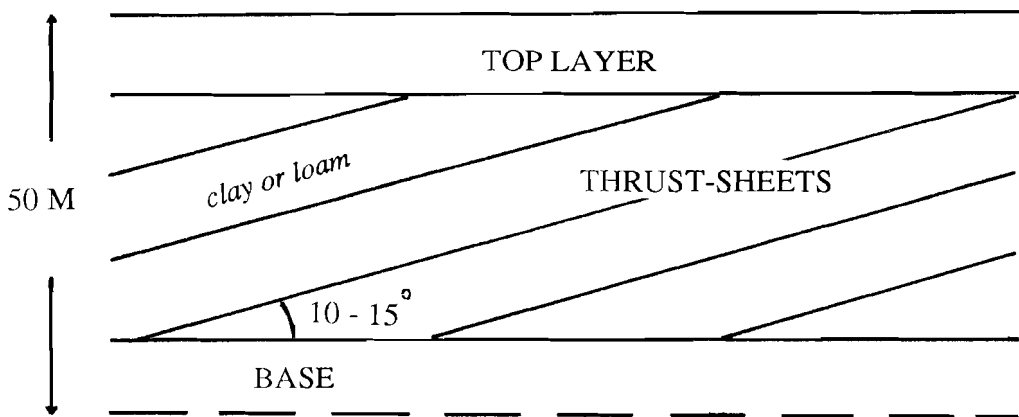


Fig. 3.11a. Model belonging to the Zwolle survey.

## 3.4.4.2 Acquisition Parameters

AREA	ZWOLLE
SOURCE	SHOTPIPE
RECEIVERS TYPE	50 Hz GEOPHONE
UNIT DISTANCE	3 m
IN-LINE OFFSET	15 m
ACQ/PROC RATIO	2
SURFACE CONDITIONS	PASTURE
COSTS PER SHOT	\$ 20,-
NOISE SOURCES	---

**Table 3.3.** Acquisition overview Zwolle.

## 3.4.4.3 Results

The results are presented as Common Offset sections (figure 3.11), because C.D.P. stacking suffered from badly defined static corrections. The profile of figure 3.11 consists of three seismic facies zones: the lowermost (zone 1) down from 170 ms (indicated D) with horizontal reflections partly disturbed by the ground-coupled sound wave (C); a second zone between 60 - 170 ms (indicated B) with south dipping reflections covered by a third zone (indicated A) of strong and almost horizontal reflections. The ground-coupled sound wave is absent in the far offset section (figure 3.11). The seismic data show an acceptable correlation with the regional geological information and cores. Seismic zone 2 may be identified as the complex of ice-pushed ridges over a flat base (zone 1) and covered by a flat top-layer (zone 3). Indications of small scale faulting within the ridge complex are not recognizable. The seismic survey has confirmed the ideas of the global geology of the area, but could not add new information.

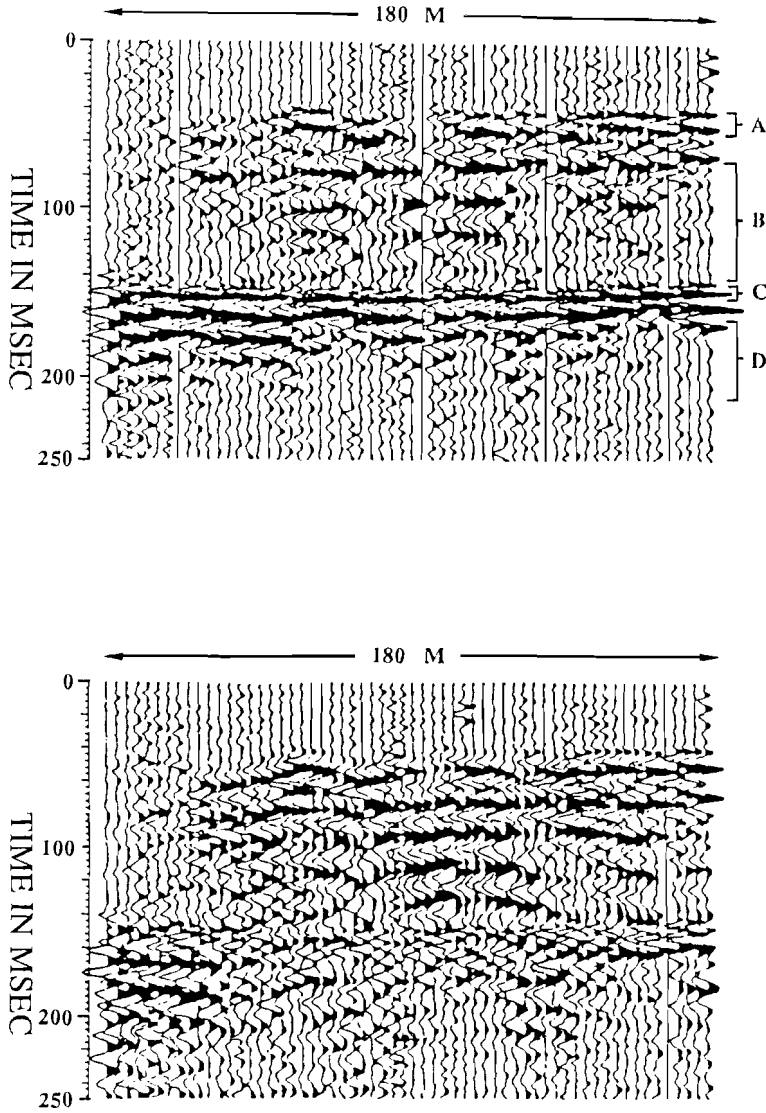


Fig. 3.11. Near-offset section (top) and far-offset section (bottom) belonging to the Zwolle survey.

### 3.4.5 Example 4: Denekamp

#### 3.4.5.1 Setting and Targets

In this area the shallow subsurface consists of slightly west dipping Mesozoic formations (alternations of thick sand and clay layers) covered by Quaternary sands with a thickness of approximately 15 meter. The study area is deformed by faults with E-W strikes. The aim of the survey was primarily to determine the seismic response of the area and to study the possibility to locate and characterize the faults. On this information future research in this area was based. Minor attention was paid to the local geology.

#### 3.4.5.2 Acquisition Parameters

AREA	DENEKAMP
SOURCE	SHOTPIPE
RECEIVERS TYPE	50 Hz GEOPHONE
UNIT DISTANCE	3 m
IN-LINE OFFSET	27 m
ACQ/PROC RATIO	1
SURFACE CONDITIONS	ROADSIDE
COSTS PER SHOT	\$ 20,-
NOISE SOURCES	----

**Table 3.4.** Acquisition overview Denekamp.

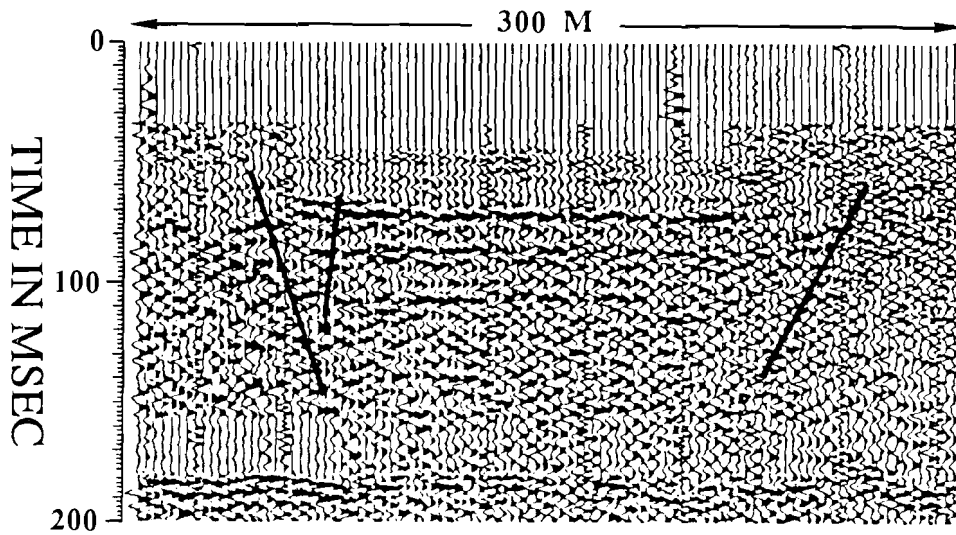


Fig. 3.12. Seismic line shot at the Denekamp location.

### 3.4.5.3 Results

The data are of good quality (figure 3.12). The common-offset section shows two major faults, recognizable by changes in reflection continuity and by the presence of diffraction hyperbolae. The seismic quality of the profile east and west of the faults is moderate. This is probably caused by the selection of acquisition parameters which was based on a test shot exactly in the middle of the profile. In this case the acquisition parameters should have been adjusted to the changing seismic characteristics caused by the faulting.

## 3.4.6 Example 5: Spain

## 3.4.6.1 Setting and Targets

The possibility to recognize channel geometries in seismic studies on tidal flats were the basic reason to study sequences of channel bodies in consolidated sediments. The study is carried out in the southern Pyrenees in the Montlobat Formation characterized by an alternation of fluvial channel sandstones and floodplain mudstones. The expected strong contrast between the sandstone bodies and the mudstones suggest the use of high-resolution seismic profiling. The thickness of the formation in the study area lies between 50 and 100 m and covers discordantly the Ager Formation (shallow marine sediments), which is slightly dipping towards the north (figure 3.13a).

## 3.4.6.2 Acquisition Parameters

AREA	SPAIN
SOURCE	WEIGHTDROP 25 kg
RECEIVERS TYPE	100 Hz GEOPHONE
UNIT DISTANCE	5 m
IN-LINE OFFSET	25 m
ACQ/PROC RATIO	.4
SURFACE CONDITIONS	PEBBLY RIVER BED
COSTS PER SHOT	\$ 35,-
NOISE SOURCES	----

**Table 3.5.** Acquisition overview Spain.



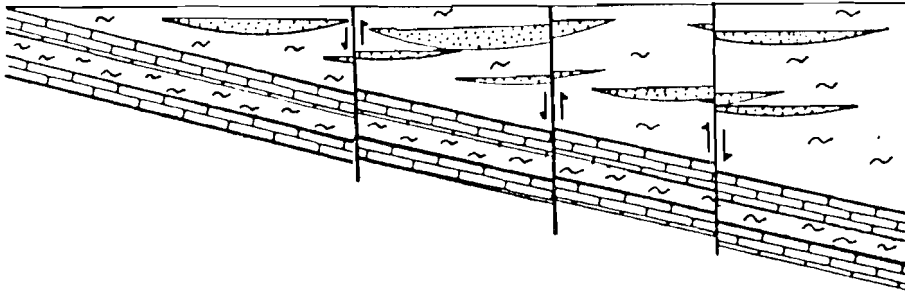
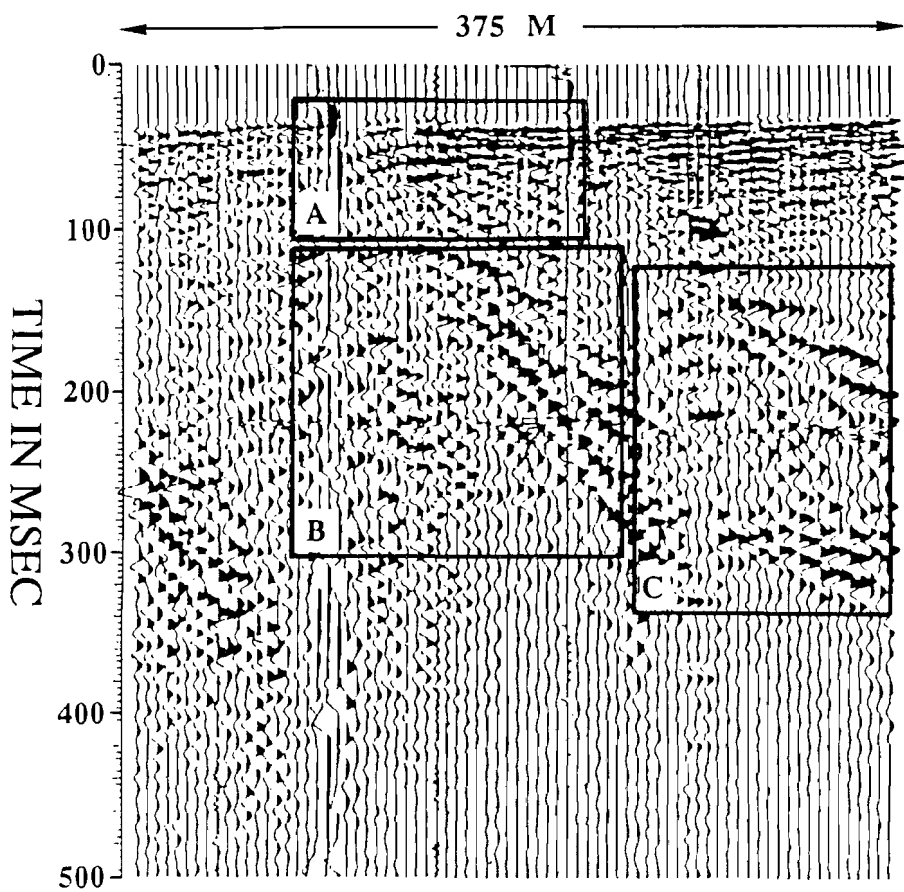


**Figure 3.13a.** Model belonging to the Spain survey.

### 3.4.6.3 Results

The data are of low quality. A remarkable result was the presence of strong S-waves in the seismogram (figure 3.13b). Box A in figure 3.13b indicates P-diffractions, boxes B and C show S-diffractions. The original aim, the study of channel bodies was not reached due to difficult surface conditions. A bad coupling between the base-plate and the ground caused a high energy loss. The total survey, from which the presented section is just a small part, shows an overall possibility to recognize the contact between the Montllobat Formation and the Ager Formation and to locate fault zones along the line.

**Fig. 3.13b.** Seismic section belonging to the Spain survey (next page).



### 3.4.7 Example 6: Texel

#### 3.4.7.1 Setting and Targets

The survey area is located on a beach of a barrier island (Texel, NW Netherlands). The upper 100 m of the subsurface consists of Quaternary glacial/fluviol deposits and Tertiary- and Holocene tidal deposits and shows lithological and morphological details on a scale from millimeters to a few meter. In this survey we tried to improve the resolution to observe some of these details down to dm scale. The data presented were acquired as a part of a survey presently carried out to study the morphological development of the system of erosion and deposition in the Marsdiep tidal inlet.

#### 3.4.7.2 Acquisition Parameters

AREA	TEXEL
SOURCE	WEIGHTDROP 7 kg
RECEIVERS TYPE	100 Hz GEOPHONE
UNIT DISTANCE	2 m
IN-LINE OFFSET	8 m
ACQ/PROC RATIO	1
SURFACE CONDITIONS	TIDAL FLAT
COSTS PER SHOT	\$ 50,-
NOISE SOURCES	WIND

**Table 3.6.** Acquisition overview Texel.

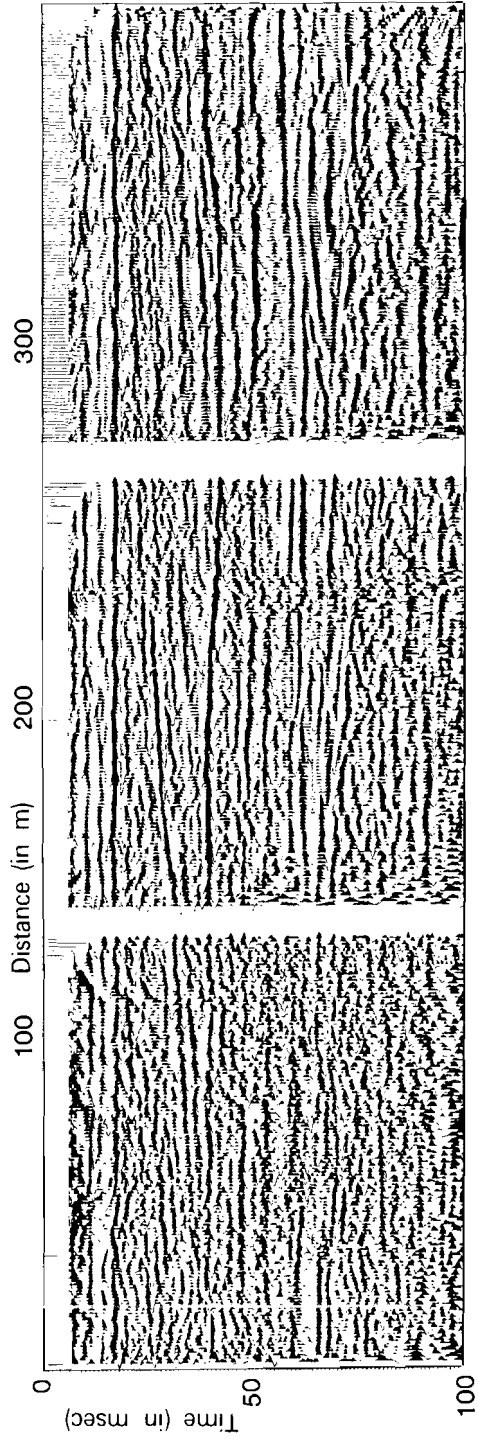
## 3.4.7.3 Results

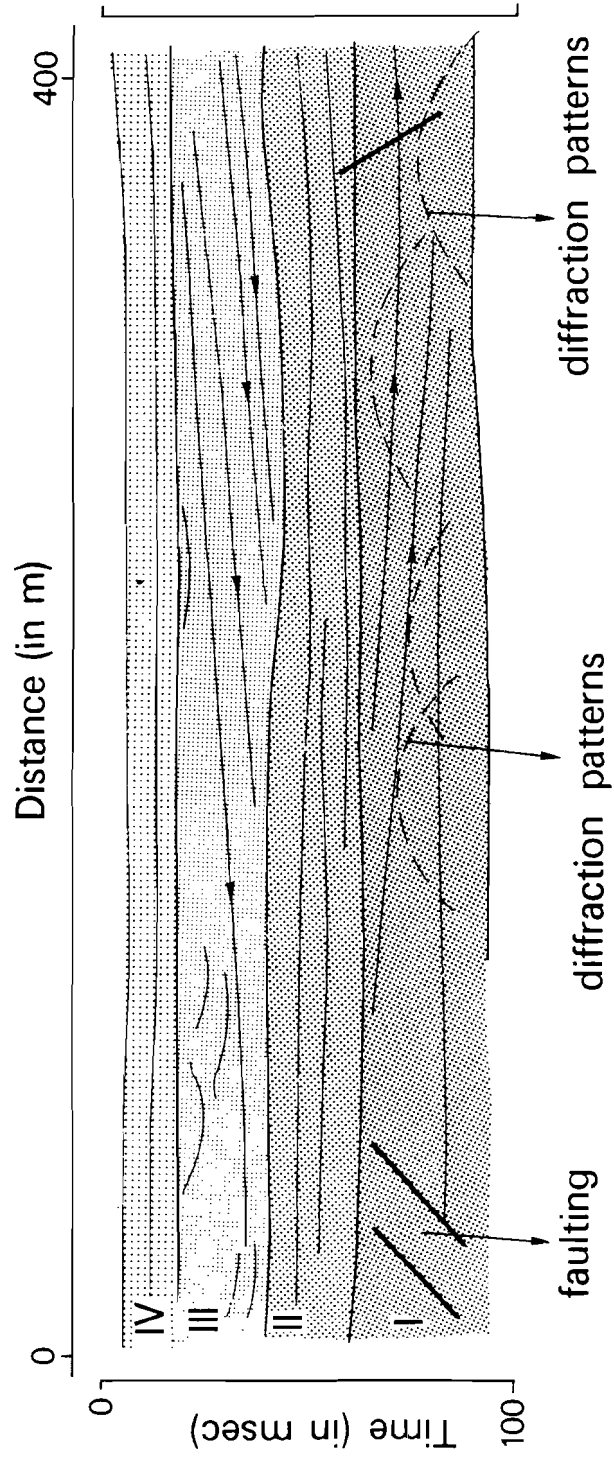
The seismic section of figure 3.14a is an example of a first attempt to get a higher resolution (0.4 m). This was achieved with a 7 kg weight dropped from a height of approximately 1.5 m. In the seismic section four distinct seismic facies units can be identified (figure 3.14b):

- unit I: Subparallel reflections with sometimes very high amplitudes and moderate continuity. Diffraction patterns are clearly recognizable.
- unit II: Subparallel reflections with moderate amplitude and continuity.
- unit III: Parallel oblique reflections with moderate continuity and amplitude with locally curved reflections.
- unit IV: Parallel reflections with low continuity and moderate amplitude.

The seismic units show a good agreement with the regional geology. The subparallel reflections of units I and II fit into a fluvial environment with channel morphologies. The reason for the distinct diffractions and high amplitudes of unit I is not clear. Unit I shows also some small scale faulting. Unit III represents the lateral accretion surfaces cut by smaller channels. The unit is bounded by two strong reflectors. The upper one corresponds to a boulder clay on top of the Saalien. The interpretation of the lower one is not clear.

**Figure 3.14ab.** Seismic section (figure 3.14a) and interpreted section (figure 3.14b) for the Texel location (next pages).





## 3.5 REFERENCES

- Doomenbal, J.C. and Helbig, K. 1983. High-resolution reflection seismics on a tidal flat in the Dutch delta: acquisition, processing and interpretation. *First Break* 1 (5) 9-20.
- Hunter, J.A., Pullan, S.E., Gagne, R.A. and Good, R.L. 1984. Shallow seismic reflection mapping the overburden- bedrock interface with the engineering seismograph, some simple techniques. *Geophysics* 49, 1381-1385.
- Hunter, J.A., Pullan, S.E., Burns, R.A., Gagne, R.A. and Good, R.L. 1985. The optimum offset shallow reflection technique: case histories. *S.E.G. Annual Meeting expanded technical abstracts*, 159-161.
- Jongorius, J. and Helbig, K. 1988. Onshore high-resolution seismic profiling applied to sedimentology. *Geophysics*, in press.
- Jongorius, P., Brouwer, J.H. and Helbig, K. 1987. Calibration of the seismic stratigraphical response of tidal deposits. *Proceedings of the 12-th World Petroleum Congress* (5).
- Ongkiehong, L. and Askin, H.J. 1988. Towards the universal seismic acquisition technique. *First Break*, 6 (2), 46-63.
- Rigdon, H. and Hoover, G. 1987. Quantitative Selection of Seismic Acquisition parameters. *The Leading Edge*, 6 (1), 18-25.
- Steeple, R.E., Knapp, R.W. and Miller, R. 1985. Field efficient shallow CDP seismic surveys. *S.E.G. Annual Meeting expanded technical abstracts*, 150-152.

## *Chapter 4*

# **HIGH-RESOLUTION SEISMIC PROFILING: A CASE HISTORY**

Data quality in onshore seismic exploration suffers most from weathering layer effects. In this chapter a case history of an onshore shallow seismic survey showing these effects is presented. The combined usage of refraction- and reflection information is discussed and the processing of guided waves is suggested. This chapter was written in cooperation with Drs. P. Jongerius.

### **4.1 INTRODUCTION**

In 1987 a high-resolution seismic survey was carried out in the vicinity of Woerden in the central part of The Netherlands (Fig. 4.1). This survey was part of a project aimed to test the efficiency of high-resolution reflection seismics in the determination of shallow geological structures (as e.g. in engineering geology) for various field conditions. The method of high resolution seismic profiling works well under favorable field conditions (Doornenbal and Helbig 1983, Jongerius, Brouwer and Helbig 1987). Even under less ideal field conditions some good results were obtained (Bredewout and Gouly 1987). The Woerden area is not the most ideal site to perform high resolution seismics and was only chosen because other geophysical methods had already been tested at this location (van Deen 1987). Major problems are caused by small signal to noise ratios due to heavy traffic on a near-by highway and a weathered layer inducing strong reverberations. Several new techniques had to be developed to cope with these problems in acquisition, processing and interpretation.



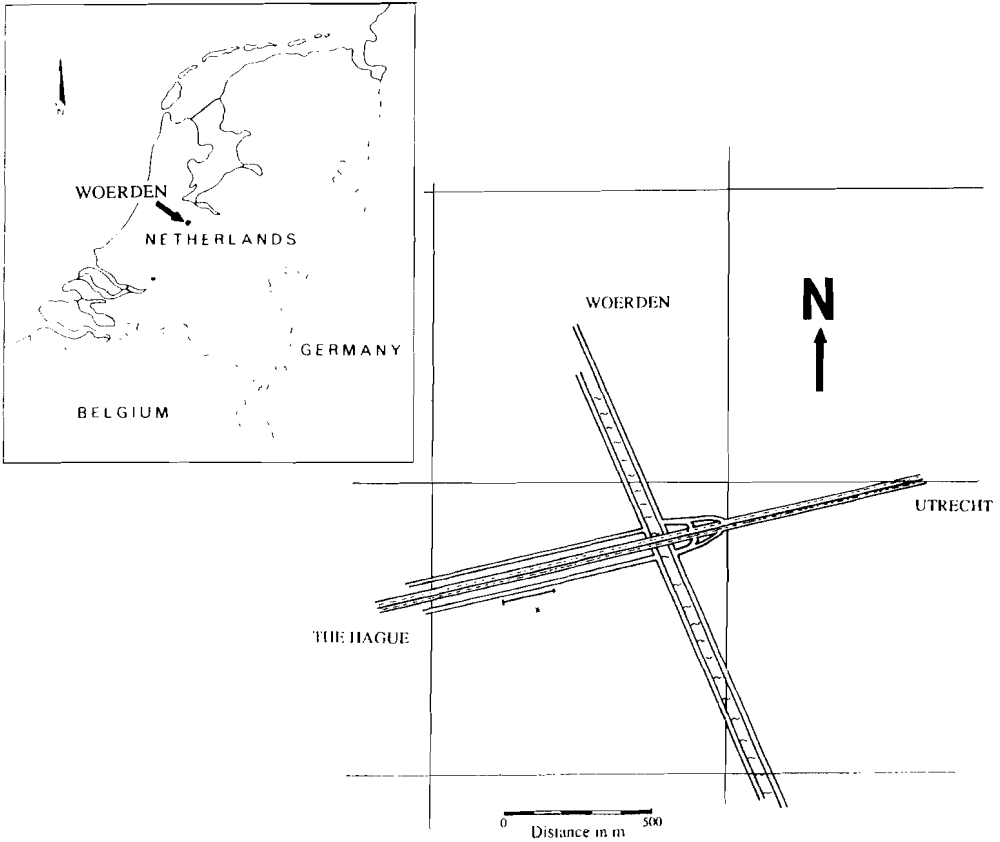


**Fig. 4.1.** Location of the seismic line south of the highway Utrecht-The Hague. Inset: topographical map of The Netherlands indicating the location of the acquisition area in the middle part of The Netherlands.

## 4.2 GEOLOGICAL SETTING

The shallow subsurface along the seismic profile consists of Pleistocene sands covered by Holocene clays and peat. The depth of the contact between the two formations is not exactly known, but nearby cores reveal a depth of 1.5 - 2 m. The depth of the groundwater probably coincides with this depth. The Holocene consists of recent humus clay overbank deposits.

The profile shown (Fig. 4.2) is based on non seismic methods (van Deen, 1987). There is no well control along the profile, and information has to be extrapolated from

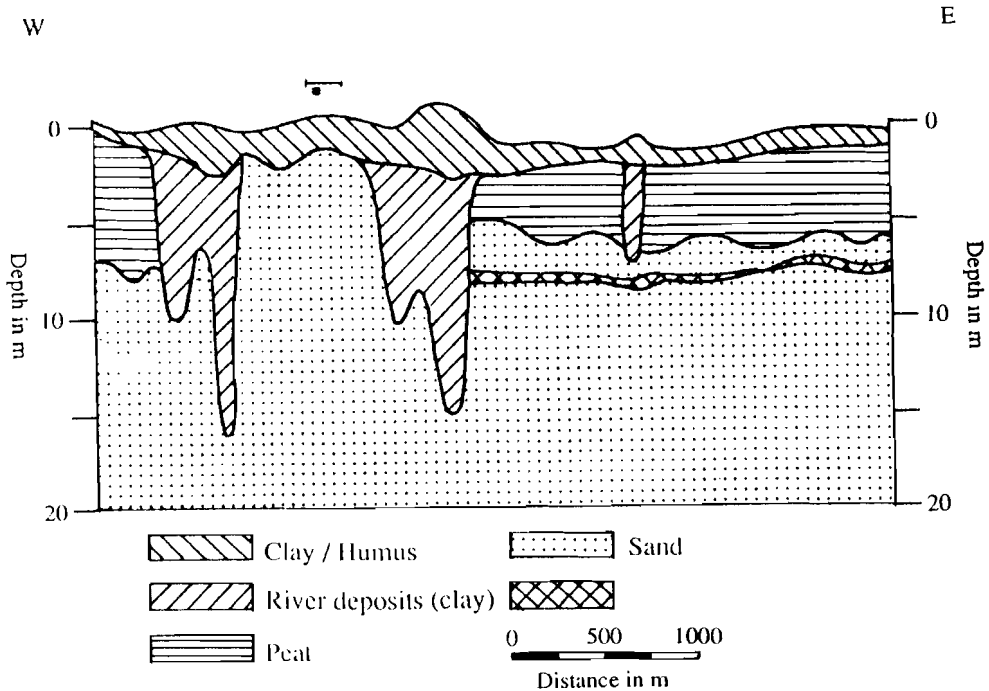
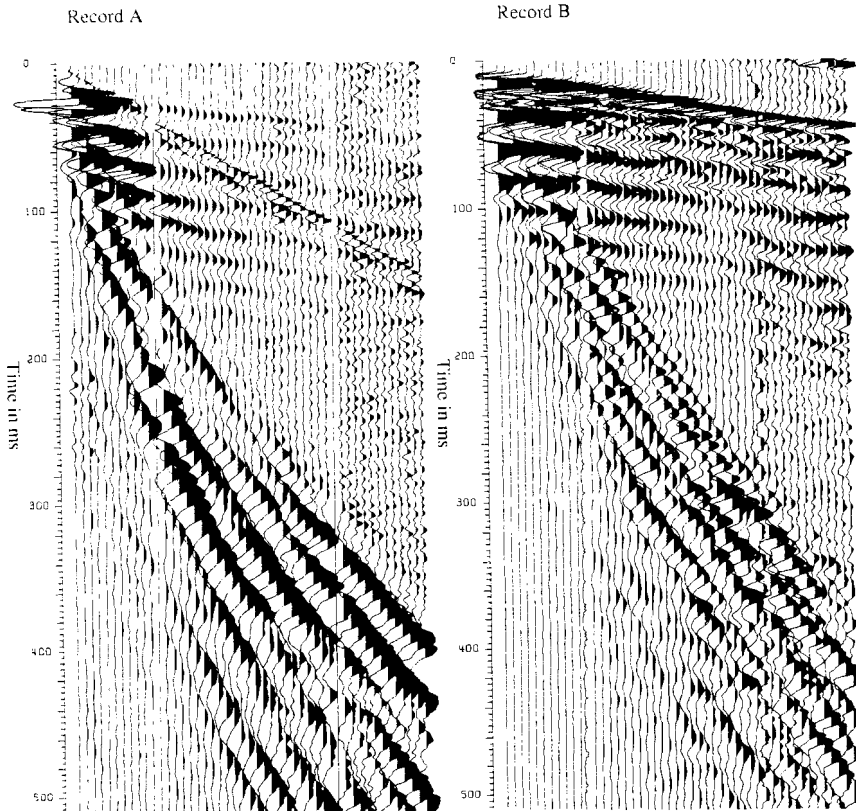


Fig. 4.2. Model of the Woerden area based on information from non seismic methods. The location of the seismic line is indicated at the top of the figure.

shallow cores north of the profile (distance approximately 100 m). From figure 4.2 it can be concluded that we deal with a two layer model in the area covered by the seismic line. Peat seems to be absent. The exact depth of the top pleistocene has to be guessed.

### 4.3 GEOPHYSICAL SETTING

The Woerden area was selected as a test site to find out which geophysical methods could be helpful in the determination of shallow geological structures. As both very shallow (1-5 m) and shallow target structures (15 m) were expected this area was suited for a geophysical survey combining both seismic and non seismic methods. The selection of the targets for the seismic survey was based on the geological model for this area (Fig. 4.2). This model was based on information from a number of non seismic investigations (including E.M soundings and shallow borings) none of which gave satisfactory lateral



**Fig. 4.3 a-b** Test shots showing the difference between a surface source record (4.3a) and a record (4.3b) using a source at depth. The surface source record (4.3a) shows a clear ground coupled sound wave and strong surface waves. Weathering layer multiples are clearly visible in both shots.

continuity (van Deen, 1987). The seismic method was expected to give better lateral resolution, eg. on the thickness of the weathered layer, the occurrence of peat layers, possible small scale fractures, and on the location of ancient beds of the river Linschoten but was expected to fail in obtaining very shallow geological information. A secondary purpose of the survey was to extract information on both P- and S-wave velocities in order to be able to calculate eg., a Poisson's ratio distribution for the different layers we interpreted. Separate P- and S-wave information can be useful for geotechnical applications.

#### 4.4 DEFINITION OF ACQUISITION CONDITIONS

Acquisition took place south of- and parallel to- the highway from Utrecht to The Hague. Distance between this road and the seismic spread was approximately 25 m. Due to the heavy traffic on this road during day time rapid changes in signal to noise ratio between shots are observed. In the far offset traces (42 m) the signal to noise ratio differs from 0.1 to 10. Continuous inspection of the actual noise level using the monitor mode of the acquisition equipment was performed in order to be able to suspend shooting if necessary because of high noise levels. Shifting of recording hours to night time has been taken into consideration. This, however, would have caused a number of logistic problems and has not yet been done.

A number of test shot records were acquired in order to determine the optimal field configuration and to find out which source and receivers we had to use.

During the test period a surface source as well as a 'shotpipe' was used to generate the seismic signal. The surface source shot record (Fig. 4.3a) shows strong surface waves and a prominent high-frequency groundcoupled soundwave. The shotpipe record is shown in figure 4.3b (the shotpipe generates a seismic signal at approximately 1 m depth). Surface waves are less prominent and a groundcoupled soundwave is not visible. The shotpipe was used in all further recordings.

The shot records (Fig. 4.3a-b) showed signal frequencies ranging from 50 to 500 Hz. In order to preserve the low-frequency part of the spectrum the use of receivers having a natural frequency of e.g. 10 Hz or 50 Hz might be suggested (10, 50 and 100 Hz geophones were available). Tests with the 50 Hz geophones already showed that these receivers were too sensitive to the low frequency traffic noise. 10 Hz geophones were expected to give even more problems. Further recordings were thus performed using 100 Hz geophones, accepting the loss of low-frequency information. In order to obtain an even better suppression of surface waves the receivers were also placed at approximately 1 m depth.

The shallow subsurface (Holocene) consists of sand and clay covered by a thin humus layer. We were not able to place the shotpipe or the receivers beneath this unconsolidated zone and thus had to be content with considerable damping of the seismic signal. Therefore, although P-reflections might be present, they are not observed at offsets larger than 40 m. From figure 4.3b it is clear that for traces at offsets smaller than 10 m useful information is obscured due to the interference of surface waves and body waves. During all further recordings a minimum offset of 9 m and a geophone spacing of 3 m was chosen resulting in a 42 m offset for the last receiver.

In high resolution seismic surveys, we generally can not afford to shift shot- and receiver positions more than a few centimeters. Since drilling had to take place at all shot- and receiver positions, problems in maintaining this accuracy were inevitable when high voltage cables, gas and drainage pipes, and paved roads had to be crossed. Whenever necessary we tried to use shots and geophones at the surface. During the processing sequence however, these recordings showed to be of inferior data quality and had to be discarded.

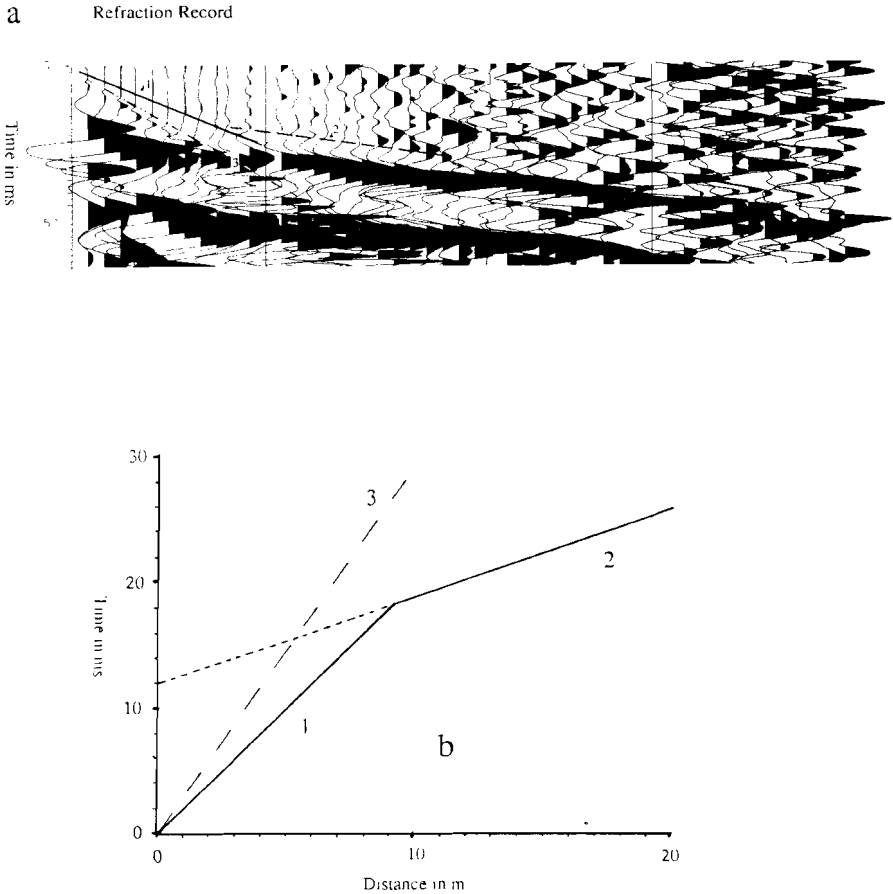


**Fig. 4.4a-b.** Refraction shot showing direct wave (1), refracted wave (2) and ground coupled sound wave (3) and the corresponding X-T graph.

#### 4.5 REFRACTION INTERPRETATION

Before the actual reflection survey took place a refraction record was acquired (Fig. 4.4a). The first arrivals of this record were digitized and plotted in an X-T graph (Fig. 4b). The direct wave is difficult to recognize since the angle of incidence is almost horizontal (the vertical geophones will not record horizontal motion). Nevertheless after an amplitude blowup a direct wave with a velocity close to 500 m/s can be found. The second branch of the X-T curve, with a velocity of approximately 1500 m/s, belongs to the wave refracted at the base of the low-velocity zone. From the intercept time of this high velocity branch with the T-axis the thickness of the low velocity zone can be calculated. This thickness is

approximately 3 m. In the X-T graph we also see a 342 m/s branch induced by the ground-coupled sound wave (a surface source was used for the refraction measurements).

The velocity contrast at 3 m depth probably coincides with the Holocene- Pleistocene boundary. Further detail within the upper 3 m is not found. As expected from figure 4.2, deeper refractions were not visible.

#### 4.6 DESCRIPTION OF THE RAW DATA

Figure 4.5 shows a collection of shots from the Woerden survey. A clear change in data quality along the line is visible. The first 20 shots are of moderate quality. The next 25 shots are rather bad and the last 15 shot records show the same data quality as the records in the first part of the profile. Obviously changes in geology occur that are beyond the lateral resolution of the model of figure 4.2.

The refraction interpretation indicated a low-velocity zone of approximately 3 m thickness. At the base of this zone we find a strong velocity contrast (500 - 1500 m/s) causing a strong refracted P-wave. Assuming a density increase at this boundary the expected reflection coefficient is at least .5 for reflection at normal incidence inducing strong reverberations in the dataset. Refraction multiples (velocity of 1500 m/s) can easily be traced in the data. The number of refraction multiples increases as a function of increasing offset. Interpretation of the first arrivals of the reflection survey might give us information on the lateral changes in the thickness of the top layer.

The critical angle for a wave reflected at the base of the Holocene is approximately  $20^\circ$ . Primary reflections at the base of the Holocene become critical at small offsets (approximately 2 m for a layer of 3 m thickness). In our data set the minimum offset used is 9 m and the primary reflections at this interface will thus be super-critical. Multiple reflections at the Holocene-Pleistocene boundary are also visible in data set. They become critical or supercritical as a function of increasing offset. An amplitude anomaly near the critical angle can be seen in the reflection multiples.

The multiple reflections at the base of the Holocene, and in general multiple reflections at the base of any low-velocity top layer, can be seen as the most disturbing factor in high resolution seismics on land since they obscure all deeper reflections. However, these multiples contain the shallowest reflection information available, since the primary reflection at a shallow interface is usually masked by surface waves and refracted waves.

Shots and receivers are not at the free surface. Due to this configuration a shot ghost and a receiver ghost is recorded. When shots and receivers are at the same depth, and also the velocity at the shot- and receiver position is the same these ghosts partly coincide. The total signal can then be seen as a primary wavelet and two 'pseudo' ghosts. For shots and receivers at 1 m depth and a velocity of 500 m/s these 'pseudo' ghosts are delayed by approximately 4 ms and 8 ms (vertical incidence), the first ghost having twice the strength of the primary signal but being opposite in sign, the second being equal to the primary (Fig. 4.6). The observed source signal can be seen as the composition of the primary signal and

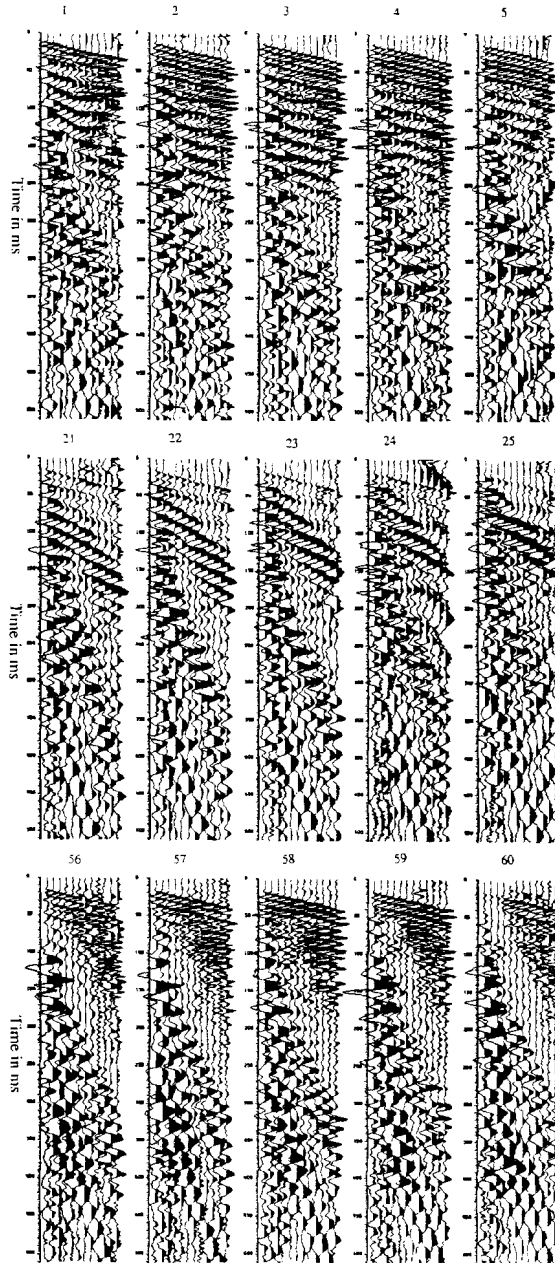
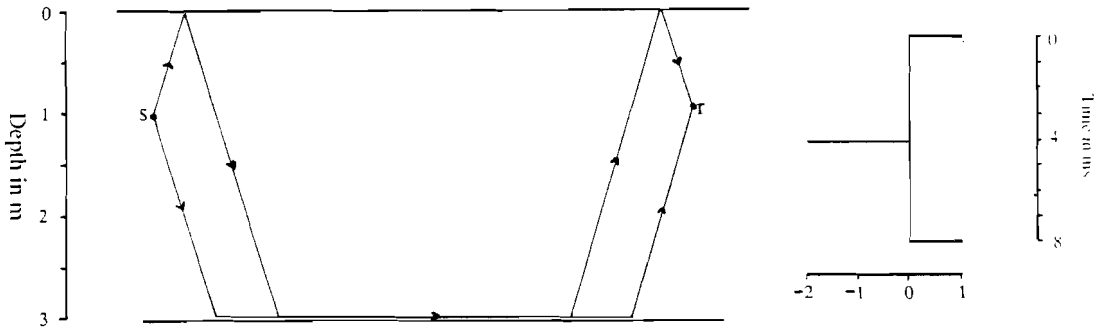


Fig. 4.5. Characteristic shots from the reflection survey. Shots 1 to 5, 21 to 25 and 56 to 60 are displayed.



**Fig. 4.6.** Shotpoint (s) and receiver location (r) relative to the surface and the ghosts that are induced by this configuration for a layer with a velocity of 500 m/s.

the two ghosts. It will therefore have a characteristic period of approximately 8 ms.

The following items have a strong effect on the shape of the frequency spectrum of the reflection data (Fig. 4.7):

- 1) the bandwidth of the source signal
- 2) the response of the receivers
- 3) the response of the recording unit
- 4) frequency attenuation in the weathered layer
- 5) reverberations in the weathered layer (Fig. 4.8)

The frequencies generated by the explosive source are limited to 500 Hz. The actual bandwidth of the recording equipment (receivers and seismograph) is approximately 100-800 Hz thus the response of the 100 Hz geophones partly disturbs the spectral shape of the source signal in the low frequency region. The bandwidth of the source signal is not assumed to change much during the survey, neither will the response of the receivers and the seismograph. Therefore changes in weathering layer properties (such as thickness and velocity) are the main causes of spectral changes during the survey. These changes manifest themselves in two ways. In the first place a thickening of this layer causes the attenuation of high frequencies to increase and will thus change the spectrum. In the second place reverberations in the weathered layer will act as a filter the spectral response of which is partly shown in figure 4.8. A change in the thickness of this layer causes a change in the shape of this response. In practice the thickening of the weathered layer results in a frequency decrease of the data.

It was hoped to find S-wave information in the data, but although these waves may be present they are not visible in the shot records. For a combined interpretation of S- and P-waves one needs two- or three-component data.



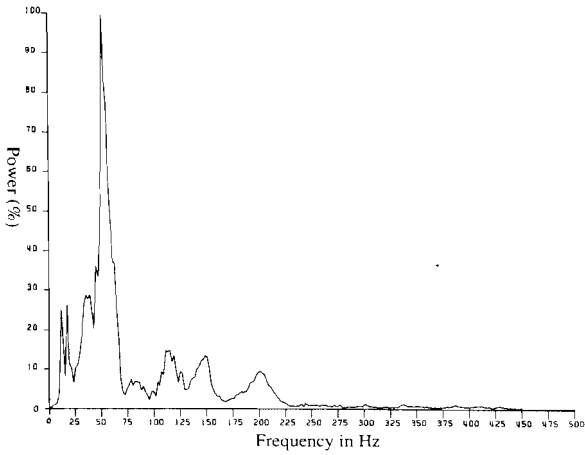


**Fig. 4.7.** Characteristic frequency spectrum of the raw field data.

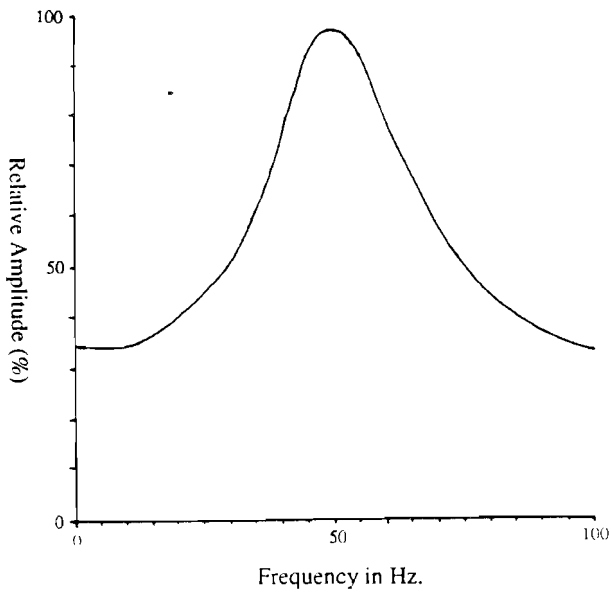


**Fig. 4.8.** Theoretical frequency response of the weathered layer based on a reflection coefficient of .5 at the base of this layer, interval velocity of 500 m/s and a thickness of 2.5 m. This response will show harmonics at 100 Hz intervals.

#### 4.7 FIRST ARRIVAL INTERPRETATION

The first arrivals of the reflection survey were used to determine lateral changes in the thickness of the low-velocity layer. Due to an initial offset of 9 m and a maximum offset of 42 m all first arrivals in the reflection survey are induced by the refraction at the base of this layer. A model of the low-velocity zone was constructed based on the assumption that only small changes in the velocity of this layer would occur and that all changes in arrival times are thus caused by changes in the thickness of this layer. Intercept times for all shot positions and all receiver positions were calculated by means of extrapolation of the high velocity branch in the X-T graph for all the shots of the reflection survey. Figure 4.9 shows lateral changes in intercept time for all field positions. Since both shots and geophones were placed at depth, we have to add these depths in order to calculate the real thickness of the low-velocity layer (depth of shot and receivers is approximately 1 m). We found variations in the thickness of the Holocene between 2.5 and 6 m.

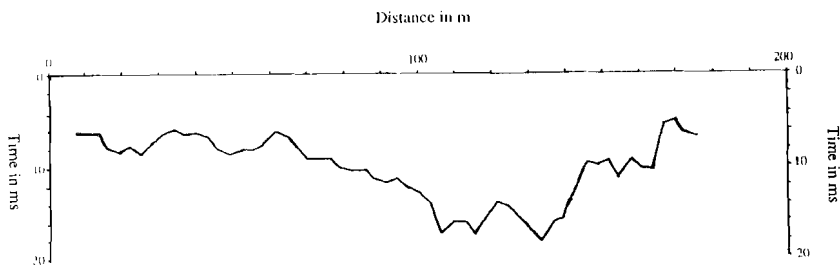


**Fig. 4.9.** Intercept times calculated for geophone- and shot-positions using shots from the reflection survey and based on a constant weathering layer velocity of 500 m/s.

The model deduced from the refraction interpretation contains the shallowest information that can be extracted from the data and is therefore part of the result. On the other hand it serves as input for the further processing sequence, since we use this model to determine static corrections. It can further be used for dereverberation filtering. However, one must realize that the assumption on the velocity of the low-velocity layer (no velocity changes were taken into account) induces an error in the determination of the thickness of this layer and thus in the geological model. The relative error in the thickness of the

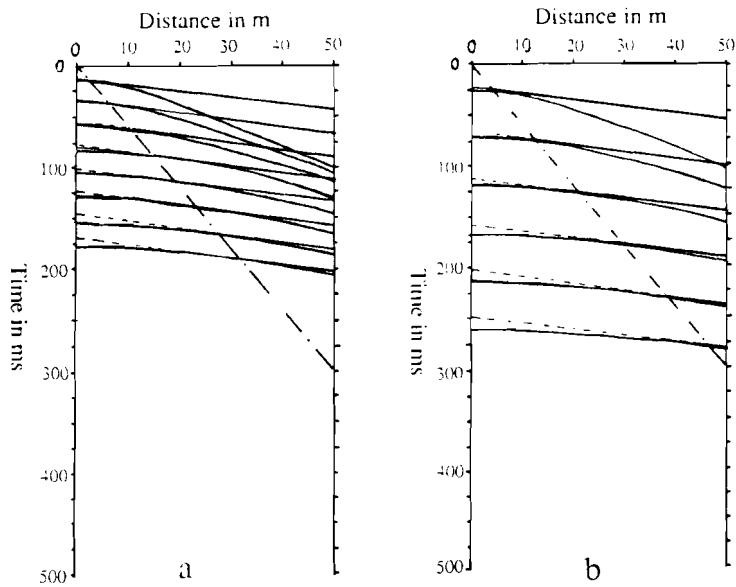


**Fig. 4.10a-b.** Expected arrival times for reflections and reflection multiples at the base of the weathered layer and refractions at this interface and their multiples. Also indicated is the critical angle as a function of offset and multiple number. Figure 4.10a shows the response for a layer of 3 m thickness. Figure 4.10b shows the response for a layer thickness of 6 m. In both cases the velocity is 500 m/s. Only even multiples are displayed. Figure 4.10a and 4.10b can be compared with shot 1 and 21 of figure 4.4.

weathered layer is approximately equal to the relative error in the velocity of this layer. The actual error in the model will be in the order of decimeters. In addition errors in the velocity of the weathered layer also affect the static corrections. Nevertheless, as long as the velocity contrast at the base of the low-velocity layer is strong a change in the velocity of this zone will only have a small influence on the static corrections. The relative error in static correction time is approximately equal to the relative velocity error multiplied with the ratio of the velocities of the low- and high velocity zone. The effect of velocity errors on reverberation filtering can be neglected as far as delay times are concerned. Reflection strength, however, is influenced by lateral velocity changes and additional information on actual multiple strength might therefore be needed.

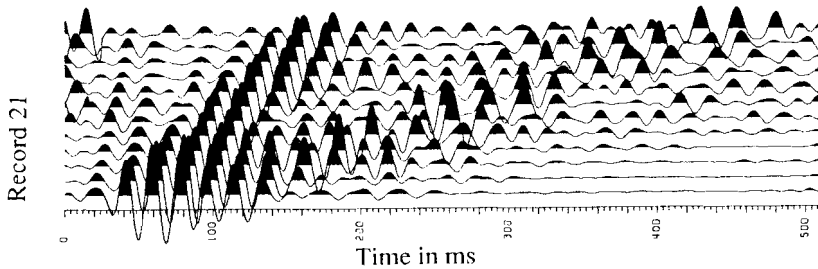


**Fig. 4.11 a.** Record 21 after the application of a low-pass frequency filter (40-80 Hz) showing strong multiple reflections at the base of the weathered layer.

#### 4.8 GUIDED WAVES

Throughout the whole survey supercritically reflected waves showing strong reverberations can be observed. These waves are known as guided waves and are generated in a low-velocity surface layer. These waves are commonly found in marine data as a result of the water layer. Guided waves are strongly dispersive when the thickness of the low-velocity layer is small compared to shot-receiver distances and wavelength of the seismic signal. Pekeris (1948) described wave propagation in a surface layer using the normal mode theory for a liquid layer over an acoustic half space. A more general approach was given by Press and Ewing (1950).

The guided wave obscures all later arrivals and is therefore often regarded as noise despite of the information it carries. Especially changes in the thickness of the low-velocity layer and in the velocity and density contrast at the base of this layer cause strong variations in the shape of the guided wave.

Figure 4.10a shows the expected arrival time curves for refraction, refraction multiples, reflection and reflection multiples at the base of a layer of 3 m thickness and a velocity of 500 m/s (this is the model derived from the refraction interpretation). Figure 4.10b shows the same curves for a layer of 6 m thickness. The line with apparent velocity of approximately 167 m/s indicates the critical offset for successive multiples. Amplitudes are strong in the vicinity of this line. The synthetic arrival time curves are remarkably similar to the observations. All events can be recognized when one takes into account a timeshift of 4 ms due to shot-and receiver depth. Even the amplitude anomaly at critical incidence can be seen (Fig. 4.5).

As stated, the guided wave contains very shallow information. To extract this information from the data the following experimental processing scheme was used:

- 1) Separation of the guided wave from all other data by means of a bandpass frequency filter and trace muting (Fig. 4.11a).
- 2) Determination of a velocity function for NMO correction that preserves multiple information. This function is independent of arrival time.
- 3) Common Midpoint stacking with this velocity function (Fig. 4.11b).

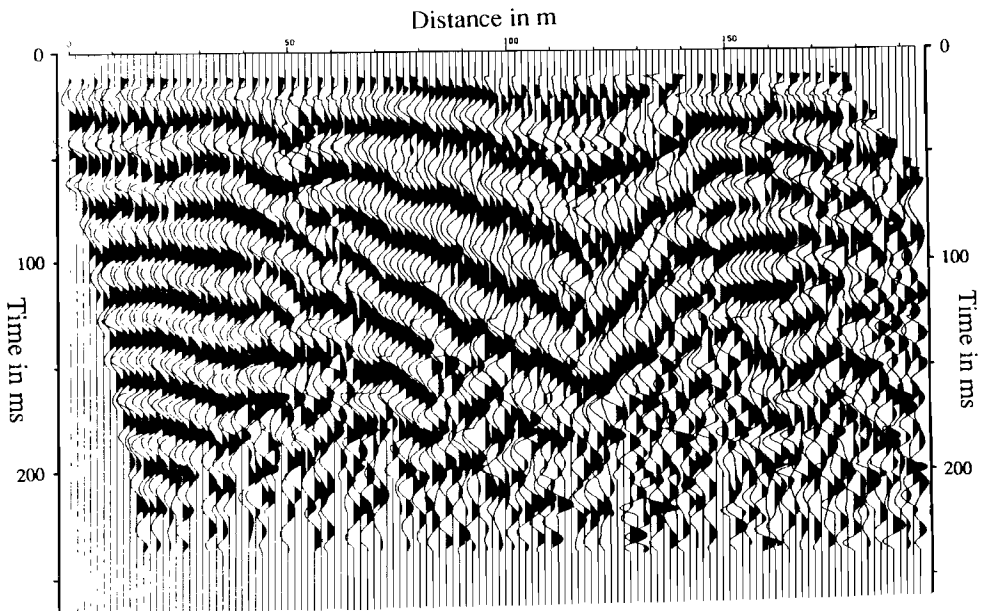


**Fig. 4.11b.** Data after Common-Mid-Point stacking using a constant stacking velocity of 500 m/s. Note the strong weathering layer multiples.

Figure 4.11b shows reflections at the base of the weathered layer with all their multiples. In addition a number of fractures intersecting the base of this layer indicated by diffraction hyperbolae are recognizable. A travel time model of the weathered layer based on this stacked section is presented in figure 4.12. Comparison of this model with the intercept times from the refraction interpretation (Fig. 4.9) shows a resemblance except for a constant timeshift of approximately 4 ms. This shift is due to the use of shot- and receiver

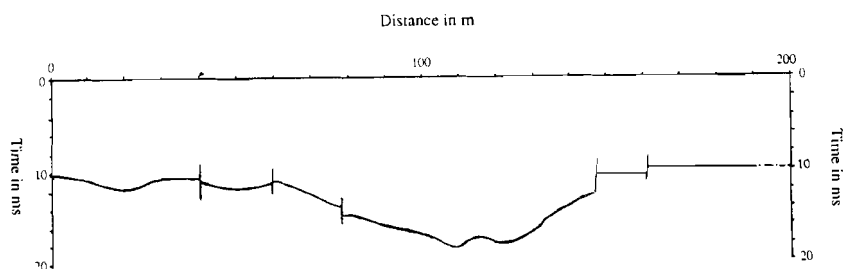


**Fig. 4.12.** Model of the weathered layer (given in two-way travel times) based on the processing of guided waves.

positions at 1 m depth.

#### 4.9 PROCESSING STRATEGY

The model of the shallow subsurface presented is based on refraction interpretation and the processing of supercritical reflections and multiples from the base of the low-velocity layer. To extract information from deeper geological structures the effects of this top layer have to be eliminated. Before continuing with a description of the processing strategy a summary of all the elements that influence the generation and distortion of the seismic signal in the weathered layer is given.

The three phenomena that more or less affect all seismic records in the survey are:

- A configuration with shots and receivers at depth introduces ghosts in the seismic records.
- A strong impedance contrast at the base of the Holocene introduces reverberations.
- High frequencies are strongly attenuated in the weathered layer.

In addition the low-velocity zone changes laterally in thickness. These thickness variations cause changes in arrival times of deeper reflections, changes in multiple delay time, and changes in frequency content of the recorded data.

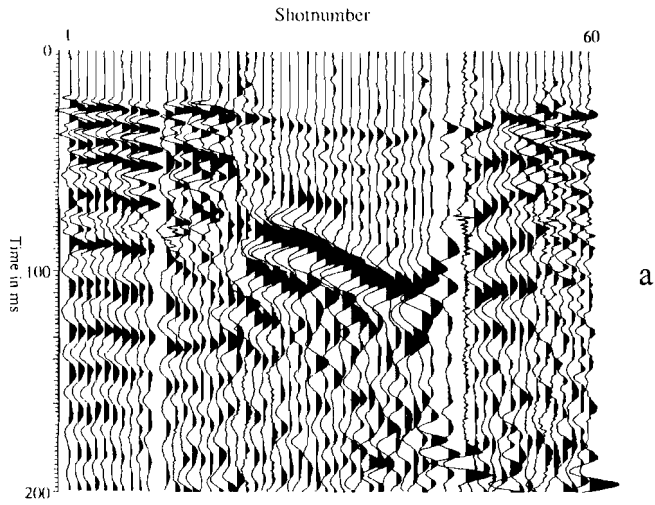
In order to correct for low-velocity layer effects multiples (dereverberation), arrival time changes (static corrections) and changes in frequency content (spectral balancing) have to be taken into account during the processing. In addition we have to correct for the ghosts (de-ghosting). After these processing steps the data set simulates the seismic data set we would acquire without the presence of a low-velocity top layer with shots and receivers at the free surface.

All the processing steps mentioned can be performed. Shot depth, receiver depth and velocity are known and deghosting can be performed. Velocity and thickness of the low-velocity layer are known thus dereverberation filters can be applied. Intercept times can be used for static corrections. Even spectral balancing can be done since spectral changes as a function of changes in the thickness of the low-velocity layer can be estimated. These operations would depend on location but this is not an insurmountable problem.

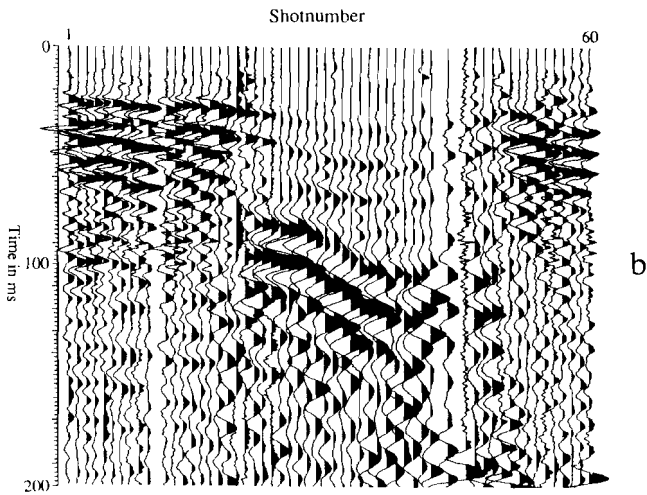
However, the delays of the ghosts are different when velocities change. The reverberation time and the actual multiple strength depend on the angle of incidence and differ for reflected- and refracted waves. Small changes in reverberation time and multiple strength are also expected as a function of reflection depth. A change in frequency content will not only occur when the thickness of the low-velocity zone varies but will also show within one trace as a function of travelled distance through the low-velocity layer. Hence, low-velocity layer multiples are expected to be of relatively low frequency in comparison with primary reflections arriving at the same time.

Figure 4.10 clearly shows the change in multiple delay time as a function of offset. A dereverberation filter that is based on the delay of the refraction multiple will not improve the data when far offset low-velocity layer multiples are dominant. This is clearly seen in figure 4.13 between shots 20 and 40. Here a simple Backus filter was applied to deal with the low-velocity layer multiples using delay times deduced from refraction and guided wave interpretation.

Due to poor knowledge of the velocities in the weathered layer and problems in the spectral balancing per trace caused by the interference of primaries and multiples another approach to permit further processing might be suggested. As a preliminary processing method a simple frequency filter (bandpass) was chosen to deal with multiple suppression and spectral balancing. This frequency filter also suppressed low-frequency surface waves and high-frequency noise. Wavenumber filters and velocity filters were tested but were not actually applied because of aliasing problems. De-ghosting did not improve data quality and was not applied. A constant velocity model was used to perform static corrections.



a



b

**Fig. 4.13.** Common offset display (offset used is 24 m) before (4.13a) and after dereverberation filtering (4.13b).



## 4.10 ACTUAL PROCESSING PARAMETERS

Figure 4.3 shows some characteristic shots of the Woerden survey. It can be seen that arrival times increase and characteristic frequency decreases as the weathered layer thickens.

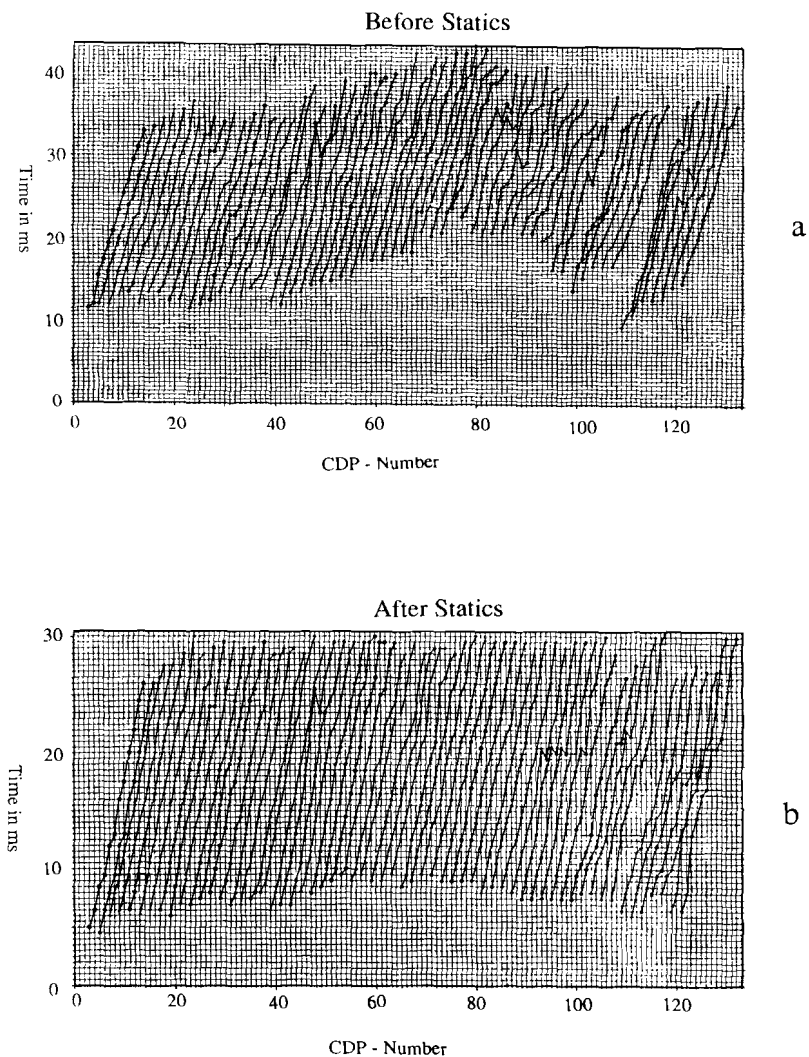


**Fig. 4.14.** Digitized first arrival times of all seismic records plotted as a function of midpoint before statics (figure 4.14a) and after statics (figure 4.14b).

In figure 4.14a all first arrival times are plotted as a function of shot and receiver position. Intercept times were calculated and static corrections were carried out. In figure 4.14b first arrivals are plotted after statics. As expected we can still see the same trend in the curves (a proper static correction will not necessarily yield constant first arrival times for all receivers with the same offset). Some errors remain due to mispicks but residual statics should deal with them.

Spectral analysis of shot 1 (Fig. 4.15a) shows coherent P-wave energy up to 400 Hz for the first shot. Shot 21 (Fig. 4.15b) shows no coherent signal above 200 Hz. Disturbance of the data due to surface waves and weathering layer multiples is most prominent below approximately 125 Hz. Based on this information a bandpass filter with corner frequencies at 150 and 450 Hz with a 25 Hz taper was applied. Using a uniform passband for the whole line induces a decrease in signal-to-noise ratio in the area between shots 20 and 45. Figure 4.16 shows some of the shots after frequency filtering. Strong reverberations of the refracted wave are still visible. They can be reduced in amplitude by means of stacking. The guided wave and all its multiples are suppressed by the frequency filter, and stacking will also decrease their strength.

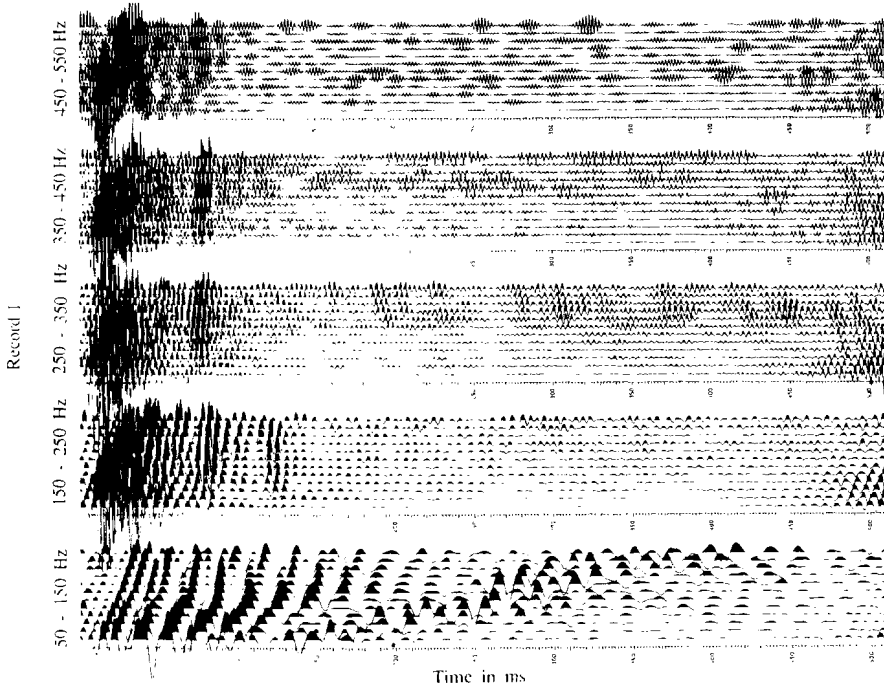


**Fig. 4.15a.** Amplitude as a function of different frequency pass bands for shot 1 (Fig. 4.15a) and shot 21 (Fig. 4.15b) indicating the changes in high frequency attenuation caused by the thickening of the weathered layer.

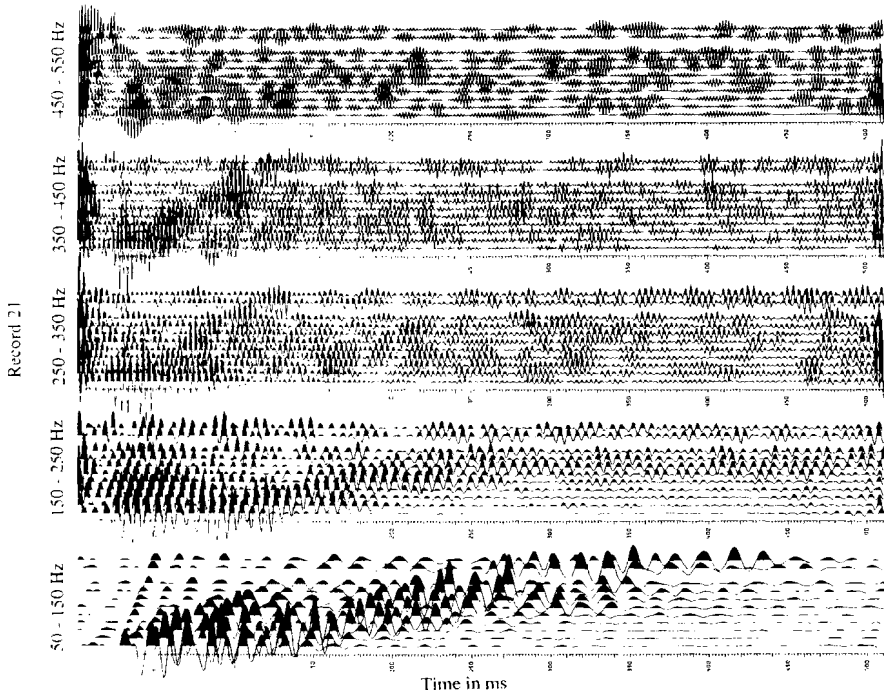


**Fig. 4.15b.**

Data were rearranged in a common midpoint assembly and a preliminary stacking velocity analysis took place. The resultant velocity profile was used for residual statics. After these statics a new velocity profile was derived and residual statics were updated. After several iterations a final velocity profile was constructed and actual stacking took place. Figure 4.17 shows the stacked section. Finally, a compilation of all the information obtained is given in the model of figure 4.18. Since no other velocities were available the stack velocity profile was used to convert times into distance.

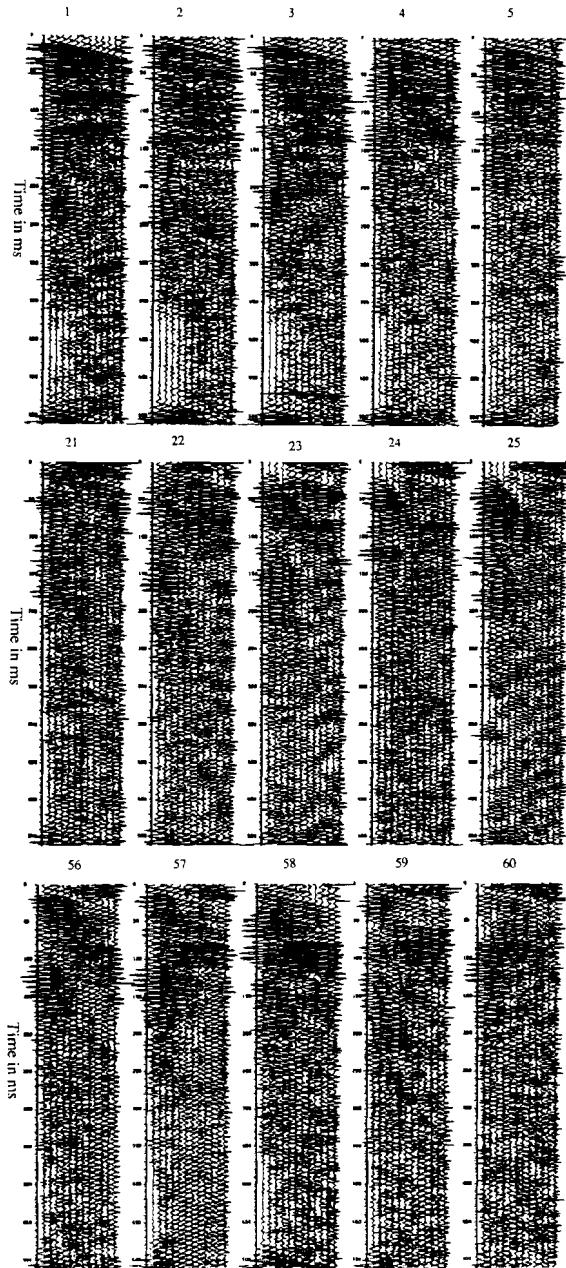
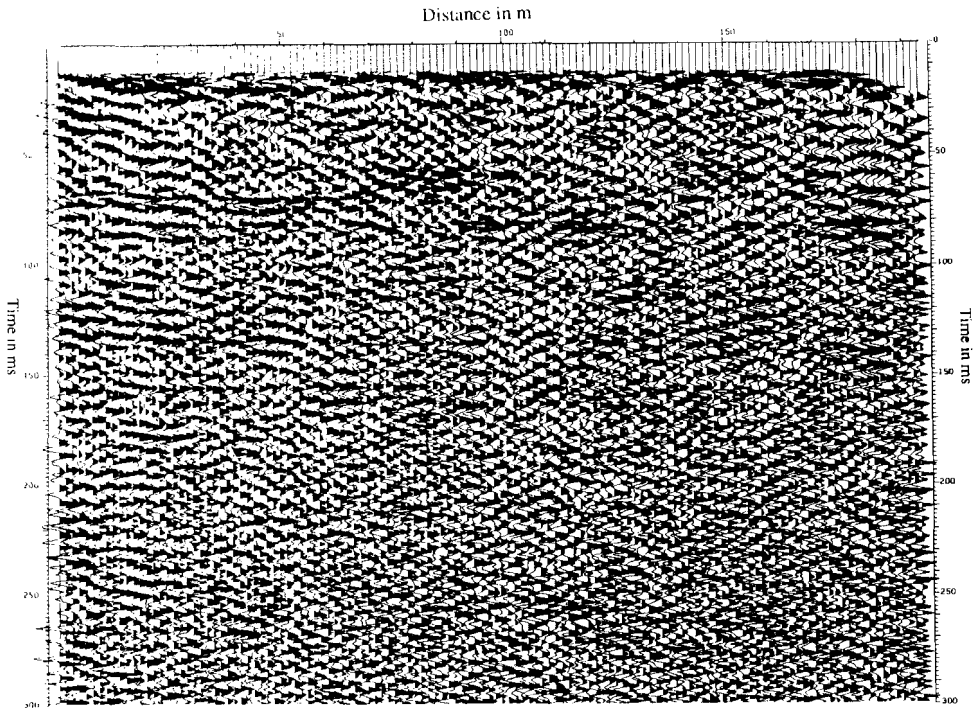


Fig. 4.16. The same shots as in figure 4.5 after frequency filtering (150-450 Hz pass band).



**Fig. 4.17.** Stacked section after frequency filtering, refraction statics, residual statics and CMP-stacking.

#### 4.11 DISCUSSION

Primary goal of this research was to determine whether seismic methods could be used to obtain information on shallow structures under difficult field conditions. The answer to this question gave rise to at least three related problems: do we physically understand the data we acquire, do we have the tools to remove unwanted information from the data set either in acquisition or in processing, and is there any relevant information in the data at all.

In this paper we gave a plausible explanation of the shape of the shot record. We know how the seismogram is physically generated and we understand - if not completely then at least part of - the data we acquire.

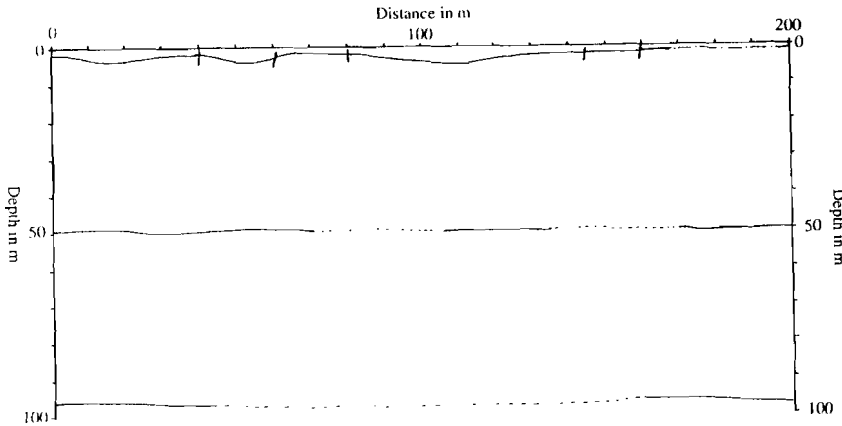


**Fig. 4.18.** Combined interpretation of the refraction information, the processing of guided waves, and the stacked section of figure 4.17.

The second problem, providing the tools to remove unwanted information from the data set is not completely solved. As far as acquisition is concerned the only way to get rid of the low-velocity layer effects (which is without question the most important operation in order to obtain deeper information) is to drill through this layer. Although this may be practically feasible the costs of a seismic survey would be significantly increased. On the other hand, knowledge of the thickness of the weathered layer is probably the shallowest information that can be acquired by seismic methods and we would like to use this knowledge in combination with information from deeper reflections. This means that we have to compensate for the blurring of deeper reflections caused by the seismic response of the weathered layer during the processing stage.

The way we handled the data during the processing sequence was far from ideal. We did perform static corrections to compensate for the time delay caused by the weathered layer but used a simple frequency domain filter to remove some of the weathering layer effects on deeper reflections. However, we tried to point out how a real 'deblurring' of the data, as far as weathering layer effect are concerned, should be performed by using dereverberation filters, multiple suppression methods, and spectral balancing.

The problem concerning the relevance of the obtained information is hard to solve. All other methods that were used to acquire information in this area either deal with other physical properties of the subsurface (as e.g. in E-M methods) or provide no lateral continuity (such as shallow borings). We can not expect to get information from P-reflections other than the seismic impedance and velocity distribution of the subsurface, thus comparing the seismic model with, e.g., a model based on electro-magnetic observations is problematic. The vertical resolution of the seismic method can not be

compared with the amount of detail in shallow borings. We deal with a wavelength of approximately 10 m and will see no more detail in the deeper reflections than 2.5 m. On the other hand the lateral resolution of the seismic survey is much better than the lateral resolution of the non-seismic measurements. The distance between the data points is 1.5 m for the seismic model. The non-seismic methods applied to gather the information displayed in figure 4.2 use at least 25 m spacing between the data points.

From the existing model of the Woerden area (Fig. 4.2) no reflections in the upper 50 m of the subsurface were expected except for the Holocene-Pleistocene boundary. Although an indication of new reflections at approximately 50 and 100 m was found in the reflection data no well control was available to verify these depths.

A preliminary conclusion that can be drawn at this moment is that from a geophysical point of view we see no unsurmountable problems in the acquisition and processing of seismic data in areas like this. Whether the information obtained is valuable for engineering geology remains to be seen. Shallow seismic profiling will certainly not improve the vertical detail. We can only hope to improve lateral resolution.

#### ACKNOWLEDGMENTS

The authors wish to thank J. Tempels for his field assistance, Prof. K. Helbig, Dr. J. van Deen, and Ir. H. den Rooijen for their constructive cooperation and discussion.

#### 4.12 REFERENCES

- Bredewout, J.W. and Goult, N.R. 1986. Some shallow seismic reflections. *First Break* 4 (12) 15-23.
- Deen, J.K. van 1987. De toepasbaarheid van niet destructieve methoden voor traceverkenning. *Report by "Grondmechanica Delft"*.
- Doomenbal, J.C. and Helbig, K. 1983. High resolution reflection seismics on a tidal flat in the Dutch delta: acquisition, processing and interpretation. *First Break*, 1 (5) 9-20.
- Hunter, J.A., Pullan, S.E., Gagne, R.A. and Good, R.L. 1984. Shallow seismic reflection mapping the overburden- bedrock interface with the engineering seismograph, some simple techniques. *Geophysics* 49, 1381-1385
- Hunter, J.A., Pullan, S.E., Burns, R.A., Gagne, R.A. and Good, R.L. 1985. The optimum offset shallow reflection technique: case histories. *S.E.G. Annual Meeting expanded technical abstracts*, 159-161.
- Jongerius, P., Brouwer, J.H. and Helbig, K. 1987. Calibration of the seismic stratigraphical response of tidal deposits. *Proceedings of the 12-th World Petroleum Congress* (5)
- Pekeris, C.L. 1948. Theory on propagation of explosive sounds in water. *Geol. Soc. Am. Mem.* 27.
- Press, F. and Ewing, M. 1950. Propagation of explosive sound in a liquid layer overlying a semi infinite elastic solid. *Geophysics* 15 111-148.
- Steeple, R.E., Knapp, R.W. and Miller, R. 1985. Field efficient shallow CDP seismic surveys. *S.E.G. Annual Meeting expanded technical abstracts*, 150-152.

## Chapter 5

# RAY-TRACING STATICS

As has been shown in the previous chapters weathering layer effects can seriously distort the seismic signal. One of the effects, changes in time delay as a function of changes in thickness and velocity of this layer, should be compensated for by means of static corrections. However, static corrections can not be performed in the usual way (i.e. a constant time shift as a function of travel time) for shallow reflection data. In this chapter a method is presented, based on a ray-tracing algorithm, that can be used to perform static corrections on shallow seismic data.

### 5.1 INTRODUCTION

Data quality in on-shore seismic exploration suffers from shallow subsurface inhomogeneities. Time shifts of several milliseconds may occur due to changes in topography and weathering layer thickness and velocity. These time shifts are recognized in standard seismic exploration, but since the depth of interest is usually large with respect to the weathering layer thickness and the velocity contrast at the base of this layer is also large the time shifts are regarded to be independent of reflector depth (record time). Hence the operation that corrects for these time shifts is called statics correction. Even if changes in time shift would occur as a function of depth these changes would be small compared to the wavelength of the recorded seismic signal.

High-resolution seismic profiling explores the shallow subsurface. Within the depth range of interest the timeshift induced by changes in topography and thickness and velocity of the weathering layer changes as a function of travel time. Even more important; the frequencies generated in shallow seismic exploration are much higher than the frequencies used in standard exploration and actual timeshifts can cover several periods. Thus, small errors in time shift will cause drastic changes in data quality during the stacking procedure.

In this paper it is shown that "static" corrections change as a function of travelled time



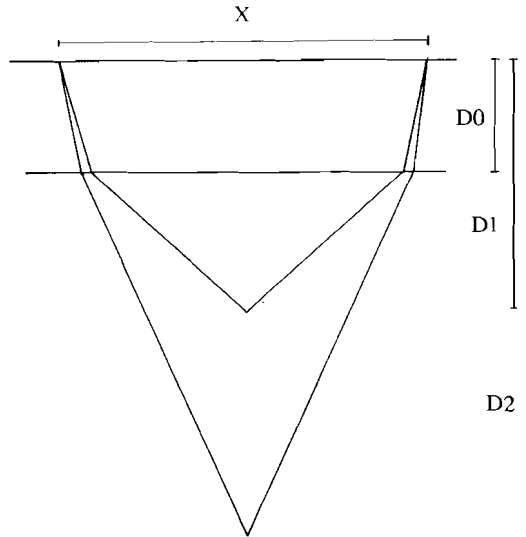


**Fig. 5.1.** Model of a homogeneous low-velocity (500 m/s) layer on top of a homogeneous high-velocity (1500 m/s) halfspace. Offset is given as  $X$ , depth of the base of the low-velocity layer and two virtual reflections as  $D0$ ,  $D1$ , and  $D2$ .

even for very simple subsurface models. Several standard algorithms for statics correction are used to process a synthetic dataset. Finally a new method for statics correction based on a stripping algorithm is introduced. Results of this method on a number of synthetic sections are given.

## 5.2 ARE STATIC CORRECTIONS REALLY STATIC?

To illustrate the behaviour of static corrections as a function of two-way travel time a simple model experiment was performed. The model consisted of a homogeneous low-velocity (500 m/s) layer on top of a homogeneous high-velocity (1500 m/s) halfspace (Fig. 5.1). Source and receivers were placed at the free surface and no topographic changes were assumed. A time-to-depth curve was calculated at 10 and 40 m offset by using a simple ray-tracing program. Because of the model symmetry only downgoing waves were taken into account.

As stated before static corrections are the time shifts that have to be applied in order to simulate the seismic record that would have been recorded with shot and geophone at datum level and without the low-velocity layer. As shots and receivers were on datum level

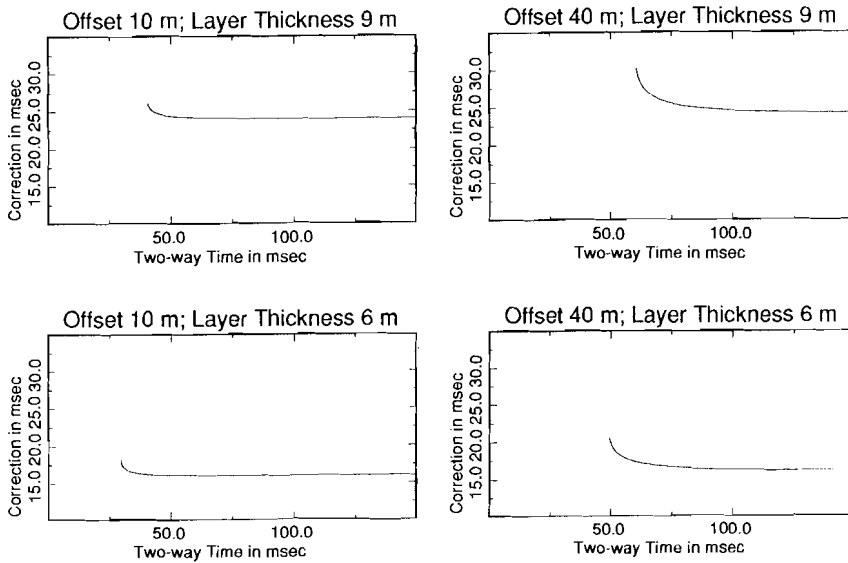


**Fig. 5.2.** Static correction time for several models and offsets as a function of two-way travel time.

in this model experiment only the low-velocity layer was taken into account.

A reference time-to-depth curve was calculated for a model without the low-velocity layer. Static corrections can now be defined as the difference between the reference curve and the actual time-to-depth curve. Fig. 5.2 shows the static corrections as a function of two-way travel time, low-velocity layer thickness, and offset.

It can be noted that static corrections are indeed static for arrival times that are large with respect to the time delay within the low-velocity layer. For shallow reflections, however, deviations of correction time are visible. These changes become more pronounced for increasing weathering layer thickness and offset. Although the effect is comparatively small actual time shift changes can be several periods in high-resolution surveys. Even more important conclusion may be that especially the shallowest reflections are affected.

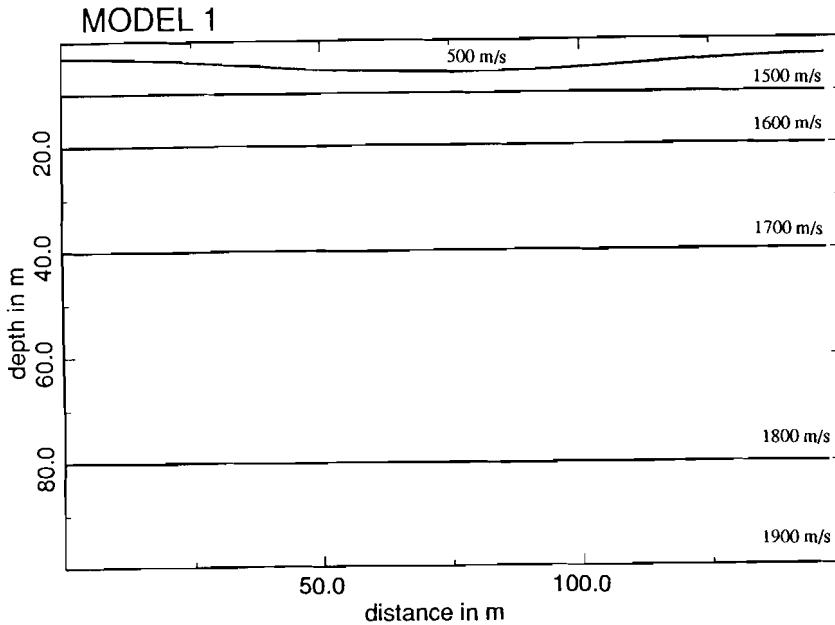


**Fig. 5.3.** Subsurface model (model 1) used to generate the seismic dataset shown in figures 5.4-5.6.

### 5.3 STANDARD METHODS IN THEORY

Methods that are used to correct for the effects the weathering layer and topography have on arrival times can be divided into field statics and residual statics.

The actual correction is defined as the sum of the time shifts needed to virtually place shots and receivers at the datum level and the time shift resulting from changing the weathering velocity into the sub-weathering velocity. Actual field statics can only take place when weathering- and sub-weathering velocities are known, when a depth model of the weathering layer is available (relative to datum level), and when source- and receiver positions are known (relative to datum level).

Residual statics basically assume the possibility to divide the total correction time into a shot related time shift and a receiver related shift. This assumption (also known as surface consistency) is extensively discussed by Hileman and Taner (1968) and Taner et al. (1974). Source corrections are constant for common-source gathers, receiver corrections do not differ within common-receiver gathers. Residual statics can handle relative time shifts between shots and between receivers. Regional effects are not covered by the theory.

Standard practice is to apply field statics to correct for structural (usually long wavelength) time shifts and use residual statics to handle residual shifts.

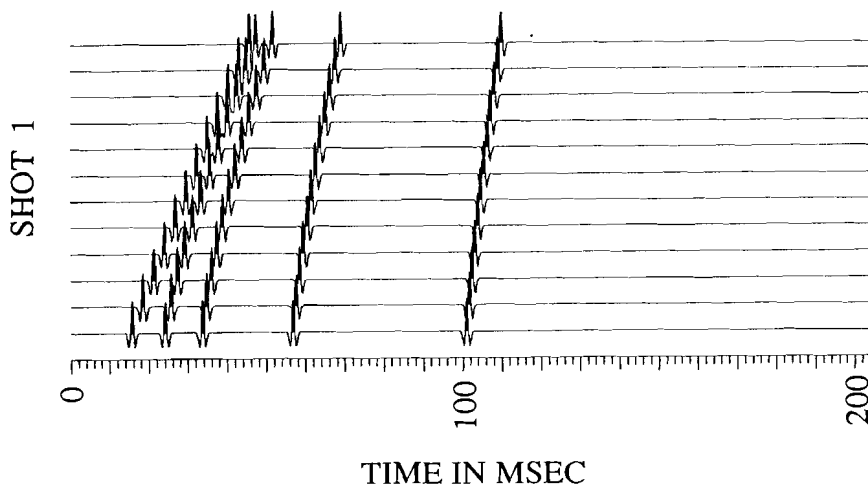
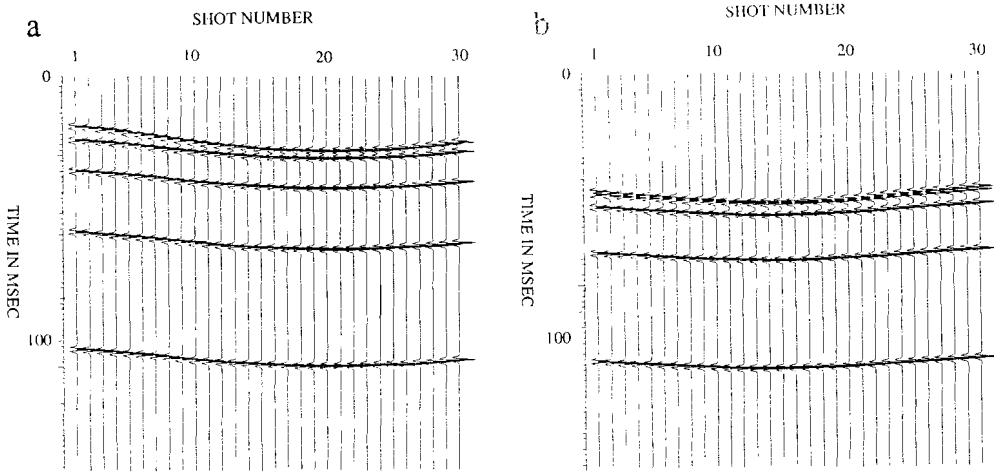


Fig. 5.4. Shot record showing the refraction at the base of the low-velocity layer and the primary reflections. Reflections at the base of the low-velocity layer are omitted.

#### 5.4 STANDARD METHODS IN PRACTICE

To test standard static correction methods for their applicability in shallow seismic exploration a synthetic dataset was generated using a simple ray-tracing program. The first model used is given in Fig. 5.3. A set of horizontal reflectors is covered by a weathered layer showing a synclinal shape. A total of 30 shot records was used. Each record consisted of 12 channels. Spacing between receivers was 3 m, offset first receiver was 9 m, and the distance between shots was also 3 m resulting in a 6-fold CDP-coverage. All shots and receivers were placed at datum level. A shot record is given in Fig. 5.4. Reflections at the base of the weathered layer are muted, deeper reflections are visible as well as the wave refracted at the base of the weathered layer. Two Common-Offset sections (Fig. 5.5) show the seismic response of this model at 9 m (Fig. 5.5 a) and 42 m (Fig. 5.5 b). It can be noted that residual statics will be of no use since the reflections show up rather smooth. Flattening of first arrival times, which is still a commonly used method, will not do any better as first arrival time curvature differs from the curvature of deeper reflection. Thus, field statics were applied, the results of which are shown in Fig. 5.6 (the refracted wave is omitted for reasons of convenience). All reflectors are more or less horizontal and no weathering effects remain at first sight. When we compare the Common-Offset section of Fig. 5.6 with the sections as they should have been without the weathered layer (Fig. 5.7) we see that shallow reflections are not correct for the far offset section.



**Fig. 5.5a-b.** Common-Offset Sections of model 1 at 9 m (Fig. 5.5a) and 42 m (Fig. 5.5b) offset.

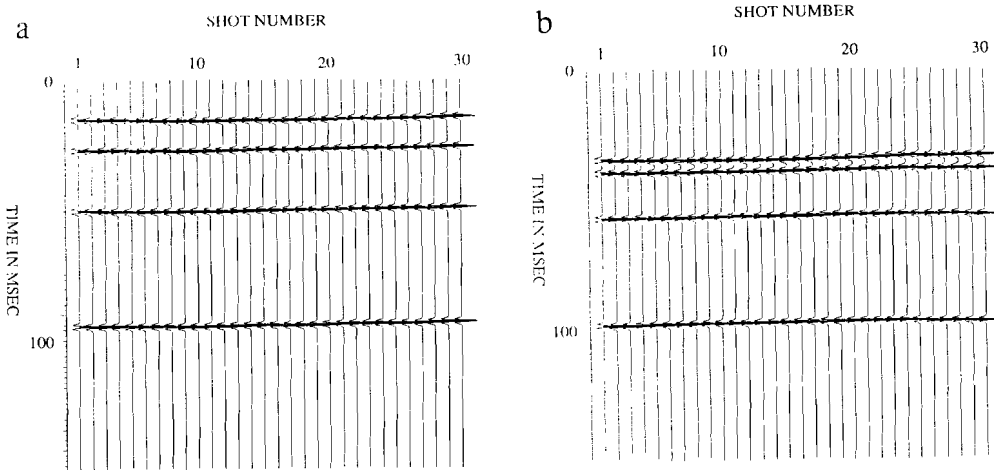


**Fig. 5.6a-b.** Common-Offset Sections of model 1 after field statics.

Model 2 was used to generate the sections in Fig. 5.9. The thickness of the weathered layer increases from 1 to 9 m. The next reflector is found at 12 m depth. Figures 5.10 and 5.11 respectively show the sections after field statics and the desired output. Some residual statics are needed for the deeper reflections. However, residual statics will not correct for the overall misfit of shallow events. From these examples it may be obvious that neither standard field statics nor residual statics will generally render acceptable results for shallow events.

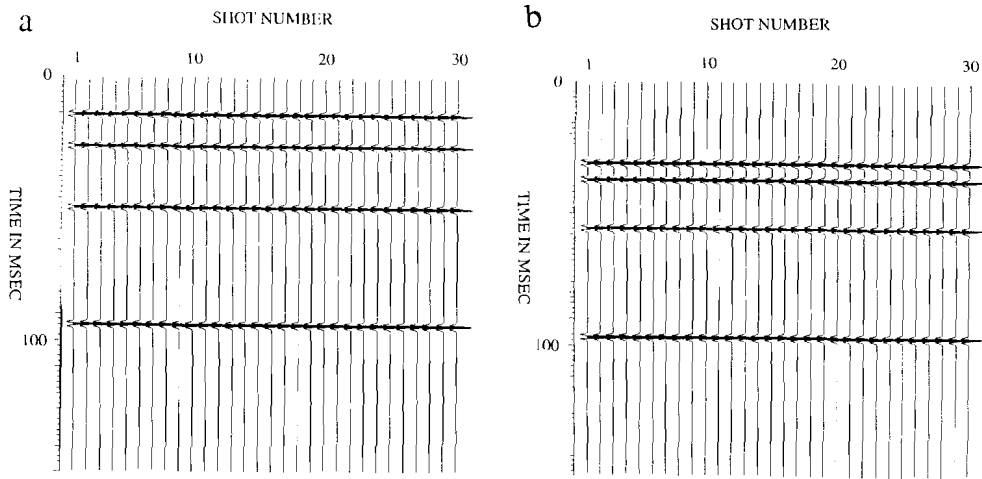


Fig. 5.7a-b. Common-Offset Sections of model 1 without the low-velocity zone.

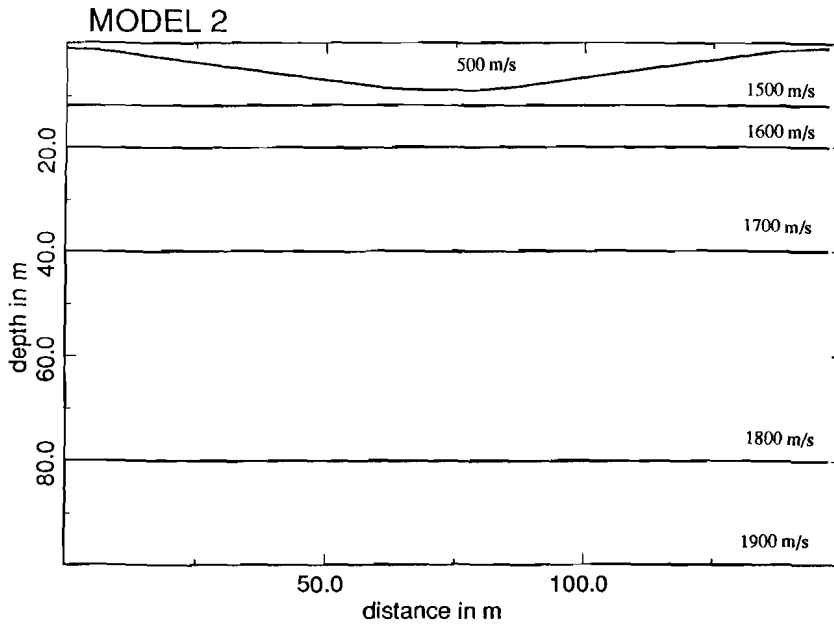
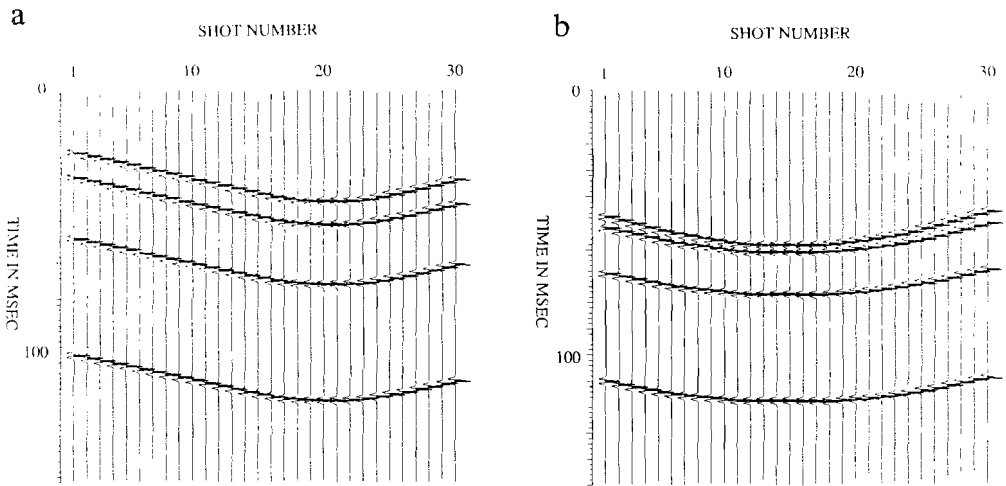
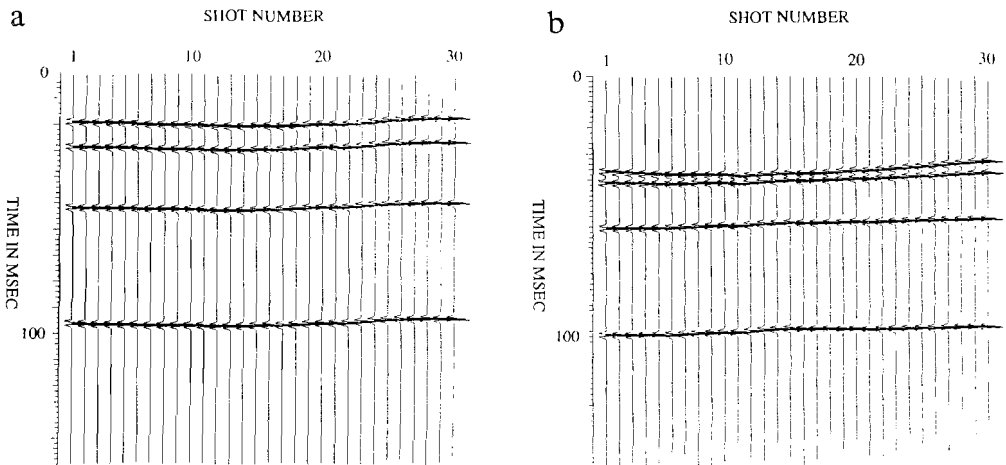


Fig. 5.8. Subsurface model (model 2) used to generate the seismic dataset shown in Fig. 5.9-5.11.



**Fig. 5.9a-b.** Common-Offset Sections of model 2 at 9 m (Fig. 5.9a) and 42 m (Fig. 5.9b) offset.



**Fig. 5.10a-b.** Common-Offset Sections of model 2 after field statics.

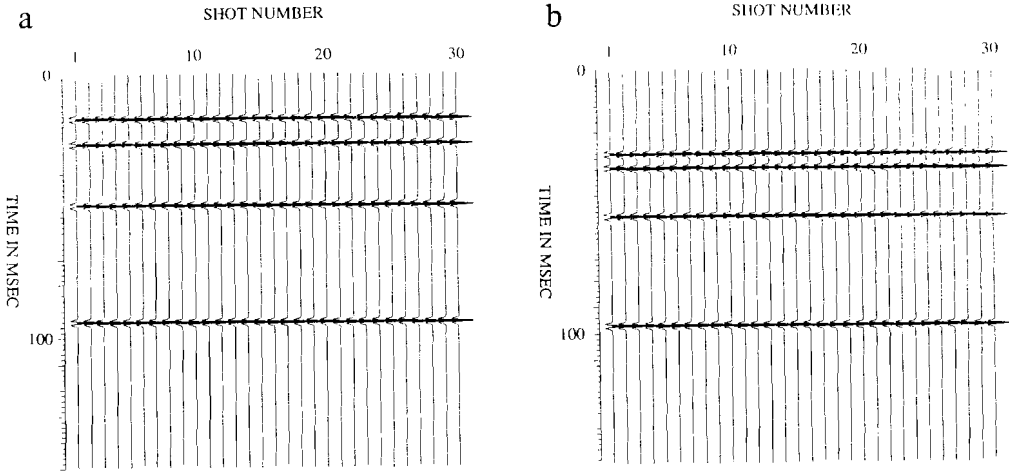


Fig. 5.11a-b. Common-Offset Sections of model 2 without the low-velocity zone.

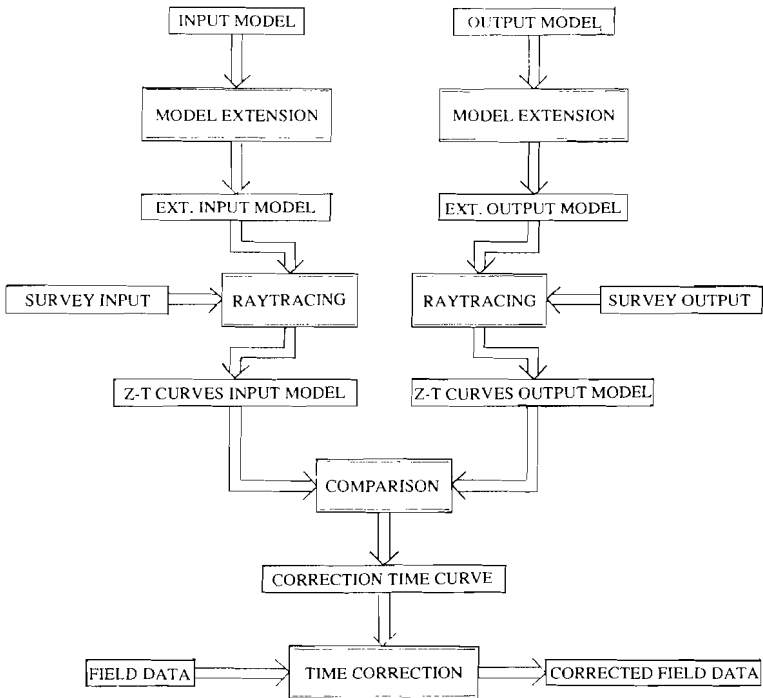


Fig. 5.12. Flow diagram of the ray tracing statics method.



### 5.5 RAY-TRACING STATICS

Since standard techniques for static corrections yield inferior results for shallow structures a new method based on ray-tracing was developed. This method was based on the following assumptions:

- a model of the structures and the velocities that need to be replaced are known.
- the replacement velocity is known.
- coordinates of sources and receivers are known.

The problem of performing "static" corrections can now be attacked by using the flow diagram in Fig. 5.12.

The layers and velocities that must be corrected for are given in the input model. The desired output, in general a homogeneous halfspace, is given in the output model. In the survey input the actual field positions of all sources and receivers are given. The survey output defines the field positions as they should be after correction (usually at datum level).

The first step in the scheme is the downward continuation of the input- and output model. This can be done, eg., by adding a laterally homogeneous halfspace with constant velocity, or a linear velocity increase with depth. Both for the extended input- and output model synthetic Z-T curves are calculated using survey input- and output parameters. This is done for all source receiver combinations. Comparison of the in- and output curves results in a time shift curve as a function of travel time. Finally actual field data are corrected using this curve.

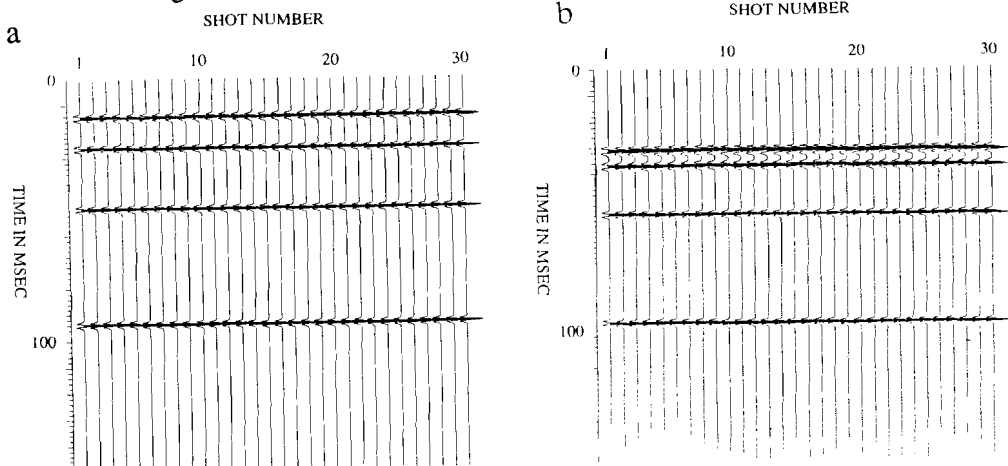
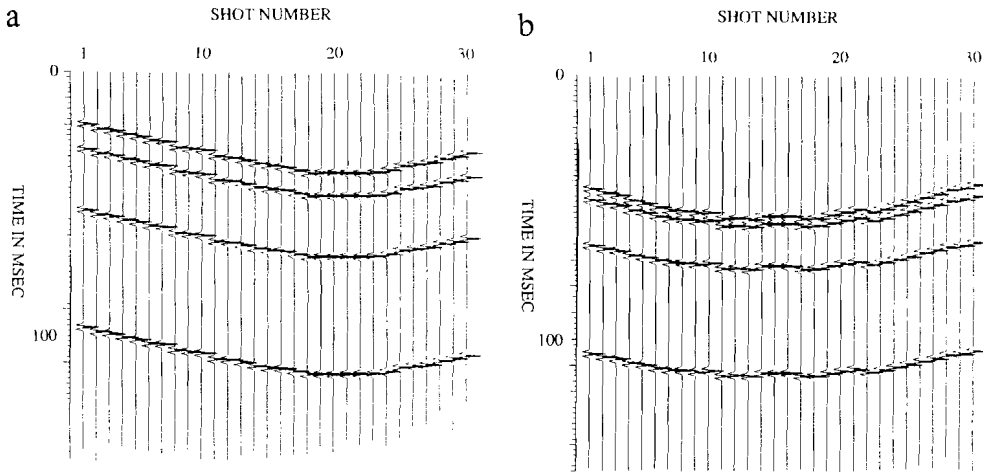


Fig. 5.13a-b. Common-Offset Sections of model 1 after the application of raytracing statics.



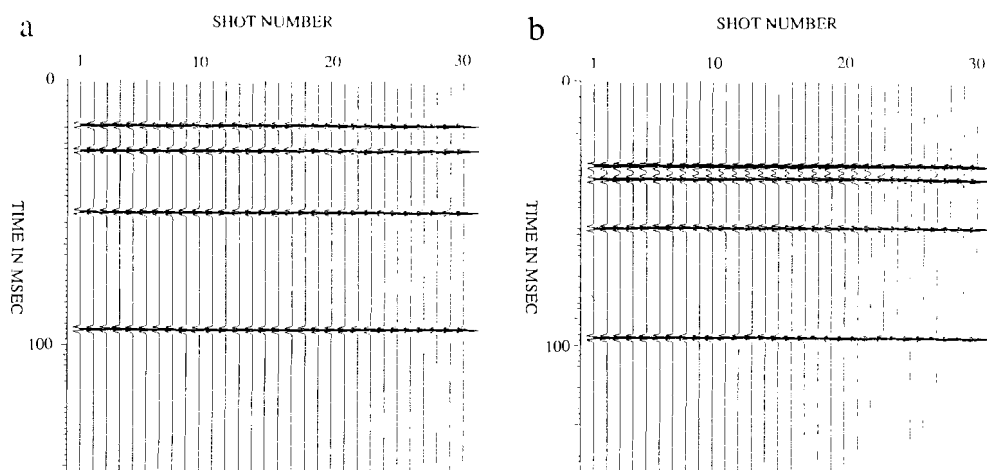
**Fig. 5.14a-b.** Common-Offset Sections of model 3 at 9 m (Fig. 5.14a) and 42 m (Fig. 5.14b) offset.

Fig. 5.13 shows the results of ray-tracing static corrections applied to the dataset of model 1 using the toplayer as input model. The corrected sections completely resemble the desired output (Fig. 5.7) although no information on deeper reflections was specified. Also the dataset belonging to model 2 could be completely corrected.

## 5.6 TOPOGRAPHIC CORRECTIONS AND LATERAL INHOMOGENEITIES

As may have been concluded from the flowdiagram in Fig. 5.12 topographic corrections are implicitly covered by the ray-tracing method. As long as all coordinates (input model and field coordinates) are known relative to the datum level and output field coordinates are specified at datum level no separate topographic corrections need to be performed. This is shown in Fig. 5.14. Model 2 was used to generate the dataset. Field positions are now randomly distributed within the weathered layer. Fig. 5.15 shows the two Common-Offset sections after the application of ray-tracing statics. Again no difference between obtained and desired output can be noticed (Fig. 5.11). Although this is not shown here, the method allows sources and receivers at all depths, including sub-weathering shots.

To study the applicability of the method for a non-homogeneous subsurface model 4 (Fig. 5.16) was used to generate a new dataset. A dipping layer (approximately  $18^\circ$ ) was added and the resultant seismic sections are shown in Fig. 5.17. The low-velocity zone was specified and ray-tracing statics were applied. In Fig. 5.18 and 5.19 the results after static corrections and the desired output is given.



**Fig. 5.15a-b.** Common-Offset Sections of model 3 after raytracing statics.

The dataset belonging to model 4 finally served as input for a standard seismic processing sequence. Both the raw- and corrected dataset were used. Fig. 5.20 shows the velocity profile along the seismic line (at CDP-points 11 and 60) for both datasets. The high velocity at 80 ms (70 ms after statics) is due to the dip of the corresponding reflector. Fig. 5.21 shows the sections after CDP-stacking. The frequency decrease of the shallowest event at 100 m distance is due to NMO-stretching of far offset traces.

Two effects may be noticed in Fig. 5.21 a:

- the shape of the weathered layer is visible in the total depth range
- at shallow depths data quality is reduced due to stacking

Fig. 5.21 b seems to be correct. However, the deepest reflection is not horizontal due to unresolved inhomogeneities in the upper zone. This effect would also have occurred in a model without the weathered layer but including the dipping event. The last step to be made is to run the statics program once more, now feeding it with the dipping layer as the model. Only the coordinates of this layer and the velocities above and below it need to be specified. Fig. 5.22 shows the final stacked section, without the apparent dip of the deepest event.

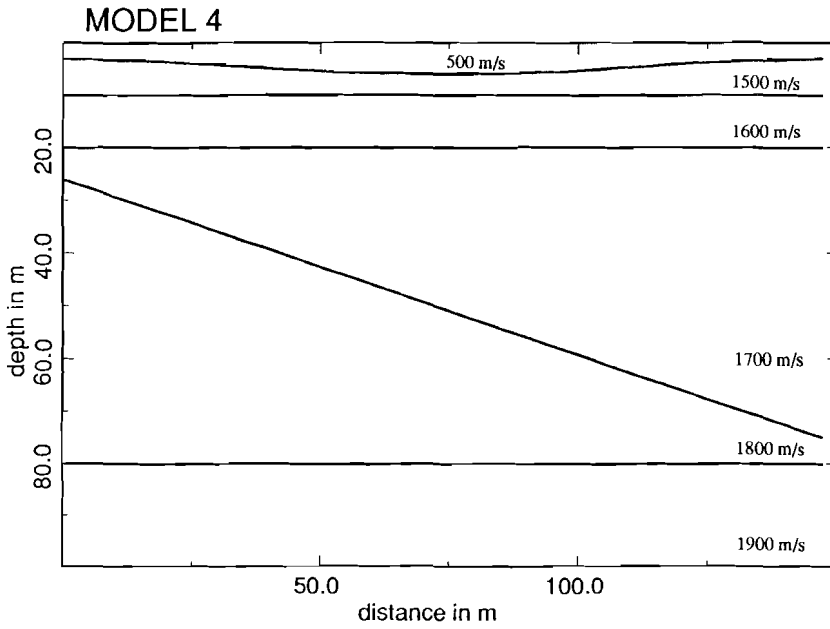


**Fig. 5.16.** Subsurface model (model 4) used to generate the seismic dataset shown in figures 5.17-5.22.

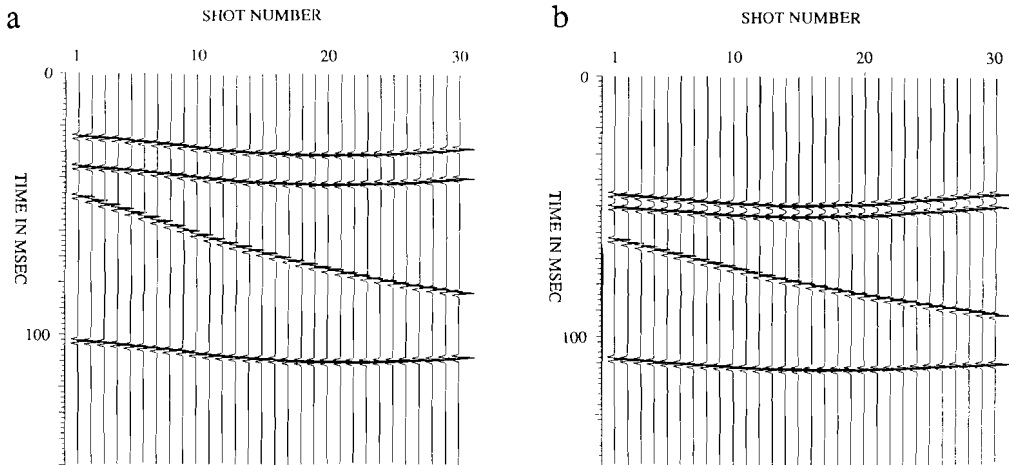


**Fig. 5.17a-b.** Common-Offset Sections of model 4 at 9 m (Fig. 5.17a) and 42 m (Fig. 5.17b) offset.

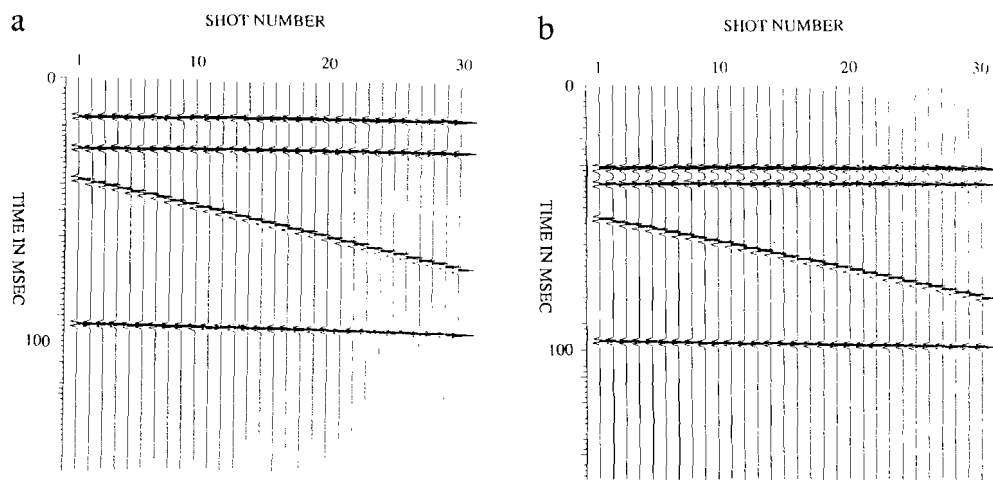


**Fig. 5.18a-b.** Common-Offset Sections of model 4 after raytracing statics.

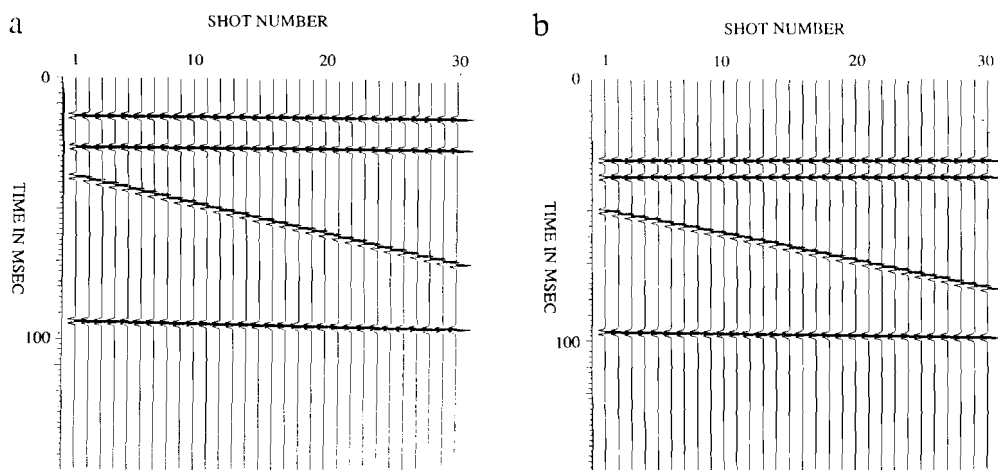


**Fig. 5.19a-b.** Common-Offset Sections of model 4 without the low-velocity zone.

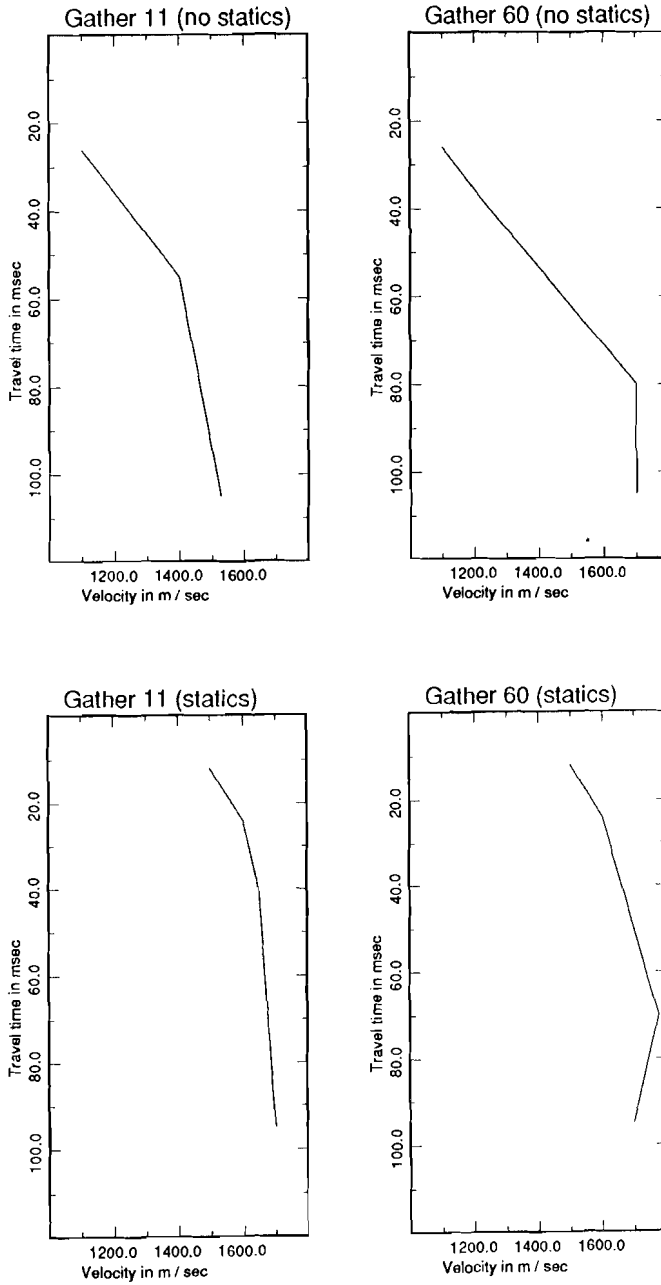
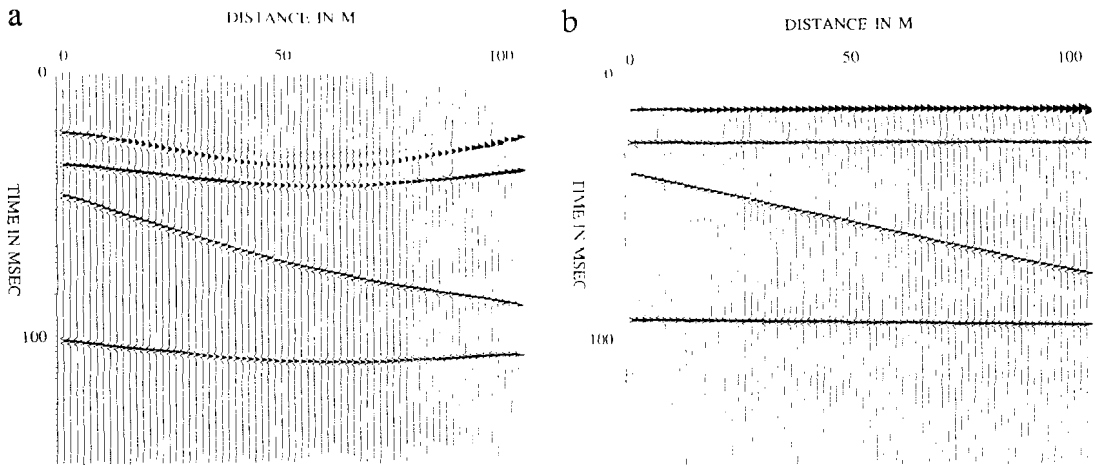
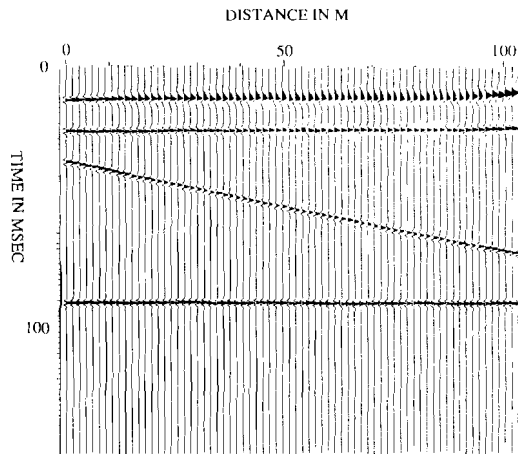


Fig. 5.20. Stackvelocity profile along the seismic profile belonging to model 4 before and after raytracing statics.



**Fig. 5.21a-b.** Stacked section belonging to model 4 without static correction (Fig. 5.21a) and with raytracing statics (Fig. 5.21b).



**Fig. 5.22.** Stacked section belonging to model 4 after correction for the low-velocity layer and the dipping event.

## 5.7 CONCLUSIONS

The use of a ray-tracing method was suggested to deal with static corrections at shallow depth. It was shown that synthetic data can almost ideally be corrected by this method resulting in a better stacking performance at shallow depths. No distinction between weathering layer corrections and topographic corrections need to be made. The method converges to the standard field statics technique for deep reflections. Inhomogeneities at large depth are treated as in standard field statics. However, the method supports the possibility to correct for known inhomogeneities at large depth, thus yielding a possible application in standard seismic processing.

The input for this method basically exists of survey coordinates, which are generally known, and a model specification. A weathering layer model can eg., be obtained from refraction interpretation or the processing of reflections at the base of the weathered layer (see chapter 4 ). The model may become more detailed by iterative processing extending the model after every processing sequence.

One should realize that the method presented only addresses the time delays caused by known structures. Amplitude effects and multiple generation are not accounted for.

## 5.8 REFERENCES

- Hileman, J.A., Embree, P., and Pfleuger, J.C. 1968. Automated static correction. *Geophysical Prospecting*, 16, 326-358.
- Taner, M.T., Koehler, F. and Alhilali, K.A. 1974. Estimation and correlation of near-surface time anomalies. *Geophysics*, 41, 441-463.



## *Chapter 6*

# **CALIBRATION OF THE SEISMIC STRATIGRAPHIC RESPONSE OF TIDAL DEPOSITS**

High-resolution seismic profiling can only be used in actual sub-surface exploration if the relationship between geological features and their expression in high-resolution data can be found. In this chapter the seismic response of tidal deposits is discussed addressing one-dimensional and multi-dimensional features. The author of this thesis was mainly involved in the processing and modelling of the data and the development of classification algorithms.

### **ABSTRACT**

An important step in the search for oil and gas is the determination of the depositional environment of the subsurface geological formations from the sedimentary facies. Analyses are carried out on various scales and with different methods, e.g., core studies, well logging and seismic facies determination. These methods are based on either theoretical or heuristic relations between observable parameters and the parameters that describe the environment of deposition. Such heuristic relations are based on the study of

---

This chapter has been published as:

Jongorius, P, Brouwer, J.H. and Helbig, K. 1987. Calibration of the seismic stratigraphic response of tidal deposits. *Proceedings of the 12th World Petroleum Congress*6 (5).

recent environments, i.e., on the direct comparison of observable quantities with the parameters controlling the deposition. Material such as that presented here from a study of the seismic response of recent tidal deposits provides such a heuristic basis for the recognition of tidal environments from seismic facies expressions.

Several significant relationships between sedimentary features like tidal channels and linear ridges, and their expression in high-resolution data have been found. To make these relationships applicable in the seismo-stratigraphic study of tidal deposits at depth, the change of both the seismic expression (due to frequency-dependent absorption and transmission losses) and the sedimentary features (due to diagenetic compaction and tectonic deformation) has to be taken into account.

## 6.1 INTRODUCTION

An important step in the interpretation of seismic sections is the determination of the seismic facies in terms of sedimentary environments. This step is generally based on theoretical and heuristic relations between seismic and geological parameters. Though this technique of seismo-stratigraphical analysis has been described exhaustively and is applied worldwide, it still contains some major gaps. One of these gaps concerns the clastics, which remain an uncertainty in every seismic interpretation. They appear in a great variety of thicknesses, shape, and lateral extent, and are formed and altered by a wide range of depositional and erosional processes. Particularly in shallow water environments clastic units tend to be thin and their lateral dimensions are often small to the seismic wavelength. The presence of shallow water clastics has often to be inferred from the depositional setting, from amplitude variations and from core information.

Study of outcrops of recent and ancient tidal deposits (Visser 1980) have revealed the presence of 'mud drapes' deposited at slack water at high and low tide. These mud drapes make the sediment body highly anisotropic for fluid flow. The small scale (cm to dm) makes it impossible to observe these features even with a high seismic resolution. However if one can observe the external geometry of sandbodies at the next higher scale (m to Dm), it is possible to infer the gross properties of the smaller features.

The heuristic and theoretical relations between depositional environment and sedimentological core information are based on the study of recent environments, i.e., on the direct comparison of observable quantities with the parameters controlling the deposition. Using a comparable actualistic method we have tried to develop a basis for the recognition of a specific clastic environment, viz., tidal areas, from seismic expressions by studying the seismic response of recent tidal deposits. This study is carried out in the Eastern Scheldt tidal inlet in the SW of the Netherlands (Fig. 6.1), where tidal deposition is investigated closely by sedimentologist and where high-resolution seismic surveys have been carried out over a few years.

In our study we try to combine these two research methods. We examine features that

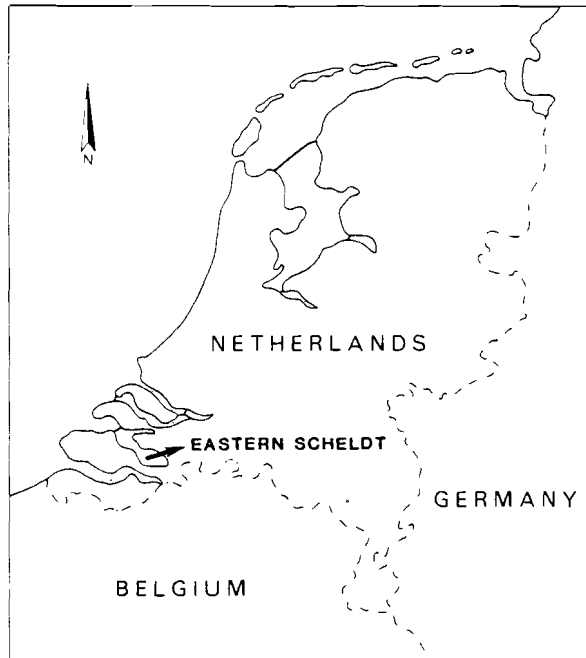


**Fig. 6.1.** Topographic map of the Netherlands showing the geographical position of the study area.

show a correlation in both seismology and sedimentology, and try to find a way to quantify them in sedimentary and seismic criteria. This paper discusses correlations between clastic tidal deposits and their seismic facies and describes algorithms that provide some numerical expressions for correlating features.

## **6.2 SEDIMENTOLOGIC FRAMEWORK:**

The last decade has seen intensive research into modern and ancient clastic tidal deposits. Despite this, fundamental diagnostic criteria based on detailed qualitative observations and quantitative measurements have been scarce. Many of the structural and textural features which collectively suggest a tidal environment may individually occur in several different environments. Most tidal areas are characterized by channels and shoals. The complex migration patterns of these subenvironments and the great variety of the

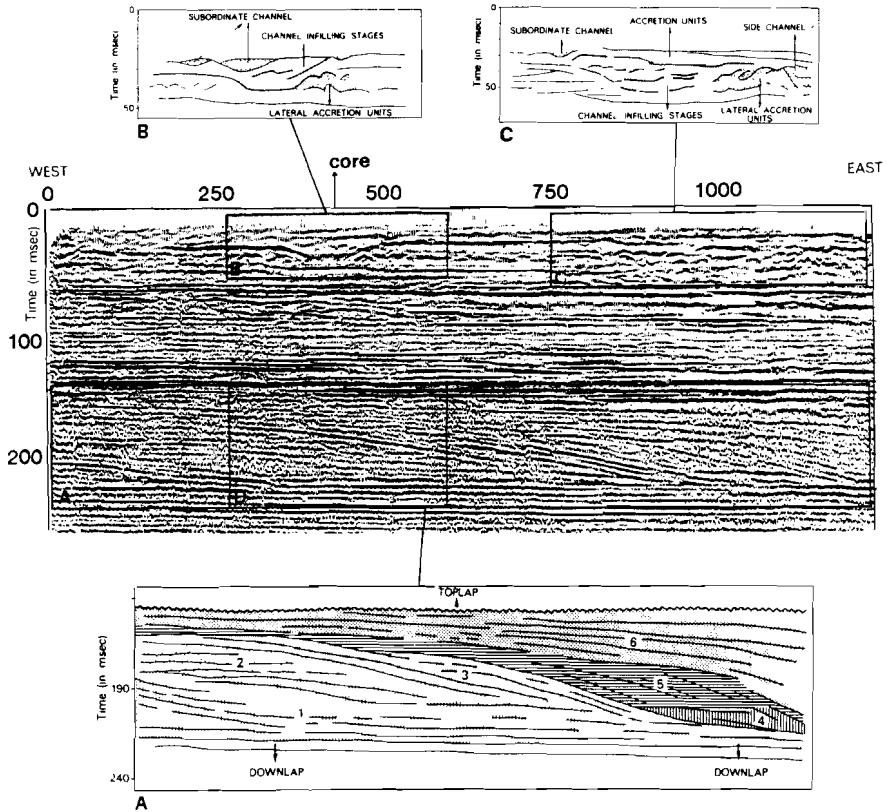


Fig. 6.2. The test section used in this paper is a high-resolution line across the central part of the *Plaat van Oude Tonge*, a tidal shoal in the Eastern Scheldt estuary. Detail a: Unit I, linear ridge striking NW-SE. Detail b and c: Unit II, distributary channels. Channel B strikes NW-SE (compare Fig. 6.3). Strike of channel C is not known.

structures they contain render it unlikely that simple commonly recurring sequences are produced. In the Netherlands, in particular the Eastern Scheldt, research into inshore tidal sedimentation has emphasized the relation between the bedform and internal structural organization.

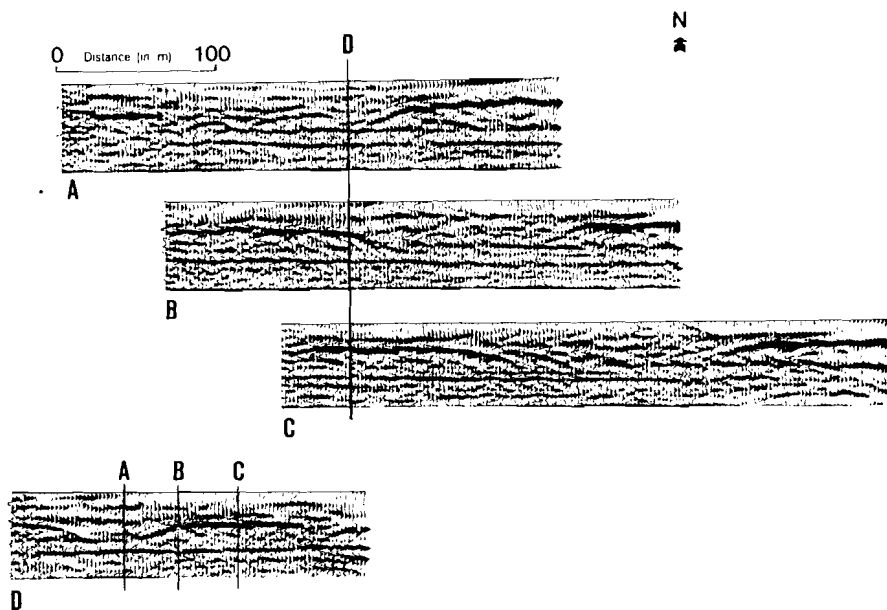


Fig. 6.3. a,b,c: E-W lines en-echelon across feature B (unit II) of figure 6.2. d: N-S line intersecting the three E-W lines.

### 6.3 SEISMIC CHARACTERISTICS

The relationship between seismic data and the geological model can either be described theoretically or heuristically. Inversion of seismic data by means of the wave equation provides us with a theoretical relation. In principle, inversion results in the geological model corresponding to a seismic data set.

The heuristic relation is established by correlation between seismic and geologic features.

In order to classify sedimentary structures on the basis of seismic data, we first have to evaluate the potential seismic characteristics. These characteristics can be divided into single-trace (one-dimensional) features and multi-trace features. Single-trace features that might be used as seismic characteristics are, e.g., signal strength, polarity, and period. After application of the Hilbert transform to determine the complex seismic trace, additional characteristics like instantaneous phase and frequency are available. Multi-trace features are essentially formed by the lateral extension of single-trace features. Among others, continuity and dip of events are of particular importance.

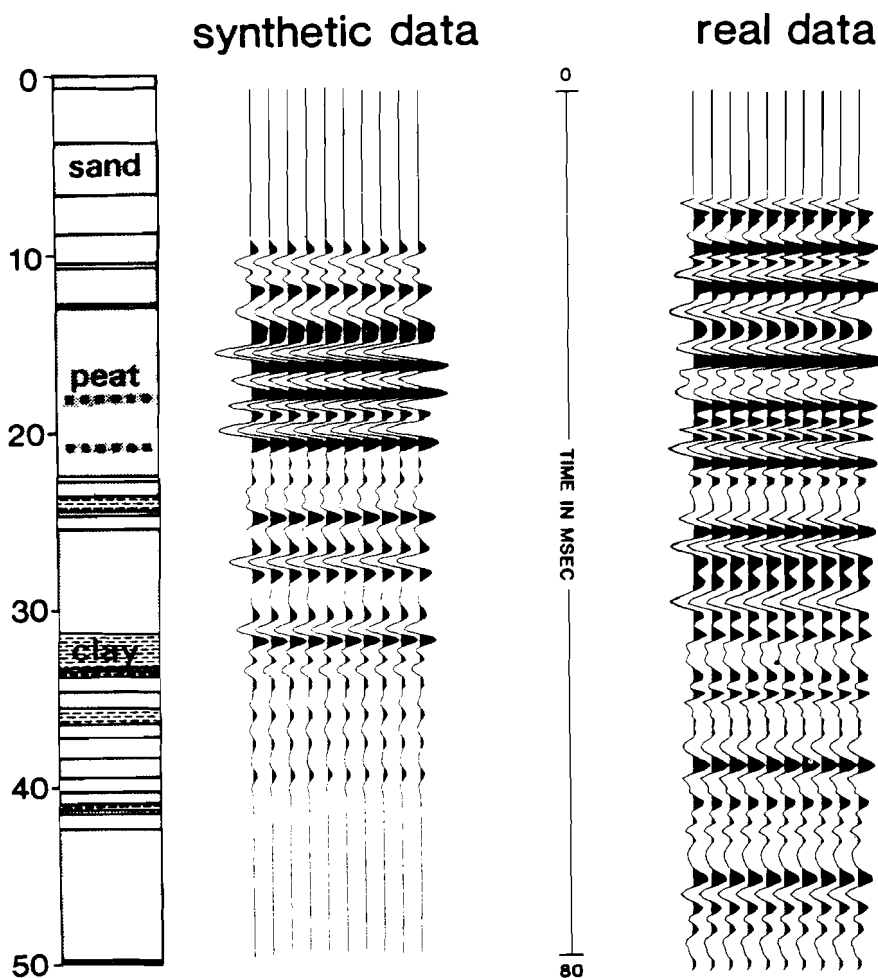
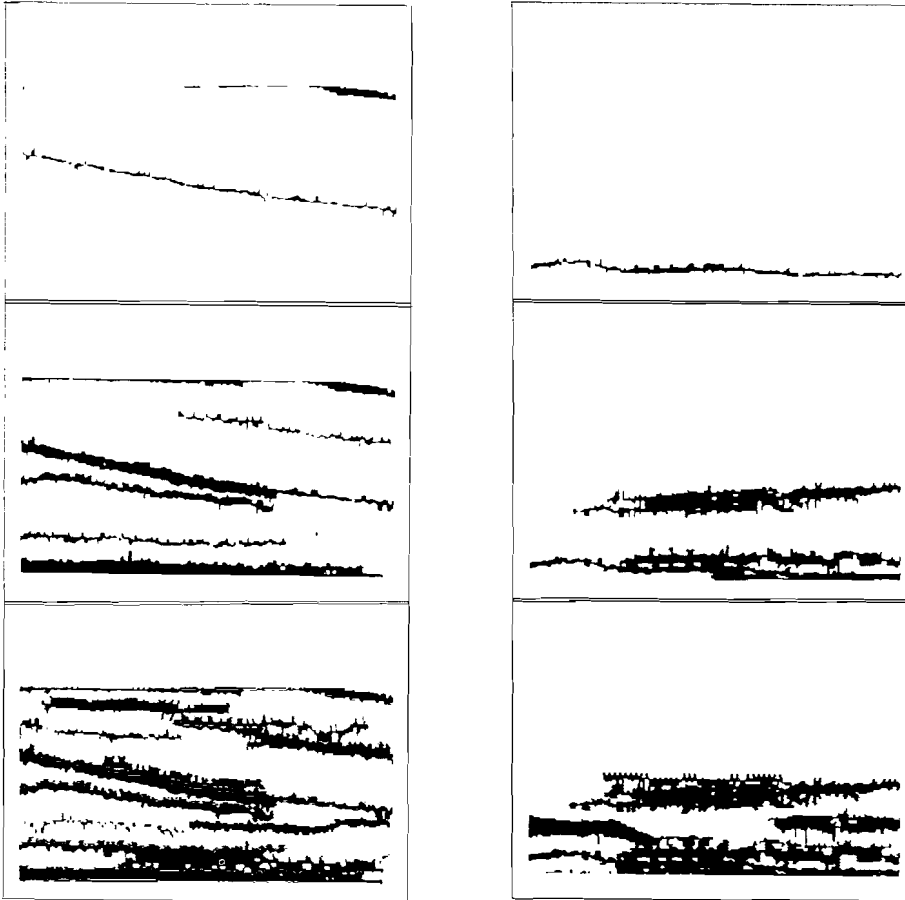


Fig. 6.4. Left: lithological log based on sand cores from well penetrating unit II (Fig. 6.2). Centre: synthetic seismogram based on impedances estimated from porosity and grain size and a Ricker wavelet centred at 350 Hz (one trace repeated 10 times). Right: Data observed at the same location (one trace repeated times).

#### 6.4 TEST SECTION

Our sedimentological investigations of the relationship between depositional processes and preserved morphologies in recent sedimentary environments are restricted to areas exposed at low tide. Standard core studies have been supplemented by some investigations in outcrops created by the recent construction works in Eastern Scheldt estuary.



**Fig. 6.5.** Continuity sections prepared from automatically picked events. Left: Unit 1 part D, right: unit II channel B. Top: all events that can be followed for at least 80% of the frame, centre: all events that can be followed for at least 40% of the frame, bottom: all events that can be followed for at least 10% of the frame.

Cores provide only information about the small-scale structures. The interpretation of structures that are significantly larger than the core diameter, which often make up a major part of the deposits, is difficult.

To extend these highly localized information we have used high-resolution seismic profiling with wave length of 2-10 m. The method supplements sedimentological studies and provides details of the sedimentary succession down to a depth of about 500 m; it thus offers the opportunity to study preserved morphologies in detail.

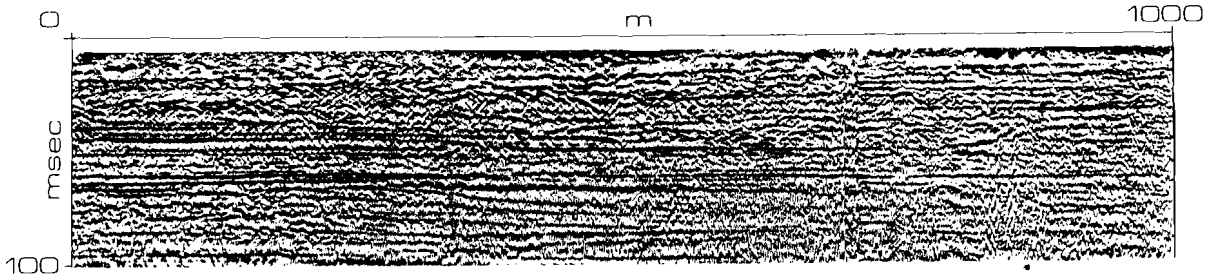


**Fig. 6.6.** Ultra-high-resolution section, position close to the test section (Fig. 6.2). The typical multi-channel features of figure 6.2 are nearly completely masked by the abundant (single-channel) detail.

The high-resolution seismic surveys were carried out using a 30- kg weight-drop from a tripod with a height of 2.7 m. A steel plate with a diameter of 30 cm is used for the impact and coupling with the ground. In view of the relatively high signal frequency (100-1000 Hz), 100 Hz geophones are used. The source- and receiver spacings vary from 1 to 10 m with an initial offset between 8 and 25 m. From the frequency spectrum and the stack velocities of 1500-2000 m/sec, a resolution of 0.5 to 5 m can be deduced.

The seismic section in Fig. 6.2 is an excellent example of a seismic survey on an intertidal shoal in the Eastern Scheldt tidal inlet situated in the SW Netherlands. Down to a depth of 500 m the sedimentary succession in the study area consists almost entirely of Tertiary shallow marine and tidal deposits, covered by a blanket of Holocene tidal sediments formed under the influence of rising sea level. Individual tidal deposits reach a thickness of 40 m.

To study relationships between lateral extensions (tidal morphologies) and their expression in high resolution seismic profiling we will focus on two time intervals of the section presented in Fig. 6.2:

- unit I, between 180 and 250 ms, consisting of inclined and semi-continuous reflections with moderate amplitude;
- unit II, between 10 and 50 ms, with undulating reflectors with a variable continuity and amplitude.

Unit I: different stages of progradation and aggradation are bounded by unconformities (Fig. 6.2A). The maximum height of the oblique sets is 40 m with a



maximum dip of 6 degrees. The extension perpendicular to strike is at least 1600 m. Due to the restricted access to the area the coverage of the unit in the strike direction is limited to about 2500 m.

The low dip, the moderate thickness and direction of progradation suggest that this is not a delta sequence. Rather the feature resembles recent linear ridges in the North Sea. In the Southern North Sea these recent sand ridges are 10–40 m high, 1–2 km wide, and up to 60 km long. Continuous seismic profiles (Houbolt 1968) show lateral accretion surfaces with dips of 4–7 degrees within the ridges. A better knowledge of the internal configuration of recent linear ridges would be needed to confirm this interpretation, but the sparker profiles across these features are still too poor to give comparable results comparable to ours.

Unit II: this unit section contains two concave morphologies with an apparent W/D ratio less than 20. Structure B has an apparent width of 250 m and a height of 20 m. The external form is accentuated by a strong reflector. It is not clear what causes this strong reflection. The unit erodes the underlying fluvial deposits. From regional geological data it is known that the top of the underlying formation is strongly dehydrated and has a higher density than the tidal sediments. This means that erosion of the older formation must cause a strong impedance contrast with the tidal infilling.

Beside this clear external channel form, different internal features can be recognized. Figure 6.2B shows an interpretation of the infill of channel B. To get an impression of the horizontal channel dimensions a three-dimensional study was carried out (Fig. 6.3). The lobe structures, which are interpreted as lateral accretion lobes, are still under discussion. They may be formed by the apices of diffraction hyperbolas. From shallow cores it is known that the channels consist partly of tidal sequences comprising medium to coarse sands at the base to medium to fine sands in the upper parts. The width-to-depth ratio is normal for coastal marine channels.

Structure C does not show a clear external morphology, but can be recognized by its internal configuration. Figure 6.2C is an interpretation of internal features. The channel has a W/D ratio less than 20 with a height of 45 m.

## 6.5 HEURISTIC RELATIONS

Seismic data are related to geologic characteristics of the subsurface. In principle it is possible to describe the seismic response of any geological model. The knowledge of recent sedimentological characteristics provides a collection of geological models, which define immediately the seismic response.

### 6.5.1 One-dimensional features

To visualize the relationship between one-dimensional geological and seismic characteristics we performed a simple modelling experiment.

Figure 6.4 shows the lithology of the unconsolidated upper unit of the seismic section in figure 6.2. As there were no wireline logs available we had to use core samples to define the one-dimensional characteristics. Changes in grainsize and sorting showed a positive correlation with impedance contrasts. Based on laboratory measurements of porosity as a function of grainsize and sorting, we determined the porosity as a function of depth. This porosity was used to calculate velocity and density under the assumption that the grains consisted entirely of quartz and the pores were filled with water.

The velocity and density were used to calculate impedance and reflectivity. The reflection coefficients resulting from the grainsize and sorting changes were in the order of magnitude of 5-10 %.

In order to compare this synthetic reflectivity log with real seismic data we convolved the reflection coefficient series with a Ricker wavelet with a peak frequency of 350 Hz.

The 1-D modelling (Fig. 6.4) is far from ideal. A real velocity- and density log would have been of great help as well as a better knowledge of the actual waveform. Nevertheless, it appears that changes in grainsize and sorting can account for reflection coefficients of 5-10%. We also see that what we observe in high-resolution seismic data is more or less the interference pattern of many small changes in reflectivity. For a better correlation one either has to increase the resolution (higher frequencies), or limit oneself to the gross changes in 1-D sedimentological features.

### 6.5.2 Multi-dimensional features

The degree to which one-dimensional sedimentological features are expressed in seismic data depends on the wavelength spectrum of the wavelet. The lateral extension of the 1-D features will show as much detail as permitted by the wavelength of our signal.

To study the multi-dimensional characteristics of the examples, the sections are digitized using an event-picking programme. From the digitized events continuity sections were prepared (Fig. 6.5). In the continuity section that shows reflectors that can be followed for more than 80% of the width of the section, only the major events are present. The channel is not recognizable, and from the linear ridge only a single dipping event is picked. A 40% continuity section (Fig. 6.5) shows the boundaries of the channel and some of the top- and downlap structures within the ridge. The third continuity section (10%) shows details of all internal structures listed above. These examples give an indication that there must be a relation between seismic continuity and sedimentary processes.

## 6.6 CONCLUSIONS

The seismic response of tidal deposits at reservoir depths differs from the above examples primarily in that the resolution is much lower: a linear ridge as unit 1 in figure 6.2 might appear as a single strong reflector. With the current acquisition technology there is little hope of observing internal structures at depth of, say, 2000 m. An apparently obvious approach to determine the seismic expression of our test features if they are situated at depth, namely low-pass filtering, does not work: low-pass filtering correctly transforms single-channel features, but multi-channel features strongly depend on the trace separation and thus on the acquisition geometry. Instead, we have compared two sections with different degrees of resolution obtained over nearly the same feature (Fig. 6.6). Comparison with figure 6.2 shows that at this high resolution the single-channel information tends to mask the multi-channel features. Though the test features are discernible in the ultra-high resolution section, the section is dominated by fluctuations in parameters like grain size, sorting and water content, i.e., by typical single-channel parameters.

The change in character from ultra-high resolution to high-resolution can be regarded as a model for the change to be expected if one goes from high resolution to standard resolution.

The high-resolution seismic response of clastic sequences shows internal details that not only give important clues to the environment of deposition and transport mechanism, but also allow inference, e.g. orientation of mud drapes that are of the utmost importance for the flow of fluids during production. Thus the developments in high-resolution seismics would result in great benefits in the study of clastic deposits.

As we can see by comparing high-resolution seismic data of different resolution, geological information that can be obtained from seismic data changes from well-described 1D changes in sediment characteristics for the ultra-high resolution seismic data to a 'low frequency' image for the high-resolution seismic data. The same change in information density may be expected in the comparison of high-resolution data with standard seismic data.

While it is not possible to infer features on the cm to dm scale from seismic data with standard resolution, the resolution of a few meters allows us to determine the external geometry of sandstone bodies in detail and to make inferences concerning their internal structure. Though this is still an order of magnitude coarser than the information obtained from cores, the gap between the two kinds of data would be considerably narrowed, thus making integration of core data and seismic data easier and more reliable.

## 6.7 REFERENCES

- Visser, M.J. 1980. *Geology* 8, 543-546.  
Houbolt, J.J.H.C. 1968. *Geol. en Mijnb.*, 47, 245-273.

## SAMENVATTING (SUMMARY IN DUTCH)

Seismische gegevens worden zowel in de seismologie als in de exploratie seismiek gebruikt voor het verkrijgen van informatie over de ondergrond. De laatste jaren is er een toenemende interesse waarneembaar voor het gebruik van deze seismische gegevens bij de verkenning van de ondiepe ondergrond. Hoge resolutie seismiek mag zich verheugen in een groeiende belangstelling met name uit de ingenieurs-geologische hoek waarbij de nadruk vooral ligt op de verbetering van acquisitie technieken.

De Rijksuniversiteit Utrecht houdt zich sinds 1976 bezig met hoge resolutie seismiek. In eerste instantie was de belangstelling voor de methode gebaseerd op de wens informatie te verkrijgen over recent afgezette sedimentaire structuren. Met name in getijde gebieden in Zeeland werd de methode met succes toegepast resulterend in seismische gegevens van ongekend goede kwaliteit. De goede acquisitie omstandigheden, de afwezigheid van een verweringslaag en een zeer hoge signaal-ruis verhouding, lagen daaraan ten grondslag. Verder onderzoek op het gebied van de ondiepe hoge resolutie seismiek hield zich dan ook voornamelijk bezig met de verwerking en de interpretatie van de gegevens aangezien de acquisitie relatief weinig problemen opleverde.

Het onderzoek dat gepresenteerd wordt in dit proefschrift houdt zich bezig met de ontwikkeling van hoge resolutie seismiek tot een methode voor de verkenning van de ondiepe ondergrond. Drie onderwerpen komen daarbij aan de orde. In de eerste plaats wordt de uitbreiding naar een volledige 3D acquisitie, processing en interpretatie techniek behandeld. Aan de hand van een project in Zeeland wordt in hoofdstuk 2 aangetoond dat het mogelijk is ook met zeer beperkte middelen hoge resolutie 3D seismiek te verrichten.

De ontwikkeling van hoge resolutie seismiek op land is het tweede onderwerp waaraan in deze dissertatie aandacht wordt besteed. In hoofdstuk 3 wordt een overzicht gegeven van de acquisitie, verwerking en interpretatie van landgegevens. De aanwezigheid van een verweringslaag is er op land vaak de oorzaak van dat de resolutie omlaag gaat. Daarnaast treden er ook bij de verwerking van de gegevens nogal wat extra problemen op als gevolg van deze verweringslaag. Een vergelijking tussen de verwerking van landgegevens en seismische data uit getijde gebieden illustreert dit.

Het gebruik van gecombineerde refractie- en reflectie informatie bij de interpretatie van landgegevens wordt behandeld in het vierde hoofdstuk. Aangetoond wordt dat het ook op land mogelijk is ondiepe informatie te verkrijgen uit seismische metingen. Multiple reflecties aan de basis van de verweringslaag zijn enerzijds zeer storend voor diepere reflectie maar bevatten anderzijds waardevolle informatie over de dikte en de snelheid van deze laag. Deze informatie kan bij de verwerking van de data gebruikt worden bijvoorbeeld voor het uitvoeren van statische correcties.

De wijze waarop statische correcties moeten worden uitgevoerd in ondiepe hoge

resolutie seismiek wordt behandeld in het vijfde hoofdstuk. Aangetoond wordt dat standaard methoden voor het uitvoeren van statische correcties ongeschikt zijn voor het verwerken van ondiepe seismische gegevens. Als alternatief wordt een op raytracing gebaseerde methode gepresenteerd die wel bruikbaar is.

Het laatste hoofdstuk behandelt de relatie tussen seismische gegevens en geologie. De correlatie tussen clastische getijde afzetting en hun seismische representatie wordt behandeld aan de hand van seismische gegevens uit Zeeland.

## ACKNOWLEDGEMENTS

I wish to thank all persons and institutions that contributed to the research described in this thesis.

I am very grateful to Prof. K. Helbig. He gave me the opportunity to benefit from his experience in the field of exploration geophysics in general and high-resolution seismics in particular. Pieter Jongerius, who cooperated in this research for more than three years, has taught me some geo-sense and helped me to keep my feet on the ground. I also thank Wim Versteeg and Job Corsmit. They initiated the work on 3D seismics at our department and have been fine colleagues during my study. Johan Tempels has been an unreplaceable technician and friend during the last five years. He never complained about the additional field tests we planned whenever this turned out to be necessary and repaired all the equipment we damaged. Jan Douma has been a roommate for three years. Although we did not work on the same research subject he was always willing to lend an ear.

**Shell and Stichting Nationaal Comite Nederland Voor Wereld Petroleum Congressen** gave financial support to visit geophysical meetings. **Grondmechanica Delft** cooperated in some of the field surveys and provided additional information on local geology.

I like to thank my relatives, neighbours, and friends for their patience and their interest in my work during my study. Liesbeth, Marloes, and Femke were just there whenever I needed them. Their contribution to this thesis need not to be emphasized.

-

## CURRICULUM VITAE

De schrijver van deze dissertatie werd op 13 oktober 1958 geboren te Leeuwarden. Hij behaalde het diploma Atheneum-B in 1977 aan de Rijksscholengemeenschap te Purmerend. Aansluitend werd begonnen met een studie natuurkunde aan de Rijksuniversiteit te Utrecht. Het kandidaatsexamen N3 werd afgelegd in 1980 waarna in 1984 het doctoraalexamen geofysica met hoofdrichting exploratie geofysica en bijvak signaalverwerking werd behaald. Sinds 1984 is de schrijver van dit proefschrift als wetenschappelijk assistent verbonden aan de afdeling Exploratie Geofysica van de Rijksuniversiteit Utrecht.